

Properties and Behaviour
of the Boom Clay
Formation within a Dutch
Repository Concept

OPERA-PU-BGS615

Radioactive substances and ionizing radiation are used in medicine, industry, agriculture, research, education and electricity production. This generates radioactive waste. In the Netherlands, this waste is collected, treated and stored by COVRA (Centrale Organisatie Voor Radioactief Afval). After interim storage for a period of at least 100 years radioactive waste is intended for disposal. There is a world-wide scientific and technical consensus that geological disposal represents the safest long-term option for radioactive waste.

Geological disposal is emplacement of radioactive waste in deep underground formations. The goal of geological disposal is long-term isolation of radioactive waste from our living environment in order to avoid exposure of future generations to ionising radiation from the waste. OPERA (OnderzoeksProgramma Eindberging Radioactief Afval) is the Dutch research programme on geological disposal of radioactive waste.

Within OPERA, researchers of different organisations in different areas of expertise will cooperate on the initial, conditional Safety Cases for the host rocks Boom Clay and Zechstein rock salt. As the radioactive waste disposal process in the Netherlands is at an early, conceptual phase and the previous research programme has ended more than a decade ago, in OPERA a first preliminary or initial safety case will be developed to structure the research necessary for the eventual development of a repository in the Netherlands. The safety case is conditional since only the long-term safety of a generic repository will be assessed. OPERA is financed by the Dutch Ministry of Economic Affairs and the public limited liability company Electriciteits-Produktiemaatschappij Zuid-Nederland (EPZ) and coordinated by COVRA. Further details on OPERA and its outcomes can be accessed at www.covra.nl.

This report concerns a study conducted in the framework of OPERA. The conclusions and viewpoints presented in the report are those of the author(s). COVRA may draw modified conclusions, based on additional literature sources and expert opinions. A .pdf version of this document can be downloaded from www.covra.nl

OPERA-PU-BGS615

Title: Properties and Behaviour of the Boom Clay formation within a Dutch Repository Concept

Authors: A. Wiseall, C. Graham, S. Zihms, J. Harrington, R. Cuss, S. Gregory, R. Shaw

Date of publication: December 2015

Keywords: Boom Clay; Mechanics; Transport; Hydraulics; Gas; Thermal; Microbiological; Netherlands; Belgium

Contents

Contents	3
Summary	5
Samenvatting.....	Fout! Bladwijzer niet gedefinieerd.
List of Figures	6
List of Tables	7
1. Introduction	8
1.1. The COVRA Boom Clay disposal concept.....	8
1.2. Geological setting.....	9
1.3. Burial history of the Boom Clay.....	9
1.4. Ice cover	10
1.5. Stress conditions	10
2. Baseline characteristics	12
2.1. Composition.....	12
2.1. Pore fluid chemistry.....	14
2.2. Geotechnical properties	15
2.2.1. Bulk and dry density	15
2.2.2. Porosity	15
2.2.1. Particle density and specific gravity.....	17
2.3. Grain scale characteristics	18
2.4. Baseline characteristics summary	19
3. Mechanics.....	21
3.1. Fundamental concepts	21
3.1.1. Stress / strain relationship.....	21
3.1.2. Elastic deformation	23
3.1.3. Inelastic deformation	23
3.2. Yield and failure	25
3.2.1. The influence of effective stress.....	26
3.2.2. Failure criteria.....	29
3.3. Mechanical properties of the Boom Clay	33
3.3.1. Elastic response.....	34
3.3.2. Compressive strength	36
3.3.3. Consolidation properties	37
3.3.4. Shear strength and frictional properties	40
3.3.5. Yield in p - q - v space	41
3.3.6. Critical state scenario analysis for the Dutch Boom Clay concept	43
3.3.7. Swelling behaviour	46
3.4. Structural characteristics of the Boom Clay	49
3.4.1. Sedimentary fabric	50
3.4.2. Fracturing and faulting	50
3.4.3. Excavation damage zone	51
3.4.4. Sealing properties	52
3.5. Mechanics summary	53
4. Transport processes.....	55
4.1. Hydraulic processes.....	55
4.1.1. Intrinsic permeability	55
4.1.2. Specific storage.....	56
4.1.3. Experimental determination of hydraulic permeability.....	56
4.1.4. Hydraulic properties	57
4.1.5. Key factors influencing hydraulic properties	58
4.2. Diffusion and Fick's law.....	63
4.3. Tortuosity	63
4.4. Osmosis and coupled flow phenomena	64
4.5. Gas migration.....	67

4.5.1.	Gas transport by diffusion.....	67
4.5.2.	Advective and dispersive transport	68
4.5.3.	Continuum approach to gas flow	76
4.5.4.	Scale-dependence and its impact on gas flow	77
4.5.5.	Impact of burial history on gas flow	77
4.5.6.	Impact of gas migration on hydraulic properties	80
4.5.7.	Gas driven radionuclide migration	80
4.6.	Transport summary	80
5.	Thermal effects.....	82
5.1.	Thermal parameters.....	82
5.2.	Elevated temperature testing.....	84
5.3.	Mechanical response and impacts	84
5.4.	Impact on hydraulic properties	90
5.5.	Impact of temperature on gas migration	91
5.6.	THM in situ studies.....	92
5.7.	Thermal summary with reference to the Dutch concept.....	95
6.	Microbiology.....	97
6.1.	Evidence for the occurrence of micro-organisms	97
6.2.	The diversity of microorganisms likely to be present	97
6.3.	Conditions necessary for the presence and survival of microorganisms	98
6.4.	Microbiology summary.....	99
7.	Conclusions.....	100
8.	References	101
	Appendix A: Symbols and Abbreviations.....	122
	Appendix B: Data and properties.....	124

Summary

This report aims to summarise the Thermal, Hydraulic, Mechanical (THM) and Biological properties and behaviour of the Boom Clay Formation. Much of the information used comes from research conducted at the High Activity Experimental Site (HADES) Underground Research Laboratory (URL), situated at a depth of approximately 220m in Mol, Belgium. A key objective of this report is to address the extent to which the THM and biological properties of the Boom Clay in Belgium may differ for a potential geological repository at a depth of 500m, further north in The Netherlands.

Initially, the baseline characteristics of the Boom Clay have been described. These are well defined in Belgium, both at the Underground Research Laboratory (URL) at Mol and also spatially across the country. However, these characteristics are less well defined in The Netherlands because the limited amount of borehole data. Spatial differences are observed across Belgium and therefore it is likely a similar degree of variability will occur in The Netherlands, primarily as a result of regional lithological differences and deeper burial conditions.

The mechanical properties of the Boom Clay have again been well defined in Belgium. A limited degree of work undertaken to predict the impact of deeper burial indicates that void ratio will reduce, but the Over Consolidation Ratio is likely to be closer to normally consolidated. The effect of greater burial depth on the mechanical properties of the Boom Clay has been analysed using Critical State Mechanics (CSM). Evidence indicates a tendency for increased mechanical stability under these conditions.

Hydraulic conductivity at 500 m depth is expected to range between 2×10^{-13} and 1×10^{-12} m/s, excluding the effects of spatial variation in mineral content. The range of magnitude reflects the uncertainty in burial history. A strong hydraulic anisotropy is likely, though current data is limited.

Coupled flow behaviour is even more poorly constrained at relevant in situ conditions. However, significant effects are expected and will need to be considered. Likely limits for the rate of diffusion of H_2 can be made, but no measurements are available for this process under the expected stress conditions for a Dutch repository. In contrast, in the case of advective gas flow, there is a significant body of evidence indicating that migration will occur by the development of pressure-induced dilatant pathways. However, further work is required to better define the coupling between gas flow and stress, and the influence of heterogeneity and anisotropy.

In terms of thermal properties, a volumetric response to an increase in thermal load is expected. However, without reliable preconsolidation data the form of strain is hard to predict. Thermal loading will also result in pore pressure build-up, to greater levels than at shallower conditions. This will further affect the hydro-mechanical evolution of a repository.

Micro-biological observations point to the presence of a small population of micro-organisms, which will mainly consist of dormant cells and spores. It may be expected that this population would decrease at greater depths, although this cannot be assumed. The presence of a population of organisms may have affect repository performance, though further research is required to assess this.

The work presented in this report is not meant to fully describe every aspect of the THM and biological properties of the Boom Clay, but is intended to show the key work already carried out and relate to the disposal concept investigated in OPERA. The report highlights areas with knowledge gaps, indicates where there are large uncertainties and recommends future work as a result.

List of Figures

FIGURE 2-1. BOREHOLE LOCATIONS NEAR THE NETHERLANDS-BELGIUM BORDER.....	13
FIGURE 3-1. THREE-DIMENSIONAL COORDINATE SYSTEM	22
FIGURE 3-2. DESCRIPTION OF FORCES ACTING ON A DISCONTINUITY.	22
FIGURE 3-3. GENERAL RESPONSE OF ROCKS OBSERVED IN THE STRESS-STRAIN SPACE..	24
FIGURE 3-4. COMPRESSION CHARACTERISTICS OF A RANGE OF NORMALLY-CONSOLIDATED MATERIALS.....	27
FIGURE 3-5. DETERMINATION OF THE PRECONSOLIDATION STRESS ACCORDING TO CASAGRANDE (1936).....	28
FIGURE 3-6. MOHR-COULOMB DIAGRAM.	30
FIGURE 3-7. THE CRITICAL STATE MODEL OF SOIL MECHANICS	32
FIGURE 3-8. THE CRITICAL STATE MODEL OF SOIL MECHANICS IN DETAIL.....	32
FIGURE 3-9. COMPILATION OF CONSOLIDATION CURVES FROM HORSEMAN ET AL. (1987)	41
FIGURE 3-10. THE CRITICAL STATE SOIL MECHANICS MODEL FOR THE BOOM CLAY AT MOL.	44
FIGURE 3-11. THE CRITICAL STATE SOIL MECHANICS MODEL FOR THE BOOM CLAY WITHIN NL.....	44
FIGURE 3-12. THE CRITICAL STATE SOIL MECHANICS MODEL – THE EXPECTED STATE OF EFFECTIVE STRESS.....	45
FIGURE 3-13. ARGILLACEOUS MATERIAL FABRIC AND STRUCTURE.....	47
FIGURE 3-14. DOUBLE LAYERS NEAR CLAY PARTICLES.....	47
FIGURE 3-15. CHEMICALLY INDUCED VOLUME CHANGE VERSUS PORE WATER Na^+ CONCENTRATION.....	49
FIGURE 3-16. LOCATION MAP	51
FIGURE 3-17. SCHEMATIC REPRESENTATION OF A VERTICAL CROSS-SECTION	52
FIGURE 3-18. SELFRAC SELF-SEALING EXPERIMENT.....	53
FIGURE 4-1. HYDRAULIC CONDUCTIVITY FOR THE DIFFERENT BOREHOLES.....	60
FIGURE 4-2. RELATIONSHIP BETWEEN HYDRAULIC CONDUCTIVITY PLOTTED AND EFFECTIVE STRESS	61
FIGURE 4-3. EXPERIMENTAL DATA FROM A BOOM CLAY SAMPLE	61
FIGURE 4-4. EXPERIMENTAL DATA FROM THE BOOM CLAY.....	62
FIGURE 4-5. POSSIBLE GAS FLOW PROCESSES IN ARGILLACEOUS MATERIALS.....	67
FIGURE 4-6. EXPERIMENTAL HISTORY T3S1 ON THE BOOM CLAY	71
FIGURE 4-7. CROSS-PLOT OF STEADY STATE GAS FLOW DATA.	73
FIGURE 4-8. (<i>LEFT</i>) STRAIN DATA FROM TRIAXIAL TEST. (<i>RIGHT</i>) POST-TEST DEGASSING	75
FIGURE 4-9. MIXED SE AND BSE IMAGE SHOWING A TRAIL OF AGGREGATED GOLD NANOPARTICLES.	75
FIGURE 4-10. CROSS PLOT OF VOID RATIO AGAINST HYDRAULIC CONDUCTIVITY	78
FIGURE 4-11. REPROCESSED DATA SHOWING THE SENSITIVITY OF GAS PRESSURE TO CONFINING STRESS	79
FIGURE 4-12. CROSS PLOT SHOWING AVERAGE BREAKTHROUGH AND PEAK GAS PRESSURES.....	79
FIGURE 5-1. CHANGE IN PORE PRESSURE PLOTTED AGAINST TEMPERATURE RISE ABOVE AMBIENT	86
FIGURE 5-2. VOLUMETRIC STRAIN PLOTTED AGAINST TEMPERATURE RISE ABOVE AMBIENT	88
FIGURE 5-4. INFLUENCE OF TEMPERATURE ON INTRINSIC PERMEABILITY	91
FIGURE 5-5. BREAKTHROUGH PRESSURE AGAINST TEMPERATURE	92

List of Tables

TABLE 1-1. STRESS CONDITIONS AT THE HADES URL	11
TABLE 1-2. REFERENCE STRESS CONDITIONS USED IN THIS REPORT.	11
TABLE 3-1. CLASSIFICATION OF CLAY SWELLING POTENTIAL, BASED ON ATTERBERG LIMITS.	48
TABLE 4-1. TORTUOSITY RELATIONSHIPS FOR POROUS MEDIA	64
TABLE 4-2. FLOW MATRIX SHOWING DIRECT AND COUPLED FLOW PROCESSES	65
TABLE B-1. REPORTED MINERAL COMPOSITION OF THE BOOM CLAY IN BELGIUM.....	124
TABLE B-2. REFERENCE MINERAL COMPOSITION OF THE BOOM CLAY IN BELGIUM	124
TABLE B-3. REFERENCE BOOM CLAY PORE WATER.....	125
TABLE B-4. SUMMARY OF GEOTECHNICAL PROPERTIES FOR THE BOOM CLAY	126
TABLE B-5. SUMMARY OF THE MECHANICAL PROPERTIES OF THE BOOM CLAY.....	127
TABLE B-6 SUMMARY OF HYDRAULIC PROPERTIES FOR THE BOOM CLAY	129
TABLE B-7. SUMMARISED GAS TRANSPORT PROPERTIES OF THE BOOM CLAY.....	130
TABLE B-8. HYDRAULIC CONDUCTIVITY DATA	131
TABLE B-9. THERMAL CONDUCTIVITIES FOR CLAYS AND CLAY MINERALS.	131
TABLE B-10. LINEAR THERMAL EXPANSION COEFFICIENTS	131
TABLE B-11. VOLUMETRIC THERMAL EXPANSION COEFFICIENTS	132
TABLE B-12. SUMMARY OF ELEVATED TEMPERATURE STUDIES CONDUCTED IN BOOM CLAY.....	133

Acknowledgements

We would like to thank Fiona McEvoy for her invaluable comments on review.

1. Introduction

The Boom Clay Formation (here after referred to as the ‘Boom Clay’) is a candidate host formation for the geological disposal of radioactive waste in the Netherlands. A benefit in the selection of the Boom Clay for investigation is the significant volume of research already conducted on this formation in Belgium, where the clay is currently the reference formation for the development of a safety case for a deep geological repository for radioactive waste. As such, a significant proportion of this research may be directly transferrable to the Dutch national programme. However, differences may occur as a result of the increased depth of burial of the formation in the Netherlands when compared to Belgium. In this report, we present an outline of the known properties of the Boom Clay and discuss the potential influence of depth and location on these properties. A list of symbols and abbreviations used is given in Appendix A. Chapters 2 and 3 examine the geotechnical and mechanical properties of the clay, respectively. This is followed by discussion of fluid flow behaviour (Chapter 4), including hydraulic, coupled and multi-phase flow, before considering the impact of elevated temperature conditions expected in a deep geological repository (Chapter 5). Though not the primary focus of this report, chemical and biological processes are also discussed briefly in Chapters 2, 3 and 6.

This report presents an assessment of the current understanding of the Boom Clay, with reference to the Dutch disposal concept. Observations are intended to be illustrative, as opposed to exhaustive. It should be noted that no new experimental work has been conducted for the purposes of this study and, where identified, knowledge gaps are highlighted in recommendation boxes and Chapter 7 (conclusion). In the following sections within this chapter, we discuss the background behind the Dutch concept in brief, and the geological history of the Boom Clay.

1.1. The disposal concept in Boom Clay investigated in OPERA

In the Netherlands, current policy on the treatment of radioactive waste involves a period of interim storage (of at least 100 years), prior to its disposal. The disposal concept for the deep geological disposal of Dutch radioactive waste (low- and intermediate-level waste, (LILW), Technologically Enhanced Naturally Occurring Radioactive Materials (TE), Naturally Occurring Radioactive Material (NORM) and high-level waste (HLW)) is based on the Belgium Supercontainer Concept (Verhoef, 2011) as well as other concepts for disposal in clay. In the Boom Clay concept it has been proposed that the waste would be disposed of in a formation with a thickness of around 100 metres. In contrast to the Belgian concept, the proposed dimensions of containers and disposal drifts are smaller, primarily a result of the amount and characteristics of the waste produced in the Netherlands, as well as the requirement for retrievability of the waste. Because of the probability of future glaciations in the Netherlands, a disposal depth of 500 m has been proposed in order to mitigate the impacts of glacial processes, including erosion.

Within Europe, several national disposal concepts propose the use of a clay-rich, sedimentary host rock (e.g. Belgium, France and Switzerland). However, the individual characteristics and properties of a specific candidate host must be carefully considered when designing a disposal facility and developing the associated safety case. A number of favourable characteristics common to clay formations are particularly advantageous for a potential host, including:

- Low permeability;
- Chemical buffering capacity;
- Geochemical characteristics that favour low solubility of radionuclides;

- High capacity to retard the migration of radionuclides towards the accessible environment, e.g. through sorption capacity and diffusion-dominated transport.

Additional beneficial characteristics specific to the Boom Clay include the presence of low hydraulic gradients (Vis and Verweij, 2014) and a propensity for plastic deformation, resulting in rapid self-sealing of fractures and void spaces. A significant body of information already exists on the Boom Clay in Belgium. The vast majority of studies relate to research conducted at (and material removed from) the Underground Research Laboratory (URL), HADES, at a depth of approximately 220 m beneath Mol, Belgium.

1.2. Geological setting

The geological and hydrogeological setting of the Boom Clay in the Netherlands has been summarised in (Vis and Verweij, 2014) and that in northern Belgium by Beerten and Leterme (2012). These papers are only briefly summarised here.

The Boom Clay (usually referred to as the Rupel Clay in the Netherlands) is of lower Oligocene (ca 28 to 34 Ma) age and forms part of the Rupel Formation. In the Netherlands the Rupel Formation has been subdivided into the Vesseem, Rupel Clay and Steensel members (Wong et al., 2007). These members are diachronous, with both the basal Vesseem and the overlying Steensel members being sandy marine deposits (Vis and Verweij; 2014) laid down close to the palaeo-shorelines. The Boom Clay is a pyritic, grey to dark brown marine clay with septarian (carbonate rich) concretions. Towards the basin margins the clays grade into sands. The formation reaches a maximum thickness of up to 250 m, with a mean thickness of around 65 m, and dips gently towards the north-east at between 1 and 2°. The formation is present beneath most of the Netherlands, both on- and off-shore, up to a depth of approximately 1500 m. Only in the Maastricht area, where older rocks crop out, is it completely absent. It is not a suitable host rock for radioactive waste disposal in all areas, because of its insufficient thickness (<100 m) or sand-rich composition.

1.3. Burial history of the Boom Clay

During the Oligocene the Netherlands was located close to the southern rim of the north-west European Paeleogene Basin and was almost fully under the influence of the Paeleogene North Sea. In this area distal marine clays merged into marine sands and clays, deposited closer to the coastline. The most complete Oligocene sedimentary sequence can be found in the Dutch-Belgian-German border area. Boreholes drilled for oil, gas and coal exploration, hydrological investigation and for research purposes, provide an insight into the depths and distribution of the Boom Clay in the Netherlands. However, the south and south-east of the Netherlands has been more fully explored than the north.

Nickel (2003) used correlation of borehole profiles to estimate the Boom Clay depth and thickness for most of the Netherlands. The Boom Clay is shallowest in the west (Hellevoetsluis-1) and south-east (Broekhuizenenvorst 52E/114) with a depth of 350 m and 416 m, respectively. The deepest the Boom Clay is found in the Asten-1 and Veldhoven-1 boreholes, with depths of 1317 m and 1122 m, respectively. This indicates that the deepest deposits of the clay have been buried close to 1.4 km beneath sea level.

The Boom Clay was mainly buried as a result of continuous sedimentation within the North Sea Basin during the Oligocene and into the Chattian. Deposition episodes for the overlying strata were disrupted by a small tectonic uplifting/tilting event at about 27 Ma, which led to some erosion of sand layers deposited onto the Boom Clay. This event resulted in about 30 m of erosion of strata overlying the Boom Clay at Mol in the north Belgium area (De

Craen et al., 2012). In this area there is no current evidence for a subsequent uplift (De Craen et al., 2012).

In the Antwerp area burial history is more complex with evidence of several uplift events (at circa 28.5, 27, 15 and 2 Ma) resulting in several phases of erosion, with an estimated maximum exhumation of about 60 m and several subsequent re-burial/exhumations of up to nearly 40 m (Beerten et al., 2013). In the deeper parts of the marine basin these events, if affecting this area, are likely only to have resulted in shallowing of the covering sea with little or no erosion of the sedimentary deposits.

1.4. Ice cover

At least parts of the Netherlands have been glaciated during the Quaternary (see for example Ehlers, 1990; Laban et al., 2011). The greatest extent of ice for which significant evidence has been identified is the older Saalian advance, which covered a large area of the Netherlands. However, an exception to this was the southwest region, reaching approximately to The Hague in the west and the Dutch/Belgian border in the south-east (Ehlers 1990). This maximum is dated at about 140 Ka (Lambeck et al., 2006; Pierik, 2010). Earlier glaciations resulted in ice cover in parts of the Netherlands, including the Elsterian (478 to 424 Ka) (Laban et al., 2011), which extended into northern parts of the country. However, none of the glacial advances since the older Saalian has resulted in ice cover on the current territory of the Netherlands (Lambeck et al., 2006). While it is possible that glaciations prior to the Elsterian had extents similar to, or even greater than, that attained during the older Saalian, conclusive evidence is currently lacking.

Estimates of ice thickness are sparsely available in the literature. The lowland continental ice sheets over the Netherlands would have been relatively thin. Ice thickness models provided by Lambeck et al. (2006) for the older Saalian maximum ice advance show regular ice thickness increase from 0 m at the ice front (roughly aligned between about The Hague and Venlo in the south) to about 700 m around Groningen (in the north of the country), increasing to around 1200 m around Kiel. Because the ice cover during other glacial maxima has been less extensive, these estimates are likely to be the maximum thickness of ice to have been present in on-shore areas of the Netherlands. Lower sea levels during glaciations and the relatively shallow nature of the North Sea in territorial waters of the Netherlands may have resulted in slightly thicker ice cover in off-shore areas. In the absence of other evidence, the Saalian estimates of ice cover thickness can be regarded as maximum past ice thickness in the Netherlands.

1.5. Stress conditions

In order to discuss the translation of known characteristics of the clay at HADES to the Dutch concept, it is first necessary to define the stress conditions from which this data has been derived.

Table 1-1 shows regularly quoted stress conditions for the Boom Clay at HADES, from which the majority of reported measurements relating to the Boom Clay have been collected. Reported effective vertical stress values are generally around 2.2-2.4 MPa. The conditions measured at Mol, generally relate to an *in situ* site depth of 223 m.

For the purposes of this report, reference pressure conditions for a Dutch Boom Clay repository have been selected (Table 1-2), so as to compare with HADES. These have been calculated based on a repository depth of 500 m, as well as for a shallower and deeper case (400 m and 600 m respectively), to allow for uncertainty in relation to burial history

and glaciation. The vertical stress (σ_v) was estimated using a density of overlying the Boom Clay of 2.03 g.cc⁻¹.

Pore pressure was estimated from a hydraulic gradient assuming an overlying density of 1 g cc⁻¹. A minor stress anisotropy has been observed at Mol in Belgium, such that the horizontal stress components (σ_H and σ_h) have been recorded to be 0.9 σ_v (Bernier et al., 2007). For the purposes of this report it has been assumed that this is consistent in the Netherlands. The resulting estimated total effective stress for a depth of 500 m is estimated as \approx 4.3 MPa. For a depth range between 400-600 m, the likely value for total effective stress lies in the range of 3.4 to 5.2 MPa, respectively. These values have been used within this report to make inferences about the likely mechanical and transport behaviour of the Boom Clay at depths appropriate to the Dutch disposal concept.

Parameter	Symbol	Units	Bernier <i>et al.</i> (2007)	Bastiaens <i>et al.</i> (2006)	Mertens <i>et al.</i> (2004)
Total vertical stress	σ_v	MPa	4.5	4.5	4.6
Effective vertical stress	σ'_v	MPa	2.25	2.3	2.4
Pore water pressure	P_w	MPa	2.25	2.2	2.2

Table 1-1. Stress conditions at the HADES URL.

Parameter	Symbol	Units	223 m	400 m	500 m	600 m
Total vertical stress	σ_v	MPa	4.4	8.0	10.0	11.9
Total effective stress*	σ_{eff}	MPa	1.9	3.4	4.3	5.2
Pore water pressure	P_w	MPa	2.2	3.9	4.9	5.9

*Values are calculated based on a linear extrapolation with depth, from differential stress measured at Mol.

Table 1-2. Reference stress conditions used in this report.

2. Baseline characteristics

A well-defined understanding of the baseline geotechnical characteristics of the Boom Clay is crucial before considering the influence of burial. These properties, as well as mineralogical composition, are key controls on the thermo-hydro-mechanical behaviour of the material (Cui and Tang, 2013; Delage et al., 2009; Tsang et al., 2012). Since the construction of the URL at Mol, the geotechnical properties of the formation have been extensively characterised. Testing at the field-scale (Bastiaens et al., 2004; Mertens et al. 2004; Gens et al., 2007; Wemaere et al., 2008; Chen et al., 2011; Areias et al., 2012) has involved in-situ experiments (hydrofracturing, dilatometer tests, etc.), visual observations and geophysical measurements/monitoring (e.g. resistivity, gamma ray logging, seismic, ultrasonics, microseismic, etc.). In addition, an extensive range of laboratory tests have been conducted to examine the physical properties of the Boom Clay, including triaxial, oedometer and isotropic consolidation tests. Specific analyses conducted to investigate baseline geotechnical properties also include standard methodologies, such as drying and wetting tests, X-ray Diffraction (XRD), Mercury Injection Porosimetry (MIP), Brunauer-Emmett-Teller analysis (BET) and extensive 2-D and 3-D imaging.

In this chapter, we summarise the primary baseline characteristics of the Boom Clay, as described in the literature.

2.1. Composition

The composition of the Boom Clay is a fundamental control on many of the key physical/chemical properties described in the following chapters. Whilst, mineralogical composition has been extensively characterised in Belgium (Volckaert et al., 1994; De Craen, 1999; Wouters et al., 1999), less evidence is available in relation to the formation in the Netherlands, though recent efforts are being made in this area (Koenen and Griffioen, 2014).

At Mol, the Boom Clay consists mainly of mixed clay and silt, with additional minor sand (Bernier, 1997). Mineralogical composition of the Boom Clay is widely reported (**Appendix Table B-1**), predominantly assessed using XRD. The clay content is generally reported to vary from between 23 and 60 % of the bulk material composition and is predominantly made up of illite, smectite and kaolinite, which is often seen in interlaminated zones (Blanchart et al., 2012; Dehandschutter et al., 2004; Wemaere et al., 2008; Yu et al., 2012). The non-clay fraction of the Boom Clay primarily consists of quartz, again widely reported to vary between 23 and 60 %. The remaining percentage of the non-clay fraction consists of feldspars, calcite and pyrite.

Whilst lithological differences may influence the widely varying quantitative mineralogies reported in the literature, Honty and De Craen (2011) attribute much of this inconsistency to the ‘application of various methodologies, often suffering from low resolution, absence of standardized procedures and independent verifiers’. In order to address these concerns, they used a new methodological approach (Zeelmaekers, 2011), requiring internal standards and additional quantitative controls, to produce an updated and refined mineralogical composition of the Boom Clay. The resulting ‘reference’ composition for the Mol site is given in **Appendix Table B-2**. Whilst in some specific zones within the formation it may be possible to measure a quantitative mineralogical composition out with these ranges (for example, in calcareous-rich layers), these layers can be considered as unrepresentative of the Boom Clay in general (Honty and De Craen, 2011).

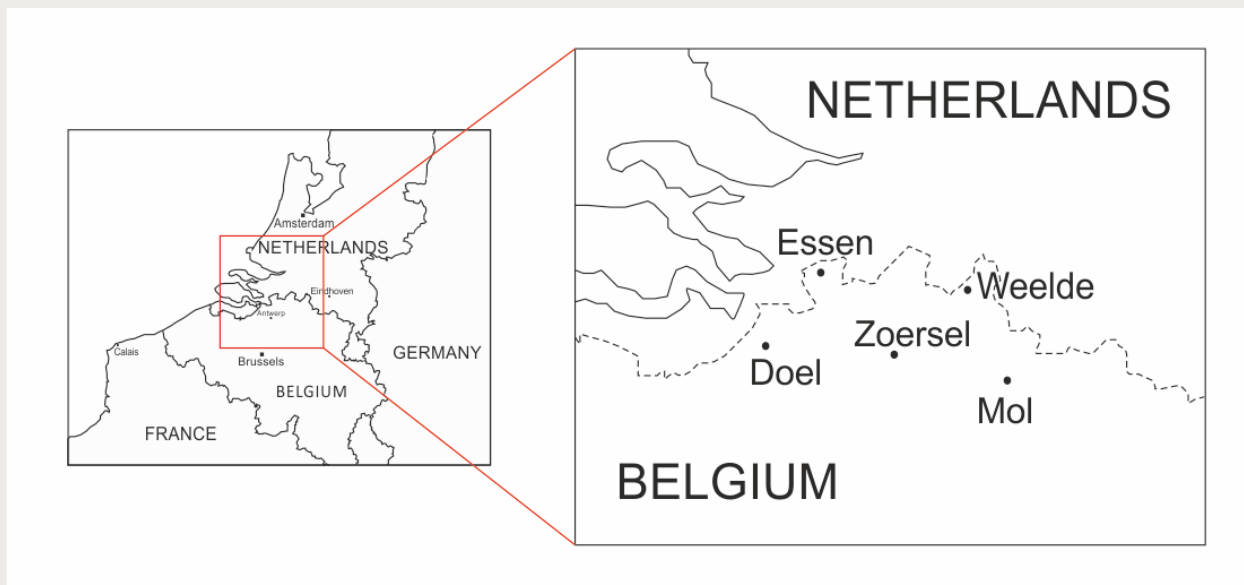


Figure 2-1. Borehole locations near the Netherlands-Belgium border.

Comparison of quantitative mineralogies to this reference composition, have indeed confirmed the presence of horizontal and vertical variation of mineral species present in the Boom Clay. Honty and De Craen (2011) observed that such variations in the vertical direction resulted primarily from layered alternations between more silty clay and clayey silt, as past sea level fluctuated. Such variation is primarily made apparent by variable quartz and total clay content and correlates with an associated coarsening and fining as a result. On a regional scale, quartz content was observed to increase with proximity to the palaeocoastline (inland), whilst clay content decreased further inland and increased in more distal regions. Nevertheless, the authors argue that from a mineralogical perspective, the Boom Clay can generally be considered as a homogeneous sediment on a regional scale, as the same overall qualitative mineralogical composition is found in the Boom Clay samples from various boreholes in the Campine Basin, as well as in outcrop.

This finding is contrary to the conclusions of Deng et al. (2011), who compared the mineralogical composition of the Boom Clay at Mol to material derived from a borehole at Essen (Figure 2-1). Quantitative methods are not described in detail, but the authors infer a higher carbonate content in samples from Essen, based on measured Methylene Blue concentrations (MB). A high degree of variability within the Essen samples was noted, reflected in the measured quartz content. In the absence of a larger dataset, it is difficult to draw conclusions relating to regional heterogeneity. Without additional data it seems just as possible that these observations relate to the small scale variations described by Honty and De Craen (2011) and do not represent large-scale deviations from the reference composition. Wemaere et al. (2008) studied vertical profiles of several boreholes located at Doel, Zoersel, Mol and Weelde, all located across the north of Belgium (Figure 2-1). Like Honty and De Craen (2011), they also report that, despite apparent small scale heterogeneity, the Boom Clay can be considered as reasonably homogeneous on larger scales.

The mineralogy of the Boom Clay in the Netherlands has also recently been examined as part of the OPERA (*Onderzoeks Programma Eindberging Radioactief Afval* programme, the third Dutch research programme tasked with investigating the geological disposal of high, as well as low, level radioactive waste in one facility (Koenen and Griffioen, 2014). A primary aim of this study was to investigate lateral and depth-related heterogeneity, with

reference to results from the Belgian Boom Clay. In total, 152 samples were taken from 17 cores, retrieved across the Netherlands, and geochemical and grain size analyses were performed. As with recent Belgian studies, analysis was conducted using the advanced approach of Zeelmaekers (2011). The resulting observations display a notable degree of variability, predominantly in relation to clay, quartz, carbonate and pyrite contents.

On a regional scale, statistical analysis indicates three distinct groups. In the southern part of the Netherlands the formation has coarser, silty upper and lower parts, whilst the central part is more clay-rich, finer grained and with occasional silty layers. The authors suggest that this is consistent with the cyclic alternation between clay- and silt-rich layers observed in Belgium (Honty and De Craen, 2011). A notably higher carbonate content is observed in samples from the south-east of the Netherlands, as compared to those from the south-west. Finally, the samples taken from the north of the Netherlands are described as significantly different from both the south-east and south-west, where the Boom Clay is fine grained and clay- and carbonate-rich throughout the total depth interval. It should also be noted that, whilst the Belgian clay samples were all found to have a carbonate content of ≤ 1.2 wt%, some Dutch samples were found to have up to 26 wt% carbonate. Pyrite content was also observed to vary considerably throughout the formation, though no geographical or depth-related dependence was detected.

2.1. Pore fluid chemistry

A sound knowledge of the pore fluid chemistry within a host formation is crucial to predicting the evolution of a deep geological repository. In particular, the capacity for clays to swell and the associated impact on other physical properties (e.g. hydraulic conductivity) may be directly influenced by the pore fluid chemistry present. This form of chemico-mechanical coupling is discussed in further detail in Chapter 3, Section 3.3.7.

In low permeability formations, pore fluid may exhibit significant chemical gradients resulting from the low transport capacity of the material and it is, therefore, necessary to understand the degree of variation within a candidate host rock. A number of techniques are available to determine characteristics such as composition, pH and salinity within clay-rich formations. These include *in situ* piezometer recovery or extraction from clay specimens by chemical leaching or ‘pore squeeze’ under pressure.

Extensive work has been conducted at the HADES laboratory in order to characterise the pore fluid composition within the Boom Clay, which can be considered as a NaHCO_3 solution, containing a significant proportion of dissolved organic matter (De Craen et al. 2004b). Pore water pH for HADES is reported to be in the range of 8.3 - 8.6 with a maximum redox potential of around -270 mV. A detailed analysis of pore fluid data for the formation was conducted by De Craen et al. (2004b) and a reference pore water composition defined for HADES (**Appendix Table B-3**). Given the importance of fluid chemistry on the behaviour of clay-rich materials, it is crucial that transport and mechanical testing is conducted using water in equilibrium with the test material and this reference composition is generally used in such studies. However, it should be noted that, in reality, the reference pore water composition only represents a small range of the pore water chemistries encountered (De Craen et al. 2004b). Statistical analysis conducted by De Craen and co-workers highlighted some variations in pore fluid chemistry with depth within the formation. These differences were attributed to spatial variability in pCO_2 and pH, the controls on which are not yet entirely clear. Whilst lateral variations in pore water composition are less ambiguous at a local scale, more significant changes are observed on a regional scale, where the influence of seawater was noted towards the West of Belgium

Given that transport within the Boom Clay is diffusion-dominated, similarities in pore fluid composition in the Netherlands might be expected, though the observations of De Craen et al. (2004b) do indicate that important differences (particularly in relation to salinity) are likely for locations and depths relevant to the Dutch disposal programme. As such, detailed analysis of pore water will be necessary in order to fully assess any effects on the favourable host properties, as part of the development of a future safety case.

2.2. Geotechnical properties

The physical response of a clay to an applied stimulus (e.g., change in stress state, temperature, the presence of gas, etc.) is heavily controlled by its material characteristics at the microscale. In particular the form and distribution of the material's constituent grains, and the associated percentage void and resulting distribution, are key impactors on mechanical, transport and thermal response. The following sections briefly describe these characteristics for the Boom Clay in Belgium as well as recent work in the Netherlands. A summary of relevant geotechnical properties found in the literature is given in **Appendix Table B0-4**.

2.2.1. Bulk and dry density

The measured density of clay is highly dependent on saturation state and is therefore usually determined specifically including or excluding water content. Standard geotechnical studies therefore generally report density in terms of the bulk and dry densities.

Bulk density, ρ_b , is defined as the total mass (inclusive of water) per unit volume:

$$\rho_b \text{ (g/cm}^3\text{)} = \text{Total mass (g)}/\text{Total volume (cm}^3\text{)} \quad \text{Equation 2-1}$$

In order to account for the presence of water, the dry density, ρ_d , of a clay is taken to be the mass of the solid phase only, per unit volume:

$$\rho_d \text{ (g/cm}^3\text{)} = \text{Mass of solids (g)}/\text{Total volume (cm}^3\text{)} \quad \text{Equation 2-2}$$

To determine the *in situ* bulk density of a clay, laboratory samples must first be allowed to fully saturate with water, before being weighed. In the radioactive waste disposal sector, the standard geotechnical approach for determining dry density requires weighing a sample which has been first heated to 105 °C for greater than one day.

Measured dry densities for the Boom Clay generally range between 1.5 and 1.7 g/cm³, and the most regularly reported values are in the 1.64-1.67 g/cm³ range (**Appendix Table B0-4**). Bulk densities in fully saturated samples mostly fall between 1.9 and 2.1 g/cm³, with a typical value at around 2.03-2.05 g/cm³. These values are consistent with the moderate degree of compaction that the Boom Clay has undergone (Bertrand et al., 2009; Chapter 1). As density is directly related to porosity and mineral content, some variation in these properties can be expected as quartz content varies. This is also likely to be the case in the Netherlands, though variations in pyrite content and the presence of higher carbonate content in some regions may also have a significant impact.

2.2.2. Porosity

Porosity is a measure of the proportion of total volume of voids, V_p , to the bulk volume of a rock, V_b , and is generally defined as:

$$\varphi_t = \frac{V_p}{V_b} \quad \text{Equation 2-3}$$

Alternatively, the total porosity can also be described as a function of the bulk density, ρ_b , and the average grain density of the mineral solids, ρ_s :

$$\varphi_t = \left(1 - \frac{\rho_b}{\rho_s} \right) \quad \text{Equation 2-4}$$

The proportion of voids to bulk rock is also often commonly expressed in terms of the void ratio, e :

$$\varphi_t = \frac{e}{(1+e)} \quad \text{Equation 2-5}$$

These parameters relate to the proportion of all voids within a rock. However, in reality not all existing porosity will be interconnected, such that the transmission of fluids is allowed through the bulk of the rock mass. As such, an additional term may be introduced, relating the total volume of the accessible porosity, V_a , to an ‘effective porosity’, φ_e , such that:

$$\varphi_e = \frac{V_a}{V_b} \quad \text{Equation 2-6}$$

In the case of argillaceous materials, it is particularly important to acknowledge the presence of accessible and inaccessible porosity, since these values may differ significantly. The determination of effective porosity within clay-rich materials is not trivial, due in part to the exceptionally small pore throat radii and the current detection limit of standard 3D imaging techniques. The task is complicated further by the involvement of complex clay-water interactions near clay mineral surfaces, leading to the presence of water in a variety of forms:

- strongly adsorbed water within the sheet structure of clay minerals;
- strongly adsorbed water on the clay mineral surface;
- loosely held water in the diffuse-layer;
- free water.

As such, the degree of perceived porosity may vary depending on the approach used and its ability to access each of these forms of water. A conventional soil mechanics approach is to define porosity in relation to the degree of water removed by oven heating test material to a temperature of 105°, for a period greater than one day. However, other methods may also lead to the removal of adsorbed water and variations between techniques must therefore be considered when comparing datasets. Geotechnical characterisation is focussed on the determination of bulk properties at the laboratory scale, but it is important to be aware of additional factors impacting effective porosity at the field scale, including the influence of larger-scale heterogeneity in porosity distributions and the presence of macrofractures and other deformation textures within the rock mass. This latter factor, and the influence of mechanical state, is discussed further in Chapter 3.

Porosity is directly related to grain morphology and distribution, but these factors are strongly controlled by environmental influences including *in situ* stress conditions and pore

fluid chemistry (discussed in Chapter 3). **Appendix Table B0-4** shows example porosities for the Boom Clay at Mol from the published literature, measured using standard geotechnical techniques, which generally range from around 35-45%. These values are relatively high for a sedimentary repository host formation and reflect the relatively small degree of burial previously experienced (see 3.3.3). A typical value for porosity at HADES depths (223m) is ~39%.

Significantly less data is available relating to the geotechnical properties of the Boom Clay in the Netherlands. In a recent study (conducted by TNO as part of the OPERA programme), a compilation of porosity datasets relating to the Boom Clay in the Netherlands is given (Vis and Verweij, 2014). Studies covered include work conducted by Rijkers et al. (1998), Wildenborg et al. (2000) and Wiers (2001) and are taken from boreholes at several locations. Porosities reported by Rijkers et al. (1998) and Wiers (2001) range between 32 and 47% and are generally higher than those measured at Mol. This is as would be expected, given the shallow depth of recovery for these boreholes (between 18 and 47m). The impact of burial and compaction processes on porosity/void ratio is discussed in greater detail in Section sections 3.2.1 and 3.3.3.

Observations by Wildenborg et al. (2000) relate to greater depths within the formation, with values of 32% and 27% measured for depths of 738-888m and 1415-1495m, respectively. These values represent rare direct measurements within the deeper parts of the formation in the Netherlands. However, there is some suggestion that core preservation may have impacted sample preservation and additional recovery of fresh core at a future date will help increase certainty in these values. Data given by Deng et al. (2011) hints at a potential correlation between carbonate content and reduced void ratio, which cannot be explained by stratigraphic changes in carbonate content with depth. However, more data is required to demonstrate any relationship with confidence and to discount the potential for carbonate to be associated with other porosity controlling minerals. In reality, porosity and the associated pore-network-distribution, are heavily influenced by small scale lateral and vertical mineralogical variations within the formation and are discussed in further detail in Section 2.3.

2.2.1. Particle density and specific gravity

Whilst dry density provides an estimate of the mass of solids per unit volume, within a clay, a number of quantities are also used which define density with reference to another known material. In particular, the mass of a given volume of clay, normalised with respect to the mass of the same volume of water, is termed the specific gravity, G_s , of the material. As such, the mass of the solid volume can be described as:

$$M_s = G_s \rho_w \quad \text{Equation 2-7}$$

where ρ_w = the density of water.

Another commonly used term is the particle density (ρ_s), which is defined as the mass per unit volume of the solid particles, or:

$$\rho_s = G_s \rho_w \quad \text{Equation 2-8}$$

The mostly regularly reported value for G_s at HADES, is 2.67 g/cm³, although only a relatively small degree of variability is observed, even for samples retrieved from reasonably disparate locations and depths (**Appendix Table B0-4**). Specific gravity values in the 2.6-2.7 g/cm³ range are typical for clay-rich materials and the Boom Clay from the Netherlands is unlikely to depart far from the measured values reported in Belgium.

2.3. Grain scale characteristics

The clay-content and associated pore size distribution within a rock or soil will strongly influence the dispersal of both stored and free water. Pores can be broadly split into the following three scale-based groups:

- Micropores, <2 nm;
- Mesopores, 2-50 nm;
- Macropores, >50 nm.

The distribution of pores within the Boom Clay at HADES has been extensively characterised using a variety of techniques, predominantly involving either injection (e.g., Mercury Injection Porosimetry (MIP), N₂ adsorption/desorption) or imaging of the sample (Scanning Electron Microscopy (SEM), Environmental Scanning Electron Microscopy, Transmission Electron Microscopy, Computed Tomography Scanning). One conventional approach is the use of MIP (Romero et al., 1999; Dehandschutter et al., 2004; Hildenbrand et al., 2004; Lima et al., 2012b), where an absolute pressure is applied to the pores using a non-wetting fluid (mercury). Dehandschutter et al. (2004) conducted MIP on intact samples from HADES and concluded that the majority of pores have radii in the order of 0.01 µm, with an estimated connected porosity (for intruded mercury) of approximately 28%. Lima et al. (2012b) also carried out MIP on material taken from HADES and observed a mono-modal pore size distribution, instead peaking at a pore size of around 0.09 µm.

In order to examine the effect of compaction on pore size distribution, Romero et al. (1999) carried out MIP on re-constituted the Boom Clay samples. Clay was pre-compacted to a low density (13.7 kNm⁻³) and a higher density (16.7 kNm⁻³). The measured pore size distributions for the higher density sample were observed to be tri-modal in nature, clustering around peaks at 10 µm, 2 µm and 50 nm. In contrast, the lower density sample exhibited a bi-modal distribution with pore sizes peaking at approximately 0.7 µm and 20 nm. The authors also conducted SEM imaging to examine clay fabric evolution and investigated the main wetting/drying paths of reconstituted samples. In describing their findings they argue for the presence of two main pore size regions: (i) an inter-aggregate porosity which responds to loading by a reduction in the interconnected macroporosity, affecting free water present, and (ii) an intra-aggregate porosity, relatively insensitive to loading processes. Their observations very clearly demonstrate that the degree and distribution of porosity within the Boom Clay is strongly related to its compaction history.

However, there are some notable disadvantages to the MIP approach when applied to argillaceous materials (Schlomer and Kroos, 1997). For example, the impacts of sample drying during storage and preparation cannot be neglected since sample damage and shrinkage-related cracking may occur as a result (Desbois et al., 2014). The MIP technique is also constrained in its application to clay-rich materials by the capacity of the apparatus to enter the smallest of the pores present within the clay (Romero and Simms, 2008).

Whilst MIP has the potential to resolve pore scale characteristics of the order of 7 nm-400 µm (meso- to macro-scale), the derivation of N₂ adsorption/desorption isotherms (N₂-BJH or N₂-BET) may be considered more suitable for investigating micropore characteristics (in the range of 0.3 nm-300 nm) within clay-rich materials. This method involves exposing a degassed sample to nitrogen at a series of precisely controlled pressures. The volume of adsorbed gas is measured at these specific pressures and the gas-adsorption isotherm is inverted for the Specific Surface Area (S₀) of the material (Brunauer et al. 1938). Hildenbrand et al. (2002) used this approach to analyse three Boom Clay samples from Molenbeersel (taken from a depth of 1053-1057 m) and one from Mol at 220 m. Their

findings indicate a lower specific surface area from the samples taken from the greater depth interval (20.1, 23.6 and 20.6 m²/g), as compared to at Mol (48.2 m²/g). This is to be expected given the greater depth of burial and indicates that, assuming a similar mineralogical composition and grain size distribution, a sample taken from the formation at 500 m depth within the Netherlands, may yield S₀ values between these two end members.

Nevertheless, limitations to this approach remain. In particular, inaccessible porosity cannot be accounted for and sample damage during preparation (and resultant desiccation) cannot be excluded. Similar limitations also exist in the application of SEM imaging. However, recent advancements in ion milling techniques (e.g., Broad Ion Beam (BIB) and Focused Ion Beam (FIB)) have led to extensive nm-scale studies under wet conditions (using cryogenic stabilisation) and allowing 3-D reconstruction of both inaccessible pore spaces and interconnected porosity.

Desbois et al. (2010) examined samples of the Boom Clay from the Mol site (Belgium) using cryo-SEM, with ion beam cross-sectioning, to prepare smooth, damage-free surfaces. They used image analysis software to compare porosity characteristics of both dry and wet samples and found that for both, the pore size distribution is unimodal; 87% of pores being of equivalent radius <100 nm. However, the total measured porosity for dry and wet samples was found to be 26.3 % and 20.4 %, respectively. In addition, the authors found that 40 % of the total porosity within the clay, resulted from pores with a radius < 100 nm. More generally, observed porosity fabrics were seen to be highly anisotropic and a close preferential alignment was found between bedding and pore orientation. Their findings were also indicative of a fractal scaling to the pore size distribution.

Further work, using BIB cross-sectioning has allowed further extensive characterisation of the Boom Clay from Mol in recent years. Findings from Hermes et al. (2011) indicate that finer-grained (higher clay content) samples show lower porosities than coarser-grained (lower clay content) material. As such, they suggest a correlation between porosity, pore size distribution and mineralogy, as well as to grain-size distribution. Comparison of BIB-SEM observations and MIP measurements also highlights a clear difference in assessed porosities (Hermes et al., 2013); 10-20% from BIB-SEM (total), as opposed to 27-35% from MIP (interconnected). Hermes et al. (2013) attribute this discrepancy to resolution limitations of the BIB-SEM approach, as well as the requirement for small sample to under-represent larger-scale characteristics.

In order to provide a cross-scale analysis of the Boom Clay pore network in 3D, Hermes et al. (2015) applied data from X-ray μ -CT, FIB-SEM and BIB-SEM in combination. They use this approach to present a well-quantified conceptual porosity model for the Boom Clay at HADES URL depths. Nevertheless, such models are not yet able to account for the impact of applied stress state and the resulting influence of mechanical and chemical compaction/swelling and associated changes in the degree of bonded to free water within the clay.

Whilst limited information is available on the bulk porosity of the Boom Clay in the Netherlands, data detailing the pore distribution is scarce. Further research will be required in order to determine whether understanding of typical pore networks quantified at Mol translates well to those in other parts of the formation.

2.4. Baseline characteristics summary

The baseline characteristics of the Boom Clay have been well defined in Belgium, particularly within the vicinity of Mol, but also increasingly on a regional scale. This work

includes compositional studies (leading to the development of reference mineralogies and pore fluid chemistries), geotechnical characterisation and grain-scale analyses. Similar work has begun for the formation in the Netherlands, but many fundamental questions remain. Particular uncertainties relate to potential differences in pore fluid chemistry and burial history, directly impacting the geotechnical characteristics and, hence, the hydromechanical properties of the clay. Whilst many characteristics of the formation in Belgium and the Netherlands are expected to be highly similar, some notable variability between the two regions seems likely. Such uncertainties are currently hindered by the absence of the Boom Clay core in a high preservation state.

Recommendations

- Recovery of well-preserved core from appropriate locations and depths would provide
 - Reduced uncertainty relating to geotechnical characteristics;
 - Likely limits on expected pore fluid chemistries;
 - An improved understanding of the impact of lithological differences on geotechnical characteristics (e.g. the influence of carbonate content on void ratio);
 - An improved understanding of the burial history of the region and associated impacts on geotechnical properties of the clay.

3. Mechanics

The mechanical properties of a host formation are fundamental to the development of a geological facility, from the initial construction and closure phases, through to the long-term system evolution, post-closure. In this chapter, some fundamental concepts are described (Sections 3.1 and 3.2), followed by current understanding of the Boom Clay mechanics and structure, as well as implications for the Dutch concept (Sections 3.3 and 3.4).

3.1. Fundamental concepts

3.1.1. Stress / strain relationship

Stress is a measure of force per unit area. It is described in terms of the SI unit, pascals (Pa), where one pascal is created by the force (F) of one Newton acting on an area (A) of one square metre (**Equation 3-1**). However, stresses within the Earth are generally several orders of magnitude larger than the pascal and so are more conventionally reported in geoscience as megapascals (MPa) where 1 MPa = 10⁶ Pa.

$$\sigma = \frac{F}{A} \tag{Equation 3-1}$$

As an applied stress has direction, as well as magnitude, it is a vector quantity. Generally, the stress field applied to rocks in the crust is heterogeneous, resulting from a vertical load applied by the weight of the overlying rock, which is partially transmitted in the horizontal sense (the Poisson effect). Further complexity in this stress field is introduced by material anisotropy, the presence of additional tectonically-induced stresses, geological discontinuities and other heterogeneities. As such, the resulting stress state is most simply described in terms of the principal stress components; three orthogonal axes corresponding to the maximum (σ_1), intermediate (σ_2), and minimum (σ_3) stresses (**Figure 3-1**).

When directed onto a discontinuity, (e.g. a fault plane) principal stresses are generally defined in relation to the plane of the discontinuity (either parallel or perpendicular). As such, the component of stress perpendicular to the plane of interest is termed the normal stress (σ_N), and the component parallel to that plane is termed the shear stress (σ_t), as shown in **Figure 3-2**. Slip along the discontinuity is encouraged by larger shear stresses and discouraged by larger normal compressive stresses. Within the field of rock mechanics, the convention is for normal stresses to be taken as positive if compressive and negative where tensile. Sense of shear is used to define the sign for shear stresses.

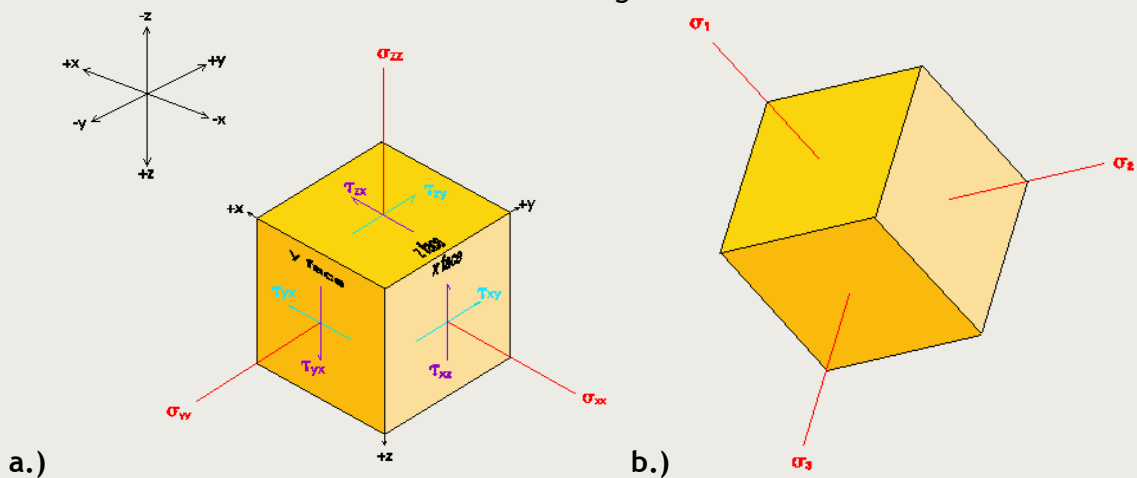


Figure 3-1. Three-dimensional coordinate system of a.) six-component stress tensor on an element cube in an isotropic medium, b.) rotation of the three-dimensional coordinate system so that it is parallel to the three principal normal stress directions (adapted from Priest, 1993).

The stresses that a rock is subjected to may cause it to deform. The degree of any resulting deformation may be quantified in terms of strain, ε , generally expressed in one-dimension as the change in length, Δl , of the material, in relation to its initial length, l_0 , such that:

$$\varepsilon = \frac{\Delta l}{l_0} \quad \text{Equation 3-2}$$

Alternatively, the volumetric strain can be found from the change in volume, ΔV , normalised with respect to the initial volume of the rock, V_0 :

$$\varepsilon = \frac{\Delta V}{V_0} \quad \text{Equation 3-3}$$

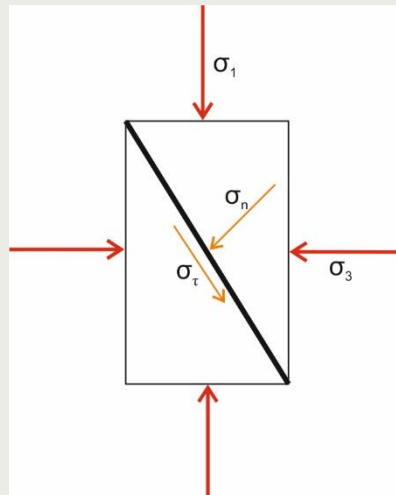


Figure 3-2. Description of forces acting on a discontinuity.

In situations where a complex stress field is applied to the material it is more appropriate to define both the applied stress state and the resulting strain response in 3 dimensions, using a 3-by-3 tensor (Jaeger, Cook and Zimmerman, 2009). This allows for simple translation of these quantities to any required components (e.g. horizontal and vertical stresses).

In order to assess the impact that applied stress conditions may have on a rock, we must also take into account the pressure exerted by fluid held within its pore spaces. This outwardly acting pressure is referred to as the pore pressure, P_p , and can be considered to oppose the principal stresses, creating an effective stress, σ_{eff} , which the rock experiences. As such, for a given applied total stress, σ_{total} , and P_p , the net effective stress is defined as:

$$\sigma_{eff} = \sigma_{total} - P_p \quad \text{Equation 3-4}$$

The introduction of pore fluid under pressure has a profound effect on the physical properties of porous solids (Hubbert and Rubey, 1961; Terzaghi, 1943). Strength is

determined not by confining pressure alone, but by the difference between confining and pore pressures. In simple drained tests, P_p remains constant and the observed effective stress is similar to the applied load. Conversely, if the pore fluid system is closed, P_p rises in proportion to the applied load as pore space is reduced, significantly lowering the overall effective stress. Thus, the mechanical response of rocks to applied load is significantly affected by the ability of fluids to drain. The mechanical response of rocks and clays, to an applied stress, is therefore impacted by the pore fluid pressure within the material, which can significantly not only affect the likelihood for deformation, but also the resultant mode of deformation. Such behaviour may occur by a number of mechanisms, which are described in more detail in the following sections.

Many rocks have been shown to follow the law of effective stress (**Equation 3-4**), including shale (Handin et al., 1963; Kwon et al., 2001) and sandstone (Byerlee, 1975; Cuss, 1999). Kwon et al. (2001) showed that the effective pressure coefficient is 0.99 ± 0.06 for Wilcox shale. This value is indistinguishable from unity and demonstrates that the law of effective stress is obeyed in this particular shale variety. The poro-elastic effect (after Biot, 1941) is added to the law of effective stress to account for the partial transfer of pore pressure to the granular framework. For the Boom Clay, Barnichon and Volckaert (2003) report a Biot's coefficient of 1.

3.1.2. Elastic deformation

A geological material subjected to an applied stress will initially respond with an elastic deformation. Such a response is not permanent and, by definition, must fully recover once the applied load has been removed. During loading, a linear relationship between the applied stress and the associated, temporary strain is expected. However, in an ideal elastic medium the net strain, as compared before and after an elastic deformation, is equal to zero.

The elastic response of a material can be defined in terms of a number of physical quantities, termed the elastic moduli. These quantities include Young's modulus (E), bulk modulus (K) and shear modulus (G), as well as an additional term known as Poisson's ratio (ν). These terms are defined and discussed in greater detail in Section 3.3.1. In a homogeneous material, the elastic constants will be equal in all directions. However, such homogeneity is uncommon in natural geological materials and the elastic constants in an argillaceous formation will be strongly anisotropic in relation to its fabric. Purely elastic responses are also rare in geological materials and perfect elastic behaviour may only occur at small strains.

3.1.3. Inelastic deformation

Inelastic deformation is defined as that which leads to permanent, irreversible strains in a loaded medium. Material properties will govern the point to which elastic deformation may occur within a rock or clay. This point is termed the elastic limit, beyond which inelastic deformation dominates. The resulting inelastic deformation may be plastic, brittle or ductile in nature, depending on the intrinsic material properties, the applied stress conditions and associated environmental factors (e.g. temperature). Some idealised stress-strain responses are given in **Figure 3-3**, highlighting different forms of inelastic response beyond the elastic limit. The following sections describe perfect plastic, brittle and ductile behaviour in greater detail, as well briefly providing an overview of the primary mechanisms for inelastic deformation.

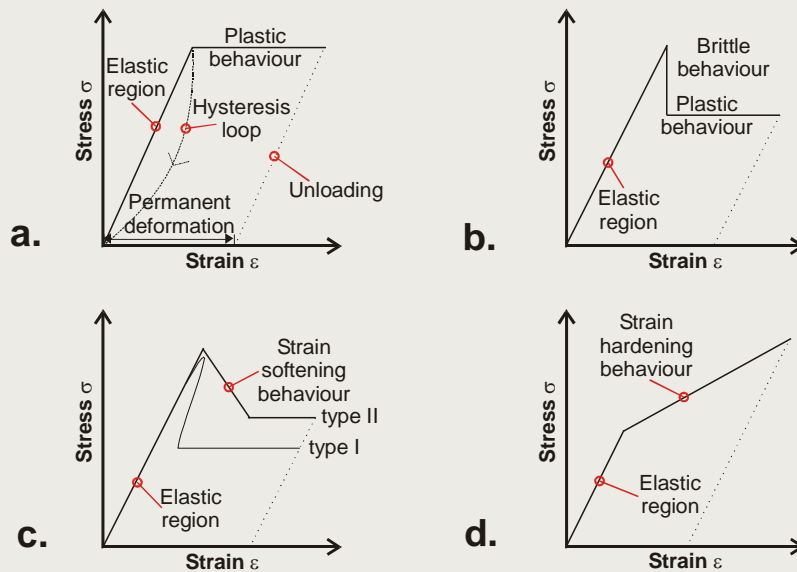


Figure 3-3. General response of rocks observed in the stress-strain space. a) Elastic-plastic behaviour. b) Elastic-brittle-plastic behaviour. c) Elastic-strain softening-plastic behaviour. Two types of strain softening are shown; type I is unstable and requires axial load to be relieved by the testing apparatus, whereas type II softens as axial displacement is increased. d) Elastic-strain hardening behaviour.

3.1.3.1 Perfect-plastic behaviour

Perfect-plastic behaviour initiates at a critical threshold of yield stress, permanent strain continuing rapidly and indefinitely while the magnitude of stress is maintained (Figure 3-3a). Granular media are among the best examples of plastic materials (Vardoulakis and Sulem, 1995). Generally, rocks are not perfect-plastic media, being subject to strain hardening or strain softening. Strain hardening results from granular inter-locking or porosity collapse, requiring increasing amounts of stress to continue strain. Strain softening results from granular fragmentation and bondage severance; less stress is required to continue strain at higher deformations.

The plastic behaviour of clays is described by index properties known as the Atterberg limits, which are reported in weight percent water. The plastic limit and liquid limit are, respectively, the water contents at which the material begins to exhibit plasticity or behave as a liquid. Plastic behaviour occurs only within a limited range of water content, defined by the plasticity index ($L_p = \text{liquid limit} - \text{plastic limit}$). Atterberg limits are strongly affected by clay mineral content, clay mineralogy, particle sizes, and the degree of aggregation of clay particles. Wroth and Wood (1978) provide a useful insight into the true significance of these simple index properties.

3.1.3.2 Brittle deformation

Brittle behaviour represents a near-instantaneous stress reduction (Figure 3-3b) involving some combination of fracture and frictional sliding, and is common in rocks at low pressures and temperature. Usually less than 1% elastic strain occurs before failure or fracturing. Stable frictional sliding along fractures requires less energy than fracture initiation, resulting in a stress-drop. Failure is observable on a wide range of scales, from microscopic to regional scale, as observed in the upper crust from microcracks to continent scale strike slip zones (Engelder and Price, 1993). Low porosity, well-indurated argillaceous rocks (e.g., shale) behave as hard rocks, whereas poorly indurated argillaceous rocks (e.g., some clays) behave as soils.

3.1.3.3 Ductile deformation

Certain rock types display a stress-strain relationship where yield-stress is achieved, but a peak-stress is never attained as a result of continual work-hardening (Figure 3 3d). These conditions are said to be fully mechanically ductile (Jaeger, Cook, and Zimmerman, 2009). Ductility can be viewed as rock 'flow', with rupture occurring, if at all, after at least 10% shortening.

At elevated temperature and pressure, rocks deform through purely ductile mechanisms. These include diffusive mass transfer, pressure solution, superplastic creep and intracrystalline plasticity. These processes usually occur at temperatures above those experienced in radioactive waste repositories, although pressure solution may be expected. In some rocks, an increase in temperature decreases yield strength, enhances ductility, and lowers ultimate strength. A mechanical transition occurs from elastic-brittle to elastic-plastic deformation, representing brittle to pure-ductile deformation. This is generally referred to as the brittle-ductile transition and is both material and condition dependent.

3.1.3.4 Inelastic deformation processes

There are three main categories of deformation mechanisms for rocks and soils (Jaeger, Cook and Zimmerman (2009) and references within):

- 1). **Shear-localisation and brittle faulting** in rocks with a low initial porosity: damage is localised in a shear zone angled approximately 30° to axial load. This is the deformation mechanism seen in test samples that exhibit brittle behaviour.
- 2). **Cataclastic flow and shear-enhanced compaction** in initially porous rocks: damage is pervasive, and progressively fragments granular material. This is the deformation mechanism observed in samples that show ductile behaviour. The progression between these failure modes represents the brittle ductile transition from localised brittle faulting to macroscopic continuous flow in the form of homogeneous cataclastic flow (Rutter, 1993). The transition occurs at an effective pressure of P_{bd} (Wong et al., 1997) in response to an increase in confining pressure and/or temperature.
- 3). **Pressure solution** is the most common intergranular deformation mechanism near the surface of the crust. The basic process involves dissolution of material from highly stressed grain contact points, followed by diffusion of this material into the pore spaces of the rock, where stresses are lower. Certain grains will dissolve faster than others, resulting in stylolites in fine-grained rocks. Whilst described here for inclusiveness, this is not a process of primary interest within the remit of this report.

3.2. Yield and failure

Various approaches have been considered in the literature in order to determine yield stresses. In the case of soft and structured clays sheared at constant confining pressure (see Tavenas et al., 1979), yield is often taken at the maximum deviator stress or at the peak of the stress-strain curves. In isotropic compression tests, yield is taken at the intersection of the two linear segments which best fit the curve in the $e\text{-log}(P')$ plot (Section 3.2.1). In more dense soils, such as compacted soils, no peak is generally observed and a volumetric criterion can also be used (Delage and Cui, 1995, Cui and Delage, 1996).

3.2.1. The influence of effective stress

As discussed in Section 3.1.3, rocks and clays may deform inelastically, by way of a number of different mechanisms, if subjected to sufficient stress conditions. In the case of porous materials, the influence of effective stress is key to determining the response of the material. Changes in effective stress may be caused by an alteration in confining pressure (i.e. a change in burial depth through exhumation or burial) or by a change in pore fluid pressure (pressure build-up or release). For an argillaceous clay or rock, burial and exhumation history can have a profound influence on the hydro-mechanical properties of the material (e.g. Bjerrum, 1967). As sediment is buried, the resulting increase in effective stress leads to consolidation, by way of compaction and dewatering processes, and a reduction in porosity.

Consolidation of an argillaceous material can be considered as a time-dependent loss of both volume and porosity during burial, resulting from the associated increase in total stress. The time required to reach full consolidation is partly related to the initial porosity and permeability of the material. Such behaviour is often subdivided into: (i) primary consolidation, which is associated with the gradual increase in effective stress caused by the dissipation of excess pore pressure, and (ii) secondary consolidation (or volumetric creep), which is the time-dependent loss in pore volume that occurs under a sustained, but not necessarily constant effective stress.

In general, sediments are described as being fully consolidated (at a given *in situ* stress) if all excess pore pressures have been dissipated. A standard approach to describing the consolidation state of a clay is to quote the Over Consolidation Ratio (OCR), as follows;

$$OCR = \frac{\sigma_{max}}{\sigma}$$

Equation 3-5

where σ_{max} is the maximum stress experienced by the rock and σ is the present stress state. As such, a clay with an OCR = 1 is described as ‘normally consolidated’, whilst ‘underconsolidated’ clays and ‘overconsolidated’ clays will have OCR values of less than one and greater than one, respectively.

Considerable effort has been focussed on the relationship between porosity and depth of burial in clay-rich materials (Been and Sills, 1981; Burland, 1990; Gibson, 1958; Leddra et al., 1992; Skempton, 1970 and Olgaard et al., 1995). These early datasets provide a large resource on which to summarise this relationship and examine trends across various materials and conditions (Rieke and Chilingarian, 1974; Dzevanishir et al., 1986; Novello, 1988).

Figure 3-4 shows the variation of void ratio with effective confining stress, for a range of normally consolidated geotechnical materials (as presented by Novello, 1988). Void ratio decreases once consolidation is initiated, usually at stresses above 10 MPa. These observations clearly demonstrate the similarity of compressibility behaviour between soil and rock (Haberfield, 1998).

In its simplest form the effects of burial on porosity can be approximated as follows (Athy 1930);

$$\varphi = n_0 e^{-cz}$$

Equation 3-6

for a depth, z , below surface. The parameters n_0 and c are functions of several contributing factors, such as position within the sedimentary basin, regional tectonic stresses, mineralogy and formation age.

In reality, variability in these parameters means that it has not proved possible to construct a reliable master curve of porosity versus depth (or effective stress), which encompasses all sediments. However, a number of empirically derived functions have been proposed for specific lithologies, where there is sufficient available porosity data and the diagenetic history is well understood. Secondary mineralisation can have a significant influence on the consolidation properties of clay and this effect (particularly in older sediments) can lead to a 'pseudo-consolidation' state.

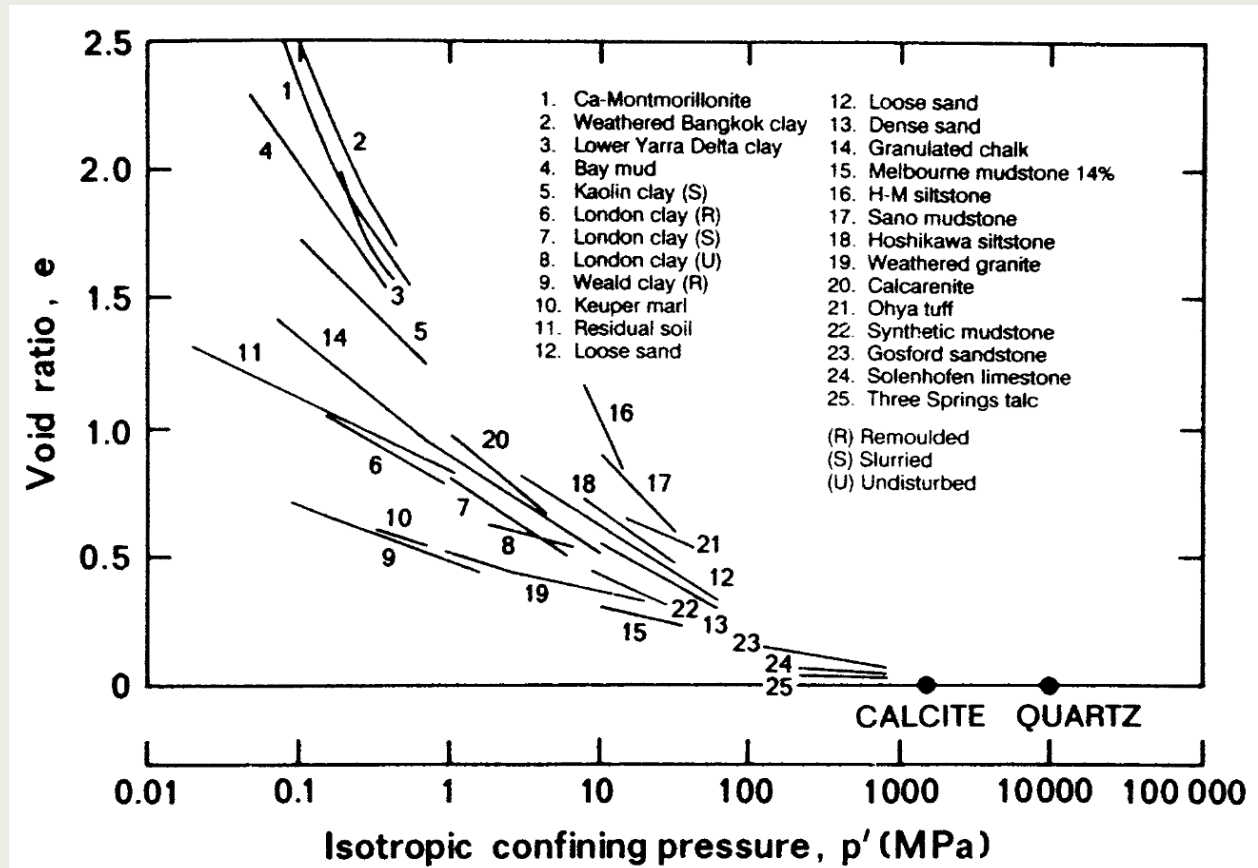


Figure 3-4. Compression characteristics of a range of normally-consolidated geotechnical materials (from Novello, 1988).

The relationship between void ratio and effective stress can be examined in the laboratory, often using a standard oedometer set-up with a saturated sample of specified geometry. The sample is radially constrained whilst axially loaded and unloaded in increments. Volumetric changes and/or net pore fluid loss are measured in order to ascertain the material response to a specified loading/unloading path. In soil mechanics testing, sample response to compression is typically described in $e-\log(P')$ space (where e is void ratio and P' is effective stress). An idealised response is shown in

Figure 3-5. On initial compression, the void ratio of a normally consolidated clay will decrease linearly with increasing effective stress; this is known as the Virgin Compression Line (VCL). As such, the virgin consolidation response of a clay can be quantified by the slope of the VCL, termed the compression index, C_c . For two points on this line:

$$C_c = \frac{e_0 - e_1}{\log \frac{\sigma'_1}{\sigma'_0}}$$

Equation 3-7

An overconsolidated clay (for a given effective stress) will plot on the Recompression/Rebound Line (RRL) (also referred to as the expansion/swelling line) as effective stress is relieved. On recompression, the clay state will ultimately re-join the VCL. The swelling response of the sample is often described in terms of the slope of the RRL, termed the swelling (or expansion) index, C_s .

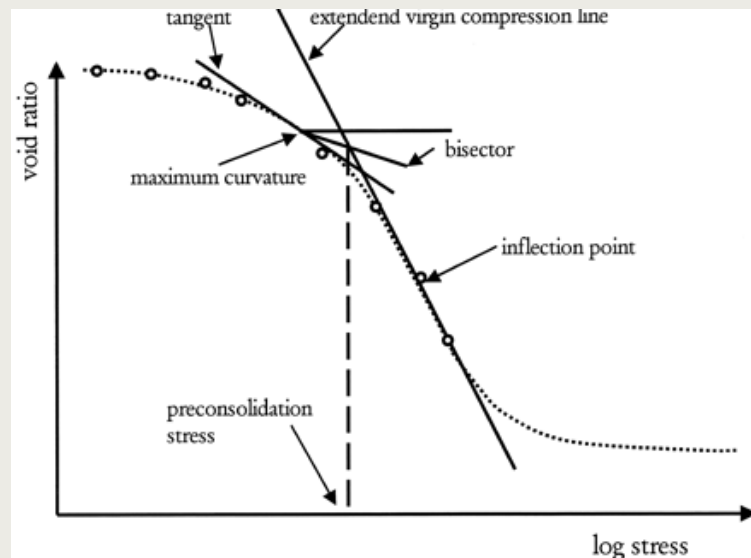


Figure 3-5. Determination of the preconsolidation stress according to the method of Casagrande (1936).

Experimentally derived e - $\log(P')$ curves are also used to estimate the maximum effective stress that the formation has previously been subjected to, generally termed the preconsolidation pressure, P_c' . This provides a simple estimate of stress history and can be used to determine the over consolidation ratio (OCR). For many geological situations in sedimentary basins this is a sufficient description of stress history. Despite being an intrinsic parameter, accurate estimation of P_c' can be non-trivial in practice and a variety of approaches to its derivation have been developed. A widely recognised method for interpreting preconsolidation stress during a consolidation experiment is the Casagrande (1936) method, which is derived in e - $\log(P')$ space. The preconsolidation stress is found based on the inflection point and maximum curvature, as shown graphically in Figure 3-5.

As may be expected, the Casagrande method can be highly subjective and is relatively sensitive to the limitations of a given dataset; a paucity of data is likely to introduce a significant uncertainty in the estimated value of P_c' . Experience is also needed in order to select the best fit to the sparse data, the locations of the inflection point and maximum curvature, as well as the slopes of the VCL and the tangent. Alternatively, a number of appropriate methods exist in order to determine these parameters in a more statistically rigorous fashion (e.g., Dias Junior and Pierce, 1995).

Şenol and Sağlamer (2000) report an experimental study where samples of a known preconsolidation stress were tested in order to validate the effectiveness of several commonly used methods, including the approach of Casagrande and a methodology proposed by Şenol (1997). Şenol and Sağlamer (2000) found that the Casagrande and Şenol

methods delivered values for the preconsolidation pressure with correlation coefficients of 77 - 82 % and 90 - 92 % respectively. As such, the methodology selected clearly plays a role in accurate determination of the preconsolidation pressure, though approximate values can generally be derived with relative ease. Determination of P_c' is discussed in further detail in relation to the Boom Clay in Section 3.3.3.

3.2.2. Failure criteria

Previous sections have discussed the influence of effective stress on material properties, which directly influences strength. However, in order to predict the inelastic deformation and eventual failure of a clay, the determination of appropriate failure criteria is required. Such criterion for a given material can then be used to assess performance within an evolving repository environment. A number of criteria are regularly used, each with specific advantages and disadvantages. Care must therefore be taken in the selection of an appropriate criterion for a given scenario and material. The following section outlines a number of these approaches, which consider the influence of differential stress ($\sigma_1 - \sigma_3$), in addition to effective stress. The determination and form of failure envelopes for the Boom Clay are discussed in Sections 3.3.5 and 3.3.6.

3.2.2.1 Mohr-Coulomb criterion

A simplified approach is the Mohr-Coulomb failure criterion. Strength is assumed to increase linearly with confining pressure, with peak, yield and residual strengths being related to the maximum, intermediate and minimum strengths respectively. In this approach, when shear failure takes place across a plane, the normal and shear stresses across the plane are related by a function that is characteristic of the material. **Equation 3-8** describes the linear Mohr-Coulomb relationship, using σ_d / σ_3 co-ordinates, where σ_d is differential stress, q_u is uniaxial compressive strength, b is a constant in the range 0-10 and p is σ_3 in a compressive test.

In terms of τ_c / σ co-ordinates, Coulomb's law becomes that shown in Equation 3-9, where $\tan \phi$ is related to frictional properties, τ_c is shear stress at failure, and τ_o is cohesion (i.e. extrapolated shear strength when $\sigma = 0$), where $\sigma_o = 2\tau_o / b$. The parameter ϕ is termed the angle of internal friction and can be related to **Eq. 3-8** by **Eq. 3-10**. **Eq. 3-9** represents the linear relationship observed between tangents to Mohr circles at failure (**Figure 3-6**). It predicts failure angle, normal and shear stress at failure, and stress states necessary to reactivate previous fractures (Jaeger, Cook and Zimmerman, 2009).

$$\sigma_d = \sigma_1 - \sigma_3 = q_u + pb \quad \text{Equation 3-8}$$

$$\tau_c = \tau_o + \sigma \tan \phi \quad \text{Equation 3-9}$$

$$b = \frac{1 + \sin \phi}{1 - \sin \phi} \quad \text{Equation 3-10}$$

The Mohr-Coulomb criterion is commonly used to predict failure in a wide variety of materials. However, the approximation of linearity may be inappropriate for a range of materials, from incohesive soil to granite (Schofield, 1998; Ohnaka, 1973; Byerlee, 1975). The use of the linear Mohr-Coulomb relationship in mathematical models of geological problems has also been shown to introduce significant errors (e.g. Wang, 1994). Whilst representing an appropriate failure criterion for specific materials over a restricted interval of stress conditions, the Mohr-Coulomb criterion is not generally considered appropriate for use in repository assessment, where more detailed data should be available.

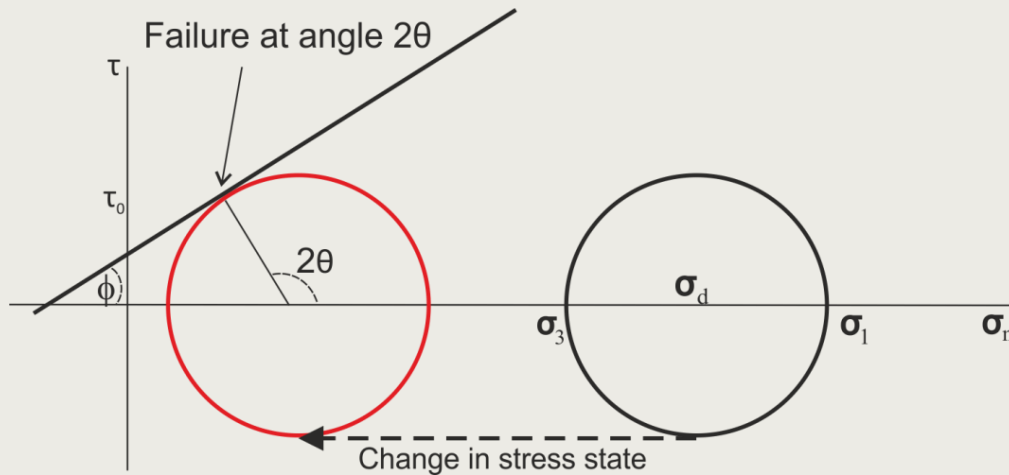


Figure 3-6. Mohr-Coulomb diagram showing change in stress state promoting failure at an angle of 2θ to the failure envelope.

3.2.2.2 Griffith-type failure criterion

The Griffith-type failure criterion is formulated around the concept of failure under tension, resulting from the development of a pre-existing microcrack. The propagation of this defect is then dependent upon provision of sufficient energy to the crack surface for growth to occur. When considering failure under compression, this criterion is not generally satisfied, and is instead combined with the Mohr-Coulomb relationship. This leads to the modified Griffith-type failure criterion (McLintock and Walsh, 1962) under compression:

$$\sigma_c = \sqrt{4T_o\sigma_N - 4T_o^2} \quad \text{Equation 3-11}$$

This relationship, therefore, suggests that the critical shear stress required for failure of a fracture is a function of both the magnitude of the normal stress on the fracture and the tensile strength, T_o , of the material. In reality, this criterion relates to the onset of microcracking, as opposed to the final stages of localisation and, as such, predicts fracture onset and not ultimate failure strength.

3.2.2.3 Hoek-Brown failure criterion

To address deficiencies in the Mohr-Coulomb approach, Brown et al. (1983) and Hoek et al. (1992) investigated non-linear failure criteria. The widely applied Hoek-Brown (Hoek and Brown, 1980) empirical strength criterion takes account of material anisotropy and has the form:

$$\sigma_1 = \sigma_3 + q_u \sqrt{\frac{m\sigma_3}{q_u} + s} \quad \text{Equation 3-12}$$

The parameter m is related to the degree of particle interlocking and is high for intact rock. The parameter s relates to the degree of initial fracturing, representing cohesion, such that for intact rock, $s = 1$. In contrast, for highly fractured rock, s reduces and tends towards zero as the strength is reduced from peak to residual. The material-specific parameters, m and s , must be empirically derived and, as such, a degree of physical interpretation is associated with this approach.

3.2.2.4 Non-linear Mohr-Coulomb failure criterion

Another empirical criterion is the non-linear Mohr - Coulomb relationship:

$$\sigma_c = \sigma_o + \tan \phi \left(\frac{\sigma_N}{\sigma_o} \right)^\eta \quad \text{Equation 3-13}$$

where η = empirical constant. This is a better approximation of porous media behaviour and has been shown to fit the response of argillaceous rocks closely.

Many other failure criteria are also utilised in the literature (e.g., Modified Lade failure criterion (Lade, 1977; Ewy, 1999), Drucker-Prager failure criterion (Drucker and Prager, 1952), Modified Wiebols-Cook failure criterion (Wiebols and Cook, 1968; Zhou, 1994), to varying degrees of complexity. Each provide good approximations of rock strength for specific rock types, under specific conditions. The Mohr-Coulomb criterion does not usually apply well to rocks, although its underlying mathematical simplicity explains its continuing importance, and it may be acceptable as a first approximation. The Griffith-type criterion is widely applied to studies of brittle deformation, with some validity. However, empirical evidence generally suggests that the Hoek-Brown and non-linear Mohr-Coulomb criteria provide the best predictions of rock strength. However, substantial testing of material is required to establish the empirical data for a given material. For complex triaxial stress states, as experienced within the Excavation Damage Zone (EDZ) surrounding a repository, more appropriate polyaxial criteria are required.

3.2.2.5 Critical state mechanics

Whilst the criteria described in the previous sections provide a methodology for prediction of failure in a given material, in many geological scenarios (and particularly for argillaceous materials) the role of mode of failure must also be considered. Ideally, a suitable failure model should describe the influence of stress state on yield mechanism and the associated deformation. The critical state theory was initially proposed by Roscoe et al. (1958) as a unified model which relates volume changes to stress states for soils. Additional modifications made in the application of critical state to rocks include accounting for brittle or work-softening behaviour (Gerogiannopoulos and Brown, 1978) and the influence of tensile strength (Shah, 1997). The state of a rock/clay subjected to a simple stress field is defined by its position in the effective stress (p') - differential stress (q') and specific volume (v) parametric space (**Figure 3-7**). A change in this state, or stress path, is then represented within the p' - q' - v space. The stress path can therefore be used to describe the deformation history of the material, as well as its current state.

The initial model proposes an isotropic soil which yields, at a critical specific volume ($v_c = 1 + e_c$). Yielding or shear slipping is considered to occur as a combination of the effective stress and specific volume, coinciding with a state boundary surface. Experimentation has shown that when sheared, a deforming rock will tend towards criticality, a state where large shear distortions will occur without any further changes in p' , q' or v (Schofield and Wroth, 1968). The Critical State Line (CSL) is the locus of all possible critical states in p' - q' - v space.

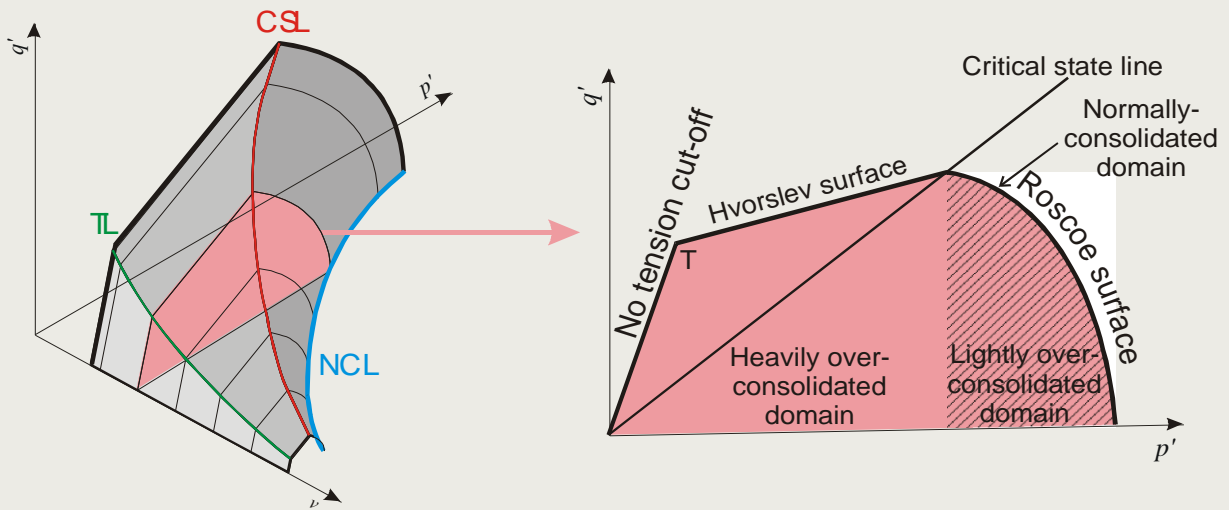


Figure 3-7. The critical state model of soil mechanics, showing the relationship of the tension line (TL), normal consolidation line (NCL) and critical state line (CSL). These lines bound the Hvorslev and Roscoe surfaces in the p' - q' space.

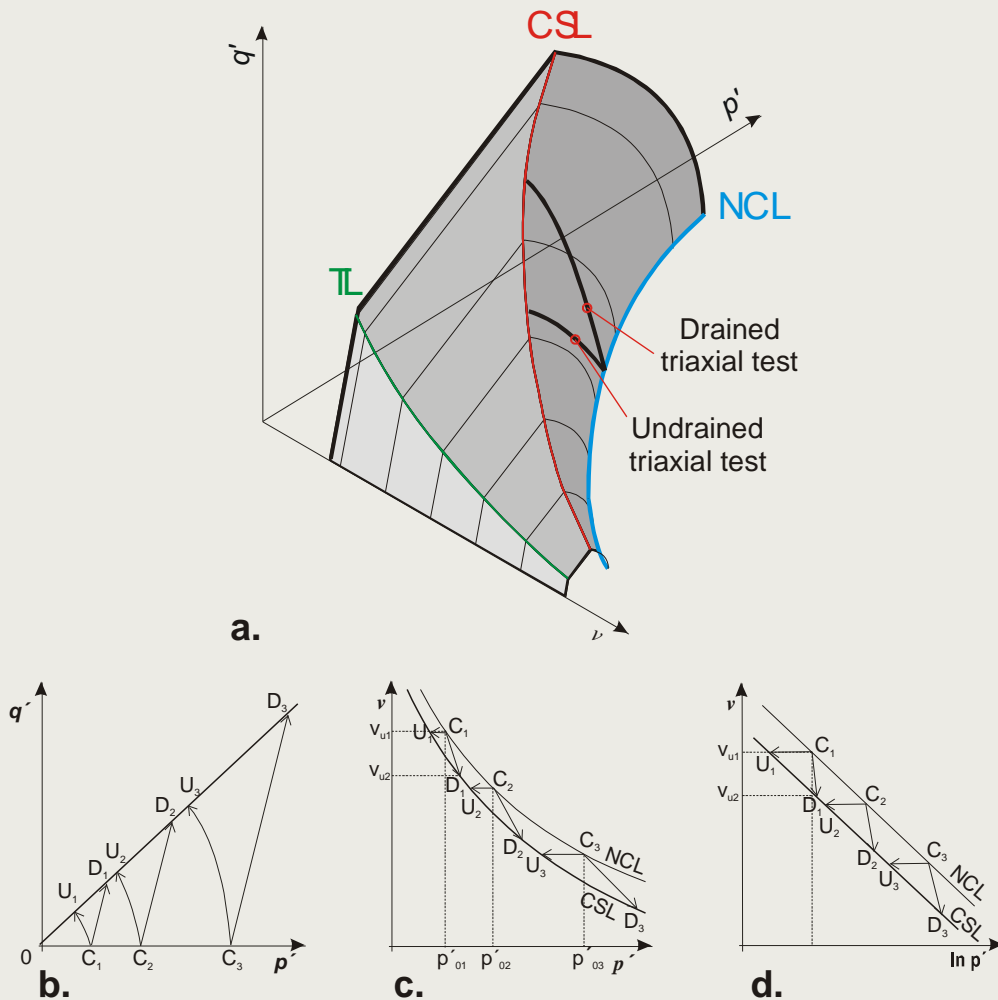


Figure 3-8. The critical state model of soil mechanics in detail. a) The state boundary surface for a particulate sediment (after Atkinson and Bransby, 1978). b-d) p' - q' - v plots of triaxial test results for drained (D) and undrained (U) tests. The stress path for all tests tends towards the critical state line where critical state deformation continues.

Figure 3-7 shows the CSL in relation to a yield surface. This yield surface can be split into three separate surfaces; the tension, Hvorslev and Roscoe surfaces. These regions are bound by the tension line (TL), the CSL and the Normal Consolidation Line (NCL).

During consolidation under isotropic stress, the volume change path will move along the NCL, which is in the plane of zero deviatoric stress (i.e. when stress in all directions is equal). The volumetric strain during consolidation is considered to have elastic (recoverable) and plastic (non-recoverable) components (Schofield and Wroth, 1968). Where a differential stress is also involved,

Figure 3-8 (b) shows the paths a material would take in drained (reducing volume path C→D) and undrained (constant volume path C→U) tests. Yield occurs at U1, D1, U2, D2, U3, and D3; in the $p' - q - v$ space this line represents the CSL. On unloading, deformed sediments will only recover the elastic component of deformation; plastic deformation by definition is non-recoverable. The path then follows the rebound-reconsolidation line (RRL), also known as the swelling line.

Although critical state concepts have generally not been applied to rocks, Novello (1988) showed that a wide range of materials, from soft clay to hard rocks, display similar strength behaviour. Cuss et al. (2003) and Cuss and Horseman (2003) applied the concepts of critical state mechanics to sandstone and shale. These studies concluded that the dry-side represented the brittle (dilatant) regime and the wet-side the ductile (contractant) regime. From this, it follows that the transition between the two states, be it the brittle-ductile transition or the dilatancy boundary, are identical. Therefore observations of rock-deformation can also easily be added to the critical state model.

There are many examples within the literature of studies on soils and clays that demonstrate the validity of critical state theory and the use of the Cam-clay derived models, which define the yield surfaces between the critical state normal consolidation and rebound-reconsolidation lines (Chen et al., 2014; Delahaye and Alonso, 2002; Hueckel and Pellegrini, 1989). The modified Cam-clay/critical state approach can successfully reproduce non-linear clay deformation with only five parameters (M , slope of the critical state line; λ , slope of the normal consolidation line; k , slope of the elastic line; E , elastic modulus and ν , Poisson's ratio).

The critical state concept and yield surface provide a powerful and effective framework in which all aspects of mechanical porous sediment deformation and evolution can be described and interrelated. Complex burial and stress-porosity histories can be described using this concept. For an argillaceous shale or clay-based host formation, preferred stress conditions lie on the right side of **Figure 3-7**, where brittle deformation is avoided and yield is unlikely to increase permeability. As long as deformation is not induced by elevated pore pressures then the conditions will result in swelling and sealing of discontinuities in the clay. Critical state parameters and their application for the Boom Clay are discussed further in Section 3.3.6.

3.3. Mechanical properties of the Boom Clay

As discussed in Section 3.2, a number of methodologies exist for predicting the yield and failure response of clays and rocks, based on fundamental and empirically derived parameters for a specific material. Extensive mechanical testing of the Boom Clay has been conducted under a variety of environmental and boundary conditions, both in the laboratory and in the field at HADES. The influence of the applied drainage condition in such tests should not be neglected when utilising measured properties to predict mechanical response. In drained experiments, pore fluid is introduced or removed in order to maintain a constant pore pressure within the sample, whilst fluid volume is kept

constant in undrained testing and can result in changes in the internal pore pressure of the sample during loading, which are not allowed to dissipate (Patterson and Wong, 2005). The following subsections briefly describe a number of studies which assess the mechanical response of the Boom Clay and the influence of controlling factors on this behaviour. Data discussed is generally only from studies where material was retrieved at depth, hence avoiding weathering effects and reducing the likelihood of mechanical perturbation of the clay. A summary of key mechanical properties given in the literature is found in **Appendix Table B0-5**.

3.3.1. Elastic response

The response of a material to an applied stress is highly dependent on the internal properties of the material. The propensity for a given material to deform elastically can be quantified in terms of the elastic moduli. Both laboratory testing and *in situ* experiments at HADES, provide data on these moduli for the Boom Clay in Belgium. There is a notable degree of variation in values reported within the literature (**Appendix Table B0-5**), resulting from differences in test stress conditions, depth and location of sample material. Other potential influences may also include mineralogy and experimental methodology. A brief summary of some relevant studies related to elastic moduli, and discussion relating to some of these influences, is given in the following sections.

3.3.1.1 Young's modulus

Young's modulus, E , is a measure of material stiffness, and is defined as the stress required to achieve unit length-parallel extensional elastic strain. As such, an elastic response can be described in terms of Hooke's law, such that;

$$\sigma = E\varepsilon \quad \text{Equation 3-14}$$

where σ is the applied stress and ε is the resulting strain response.

There is a wide variation in reported values for the drained Young's Modulus, E_d , in the Boom Clay (TIMODAZ, 2007), which range from 130 to 400 MPa (**Appendix Table B0-5**). A number of studies have demonstrated that stiffness of the Boom Clay is reasonably sensitive to changes in the applied effective stress conditions (TIMODAZ, 2007; Horseman et al., 1993; Bouazza et al., 1996; Sultan et al., 2010) and the spread in quoted values, in part, results from differences in test stress conditions between studies. In addition, values for E quoted in the literature may be derived using different methodologies (secant versus tangent modulus), accounting for some of the observed divergence. The majority of reported drained values are for the expected *in situ* conditions at HADES ($\sigma_{\text{eff}} \sim 2.2\text{MPa}$) and these generally fall within the range of 150 - 300 MPa. The most commonly used value in the literature is 300 MPa, derived from *in situ* testing at Mol (Branichon and Volckaert, 2003; Bernier et al., 2007), which is consistent with a relatively high porosity clay. Values for undrained conditions, E_u , are reported in the range of ~150 - 200 MPa.

Given evidence provided by studies in a range of argillaceous materials, the elastic properties of clay are strongly dependent on the initial water content (Horseman et al., 1996; Lima et al., 2012a). Typical behaviour is observed as a non-linear decrease in E with increasing water content (Blumling and Bernier (2007)). However, there is a paucity of data on the specific impact for the Boom Clay, in spite of its importance during the excavation and closure phases of repository development. Remaining variation in values for E derived under similar conditions may be attributed to differences in the lithological state resulting from lateral variation in stress history, spatial heterogeneity in mineralogy within the formation (carbonate content, clay/non-clay fraction) or they may result from further differences in the experimental approach.

Since the influence of effective stress on Young's modulus is well established (Bouazza et al., 1996; Horseman et al., 1993), elastic moduli must be selected with care, so as to be representative of the relevant stress conditions. However, no experimental measurements of the Young's modulus for the Boom Clay in the Netherlands could be found within the literature and there is, likewise, a paucity of data at appropriate stress conditions from studies in Belgium.

Based on a relationship derived by Wroth (1972) and assuming the Poisson's ratio (as Wroth indicates) is substantially independent of effective stress, Horseman et al. (1993) proposed two linear relationships for E_u with respect to increasing consolidation stress. These are empirically-derived from triaxial testing of the Boom Clay samples from Mol and predict changes in elasticity based on the estimated secant modulus (Equation 3-15) and tangent modulus (Equation 3-16), such that;

$$\frac{E_u}{P'_c} = 37.2 + 43.4 \ln(OCR_i) \quad \text{Equation 3-15}$$

and

$$\frac{E_u}{P'_c} = 32.0 + 30.0 \ln(OCR_i) \quad \text{Equation 3-16}$$

Horseman et al. (1993) used Equation 3-15 to estimate an undrained Young's modulus (E_u) of 197 MPa for stress conditions at HADES. Using the same equation and assuming an estimated σ_{eff} range resulting from the Dutch depth criteria (Section 1.5) of 3.4 MPa to 5.2 MPa and a preconsolidation stress of 7.45 MPa (see Section 3.3.3) gives an estimated range for E_u of between approximately 400 MPa and 525 MPa. However, further additional testing is required to confirm the validity of this extrapolation under such conditions. Notable anisotropy in E has also been noted in the literature (Horseman et al., 1993), though there is a paucity of data relating to its development with increasing effective stress.

3.3.1.2 Poisson's ratio

Poisson's ratio (ν) describes the translation of vertical stresses into additional horizontal strains. Where deformation is isovolumetric, $\nu = 0.5$, axial strain is translated symmetrically into the two radial directions. Most rocks typically have $\nu \approx 0.25$, meaning that elastic volume decrease occurs as result of axial loading. The Poisson's ratio is defined as;

$$\nu = -\frac{\epsilon_1}{\epsilon_3} \quad \text{Equation 3-17}$$

where ϵ_1 and ϵ_3 are the maximum and minimum principal strain components.

Reported values for the Poisson ratio of the Boom Clay are ~0.13 - 0.14, though the associated drainage conditions are not always made clear. The most commonly reported value for the drained Poisson's ratio, ν_d , is 0.125 (Branichon and Volckaert, 2003; Bernier et al., 2007), which is derived from observations at Mol. However, there is a lack of information relating to any spatial variability in ν within the formation, either as a result of changes in mineralogy or as a consequence of greater burial depth. Whilst ν is not

expected to be as sensitive to effective stress as Young's modulus, there is some evidence to suggest that the influence of depth cannot be entirely neglected (Yu et al., 2014). Additional testing will confirm the appropriateness of such an assumption at depths relevant to the Dutch concept.

3.3.1.3 Bulk modulus

The bulk modulus of compressibility (K) describes the resistance to dimensional alteration, as described by ν and E , such that;

$$K = \frac{\delta P_c}{\delta \varepsilon_v} = \frac{E}{3(1 - 2\nu)}$$

Equation 3-18

where P_c is hydrostatic confining pressure and ε_v is volumetric strain.

Calculated Boom Clay values for K (based on E and ν in **Appendix Table B0-5**) reflect the variability in other reported elastic moduli. However, the most widely quoted values for E and ν , under the stress state at Mol, give $K = 133$ MPa, as might be expected for a lightly overconsolidated clay. Improved confidence in the source parameters for this value and their sensitivity to depth will reduce uncertainty in their application to deeper parts of the formation, such as in the Netherlands.

3.3.1.4 Shear modulus

The shear modulus, G , describes the resistance of a material to shear and can be defined as the ratio of shear stress, σ_τ to shear strain, γ ;

$$G = \frac{\delta \tau}{\delta \gamma} = \frac{E}{2(1 + \nu)}$$

Equation 3-19

Using reported values for E and ν (**Appendix Table B0-5**), gives calculated values for the shear modulus ranging from around 70 to 140 MPa. As with the bulk modulus, improved confidence in the source parameters for this value and their sensitivity to depth will reduce uncertainty in their application to deeper parts of the formation, such as in the Netherlands.

3.3.2. Compressive strength

Clay strength is often initially assessed and quoted in terms of the Uniaxial Compressive Strength (UCS), which is determined by the axial loading of an unconfined sample to the point of failure. The associated axial and radial strains are also generally measured during deformation. No confining or pore pressure is applied to the sample and care must be taken to select an appropriate strain-rate so as to ensure pore water is able to drain, if so required. Drained UCS values for samples taken from HADES, are widely reported, though often without provision of the original data source. Most of these values lie in the 2-3 MPa range, with a value of 2 being most commonly given (Bernier et al., 2007; Tsang et al., 2012). Bésuelle et al. (2013) report measuring a UCS of 2.5 MPa during compression testing of the Boom Clay from HADES (**Appendix Table B0-5**). Whilst not a direct measure of the clay's response under *in situ* conditions, this quantity does provide a first estimate of the likely mechanical strength of the material. According to its UCS, the Boom Clay would be described as a 'weak' rock (Waltham, 1994), which will 'crumble under pick blows' in the field. In the Netherlands, any differences in the compaction state of the clay are likely to result in changes to its UCS.

It should be noted that in reality, during the construction of a repository, the influence of effective and differential stresses (both past and present) cannot be excluded when considering clay strength and are discussed in greater detail in the following sections.

3.3.3. Consolidation properties

The Boom Clay, in the Belgian context, is generally described as being a lightly overconsolidated material (Horseman et al., 1987; Horseman et al., 1993; Bernier et al., 1996). This understanding is derived from a number of experimental programmes, beginning in the 1980's. Typical quantification methods generally involve a 1-D axial oedometer arrangement or an isotropic loading test. As described in Section 3.2.1, consolidation testing allows the determination of the maximum pressure experienced by the sample material whilst *in situ*. A summary of parameters measured in such studies is given in **Appendix Table B0-5**. Estimated values for the vertical preconsolidation pressure, P_c' , of the Boom Clay taken from HADES generally range from between ~5 and 6 MPa, leading to an OCR at *in situ* conditions of ~2 - 3, though there is some debate relating to these values. Nevertheless, the most commonly adopted value within literature appears to be an OCR of 2.4. In this section we describe a number of key studies relating to the consolidation characteristics of the Boom Clay and discuss the implications in relation to the Dutch Boom Clay concept.

Some of the earliest experimental work on the Boom Clay, in relation to the Belgian disposal concept, was conducted by Horseman and co-workers. They conducted 1-D axial, isotropic and triaxial loading tests (Horseman et al., 1987; Horseman et al., 1993), in order to investigate the thermo-hydro-mechanical properties of samples derived from HADES. The Casagrande method was used to estimate the preconsolidation stress using data from three 1-D consolidation tests loaded perpendicular to bedding, yielding P_c' 6.0 - 6.1 MPa, and one test parallel to bedding, giving $P_c' \sim 5.0$ MPa. There is a lack of other measurements made on samples in the latter orientation within the literature, but these findings imply a significant anisotropy (with a ratio ~0.8), which warrants further investigation. Taking the vertical loading case (perpendicular to bedding) and reported *in situ* conditions for Mol ($\sigma_{\text{eff}} = 2.3$ MPa, Bernier et al., 2007), an OCR of 2.4 is estimated. The authors state that these findings indicate a previous maximum overburden of 600 m, which they could not reconcile with the geological history of the formation. Instead, they suggest this figure may be the result of a "pseudo-overconsolidation" effect, resulting from diagenesis and ageing effects.

Wildenborg et al. (2003) combined both laboratory experiments and numerical simulation to investigate the potential influence of glacial loading on the hydromechanical properties of Paeleogene clays. Both 1-D axial and triaxial loading experiments were conducted on samples derived from material retrieved at six depths in Belgium (four locations) and in the Netherlands (one location). All but the deepest samples were derived from within the Rupel Clay member, the latter instead belonging to the Asse Member (immediately beneath the Rupel). Contrary to the findings of Horseman and co-workers (Horseman et al., 1987; Horseman et al., 1993) on clay from HADES, Wildenborg observed a normally consolidated response during most of the triaxial tests, irrespective of retrieval depth. However, they attribute this behaviour to sample swelling during long-term core storage, post-exhumation. The preservation procedure for the cores is not described, but it is conceivable that sample damage (use of drilling fluids, drying effects, etc.) may also be a contributing factor.

Wildenborg et al. (2003) also presented findings from five oedometer tests conducted on both the Dutch and Belgian clay samples. The experimental approach is not described, but they report good reproducibility in terms of the form of the stress-strain material response

on compression. Although the procedure for estimation from $e\text{-log}(P')$ data is not described, the authors estimate preconsolidation stresses ranging between 6.4 and 8.0 MPa for all five samples and an OCR ranging between 1.9 and 2.2. The degree to which this variability is the result of lithological differences, as opposed to uncertainty in quoted values is unclear. However, these values do suggest a reduction in the OCR (towards a normal consolidation state) within deeper parts of the formation, as would be expected. In particular, they report that for the Dutch clay samples (from depth intervals of 453 - 454 m and 561 - 562 m) measured values for P_c' are slightly higher.

The EC-funded project TIMODAZ (Thermal Impact on the Damaged Zone around a Radioactive Waste Disposal in Clay Host Rocks) also examined the mechanical properties of the Boom Clay from HADES, using a variety of experimental techniques. In a project report (TIMODAZ, 2007, they summarise available test data derived from sample stress-strain response under isotropic and/or oedometric conditions and suggest an OCR ranging from 2.05 - 2.64 and a preconsolidation stress of ~ 5 - 6 MPa.

In more recent studies, Sultan et al. (2010) carried out mechanical testing of samples from HADES, in order to examine the influence of stress history and of anisotropy. Testing included isotropic compression experiments and triaxial shearing. Compression experiments were carried out at a rate of 0.5 kPa/min, which the authors argue is sufficient to assume fully drained conditions (although sample pore pressures and net outflow were not monitored). During compression testing they measured a significantly lower preconsolidation pressure than in other studies (Horseman et al., 1993; Besuelle et al., 2013; TIMODAZ, 2007) of 0.37 - 0.38 MPa; a value significantly below *in situ* conditions for Mol. However, sample hydration was conducted at much lower stress ($\sigma_{eff} = 0.07\text{MPa}$) than previous *in situ* conditions and they suggest this response is the result of sample swelling.

Deng et al. (2011) also conducted hydromechanical testing of samples retrieved from HADES, as well as additional Boom Clay derived from the Essen-1 borehole (over a depth range of 220 - 260 m). Their experiments included low pressure and high pressure oedometer testing (ranging from $\sigma_{eff} = 0.05 - 3.2$ MPa and $\sigma_{eff} = 0.125 - 32$ MPa, respectively), isotropic consolidation testing and triaxial testing. They report that the geotechnical properties, mineralogy and hydromechanical behaviour of test specimens is similar for material taken from both locations, though some small variations are noted. During consolidation testing, sample equilibration was assumed based on mechanical stabilisation, rather than a constant net outflow (indicating that hydraulic equilibrium is achieved). The oedometer tests were conducted on five samples from the Essen borehole and one from Mol. Clay specimens were initially resaturated under approximate *in situ* effective stress conditions (2.4 MPa), before being incrementally unloaded to $\sigma_{eff} = 0.125$ MPa, then subjected to a further two cycles of loading and unloading. The resulting $e\text{-log}(P')$ curves give values for yield stress ranging between 1.3 - 2.2 MPa, which are significantly lower than those reported in most other studies on the Boom Clay (Horseman et al., 1987; Yu et al., 2012; Bésuelle et al., 2013). The authors suggest that their findings indicate that oedometer tests may not be appropriate for accurately deriving preconsolidation stress.

Nevertheless, the approach used by Deng and co-workers is unorthodox, in that conventional consolidation testing is generally begun by incremental loading above the *in situ* stress. By unloading from *in situ* conditions, samples are allowed to swell before reloading can take place, which the authors themselves acknowledge can potentially induce significant changes in the clay microstructure. Certainly, the observation of yield stresses below the *in situ* conditions at Mol, is counter to most observations conducted at the URL. Given that preconsolidation stress is, by definition, the maximum stress the clay

has previously experienced, it is also difficult to reconcile the observation of yield stress values below the initial effective stress conditions applied to the sample during testing. If the loading scheme has impacted on the sample behaviour, this may go some way to explaining why a different sample response was observed for the same material when tested in low pressure oedometers (where unloading was allowed to a lower stress), as compared to the high pressure oedometers.

Deng et al. (2011) also conducted isotropic consolidation tests on four samples from the Essen borehole, which were loaded to a peak stress of 20 MPa before unloading. The resulting $e-\log(P')$ curves are indicative of normally consolidated behaviour, unlike findings for clay from HADES. Unfortunately, no isotropic tests were conducted on the Mol samples, meaning a parallel response cannot be compared. The authors report values for these samples of $P_c' \sim 2.2$ MPa, though visual inspection of the $e-\log(P')$ curves show little evidence for a break in slope and modelled fits to the data are not presented. Certainly a significant level of uncertainty in the determination of these values is likely and it is therefore non trivial to draw conclusions about the comparative response of material derived from the Essen location and the influence of mineralogy and retrieval depth upon measured preconsolidation stress values.

A number of other recent studies are focussed on samples retrieved from HADES and present similar findings to those given in the early literature. Yu et al. (2012) report an average preconsolidation value of 5 MPa (OCR ~ 2), based on observations from oedometer testing. Bésuelle et al. (2013) conducted both isotropic compression and drained triaxial compression tests to investigate the influence of effective stress. Their observations of volumetric strain evolution during consolidation of the Boom Clay samples also yield $P_c' \sim 5$ MPa. Whilst slightly lower, these values are not inconsistent with the findings of Horseman et al. (1987). Bernier et al. (2007) published a synthesis of geotechnical observations from twenty-five years of operations in Boom Clay retrieved from the HADES URL. For completeness, physical properties determined from field and laboratory testing and quoted in this paper are also displayed in **Appendix Table B0-5**. These values are regularly cited in the literature and commonly used for the purpose of numerical simulation.

Figure 3-9 shows a compilation of the consolidation curves determined by Horseman et al. (1988). For ease of comparison, void ratio data has been normalised for each dataset with respect to e (at a pressure of 2 MPa). The effective stress state at HADES is indicated by the solid red line. A favourable value (6 MPa) for P_c' at HADES (Bernier et al., 2007) is indicated by the dashed red line. An estimated effective stress state at 500 m depth (see Section 1.5) is shown as a solid blue line. Based on this dataset and assuming an identical lithology, these depth conditions would likely result in a clay void ratio of -0.6 ± 0.05 . Given the greater depth of burial, it seems likely that the value of P_c' will be higher for a Dutch repository than at Mol. Based on the observations of Wildenborg et al. (2003) on core from Blija (in the North of the Netherlands), an approximate averaged value for P_c' in the Netherlands (7.45MPa) is indicated by the dashed blue line. This maximum previous burial pressure would result in an OCR at 500m of ~ 1.7 , indicating a lightly overconsolidated state a little closer to normally consolidated than at HADES.

These figures would suggest that the clay will be slightly closer to yield and more susceptible to changes in pore pressure conditions during the construction phase. However, this is an over-simplification of the material response as the influence of differential stress is neglected. This aspect of the material's stress state is considered in more detail in Sections 3.3.5 and 3.3.6, where the critical state approach can provide additional insight. It is certainly clear, however, that further data from core in the Netherlands would greatly increase certainty of the clay's past burial history and its expected mechanical response.

3.3.4. Shear strength and frictional properties

Shear strength is a commonly reported property for clays. The shear strength, S_c , of a rock is a measure of the internal resistance of a body to an applied shear stress. Undrained shear strength, S_u , is dependent upon the friction and cohesion properties of the material and is often represented in terms of the Mohr-Colomb relationship (Section 3.2.2.1);

$$S_c = \tau'_0 + (\sigma - P_p) \tan \phi \quad \text{Equation 3-20}$$

where τ'_0 is the cohesion intercept, ϕ is the angle of internal friction, $(\sigma - P_p)$ represents the effective stress, where σ is the total stress and P_p is the pore pressure.

In situations involving rapid loading (e.g. in close proximity to a tunnel face), the frictional component of shear strength cannot be mobilized. Instead, the clay will fail at its undrained shear strength S_u . However, in the case of more indurated mudrocks, failure will occur close to the UCS of the clay, q_u , often assumed to be double the undrained shear strength ($q_u \approx 2 S_u$).

Most values given for the shear strength of the Boom Clay within the literature are measured under undrained conditions. In triaxial loading tests, Horseman et al. (1987) estimated an undrained shear strength in the vicinity of 1.1 MPa. However, other observations suggest a significant variability in measured strength within the formation even at a constant depth interval. Clarke and Smith (1992) report S_u values, acquired using a self-boring pressuremeter at HADES, of 0.75 - 2.76 MPa. There is also a degree of variation in the reported values for ϕ and τ'_0 (**Appendix Table B0-5**). Typically used experimentally derived values for undrained conditions range from $\sim 2.0 - 4.0^\circ$ and 0.5 - 1.3 MPa, for ϕ and τ'_0 respectively. For drained tests values of $\sim 13 - 25^\circ$ and 0.01 - 0.3 MPa are generally quoted. Improved certainty in these values will better constrain attempts to extrapolate shear strength properties at greater depths.

As described in Section 3.2.2, in order to carry out such an extrapolation the undrained shear strength S_u , of overconsolidated clays and mudrocks is often assumed to increase more or less linearly with depth. De Beer (1967) conducted laboratory testing on Boom Clay samples collected from Antwerp to construct an empirically derived relationship for S_u (kPa), as a function of depth, z , as follows:

$$S_u = 73.6 + 3.4z \quad \text{Equation 3-21}$$

Using this relationship gives estimated undrained shear strengths of 822 kPa and 1774 kPa, at depths of 220 m and 500 m, respectively. This implies a more than two-fold increase in S_u , for proposed repository depths in the Netherlands, as compared to Mol. However, as previously discussed (Section 3.2.2), the approximation of linearity is not wholly appropriate and extrapolation from values measured at lower stress conditions may not be sufficient when considering the clay behaviour deeper in the formation. Nevertheless, it should be noted that the majority of available shear strength data is derived from experiments conducted at reasonably low effective stresses, generally not directly comparable to conditions appropriate to the Dutch concept. The following section describes a number of studies that examine the form of the yield surface in greater detail and the implications for the Dutch Boom Clay concept.

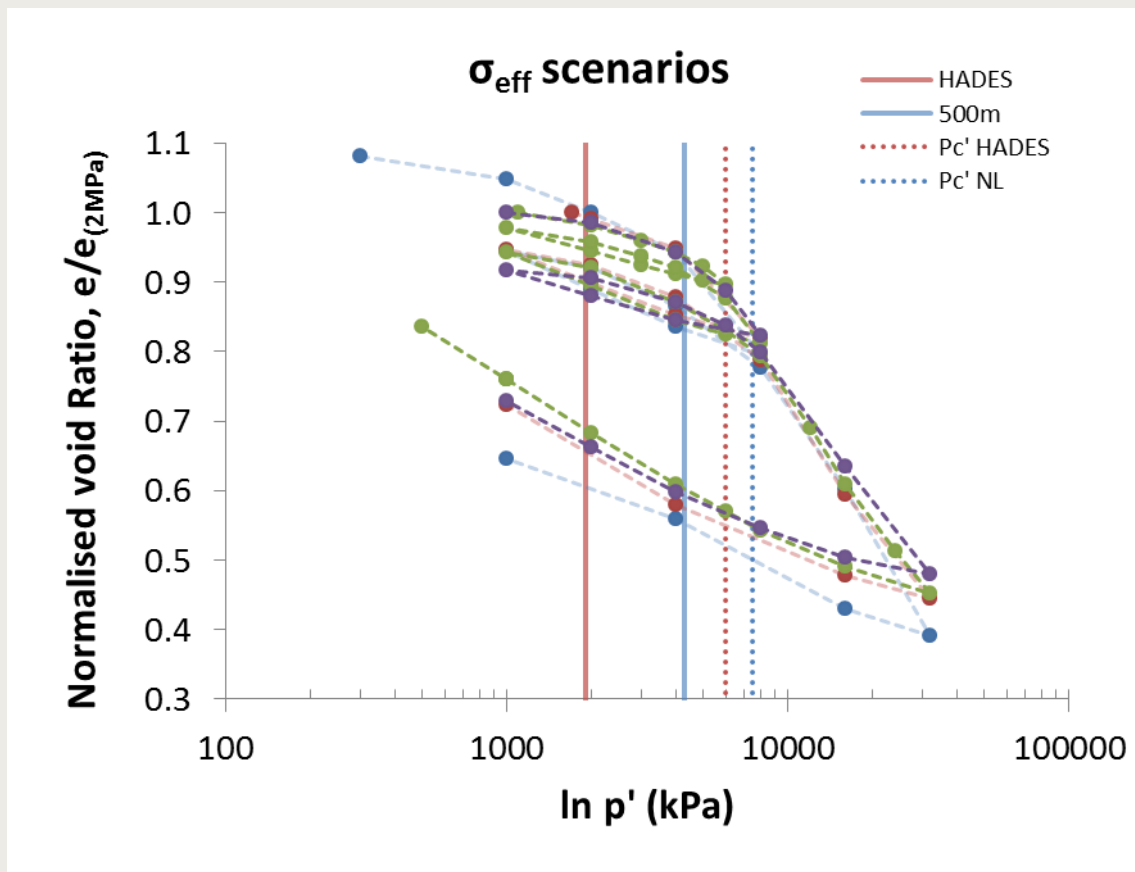


Figure 3-9. Compilation of consolidation curves from Horseman et al. (1987) displaying the stress state at HADES and a potential stress state for the disposal concept investigated in Dutch research programme OPERA.

3.3.5. Yield in p - q - v space

A range of failure criteria exist for prediction of clay behaviour under mechanical loading (Section 3.2.2). Whilst the Mohr-Coulomb approach provides a useful first-approximation within a given stress interval, in order to extrapolate data to greater depth conditions the non-linearity of the failure envelope must be addressed. Since investigation of the mechanical properties of the Boom Clay began, a significant amount of laboratory and field testing has been conducted in order to delineate the shape of the failure envelope and apply more appropriate models to predict the conditions required to promote failure within the clay.

Bouazza et al. (1996) carried out triaxial tests on normally consolidated, reconstituted Boom Clay, loading samples to failure under drained conditions. The resulting data provides a failure envelope in p - q space at very low pressures (up to q -0.25 MPa and p -0.45 MPa). However, these conditions fall significantly short of the *in situ* stress conditions expected for a repository both in the Netherlands and in Belgium. Given the substantial evidence that the form of this envelope does not allow linear extrapolation to higher pressures, this dataset is therefore of limited use when considering stress conditions appropriate for the Dutch repository concept. The reconstituted nature of the samples is also likely to have significantly reduced the shear strength of the material, resulting from a loss of sample fabric and cementation, and the authors call for further testing on intact samples.

Wildenborg et al. (2003) also present shear strength data determined from triaxial loading tests on intact samples from the Rupel Formation and construct the resulting failure envelope in p - q space. Their findings demonstrate a dramatic reduction in clay strength under undrained conditions, with failure occurring at significantly lower stress conditions than in the drained state. These findings highlight the influence of boundary conditions on the mechanical response of the clay, which will differ significantly during the lifetime of a repository. The authors also report a general trend of increasing effective cohesion and decreasing effective friction angle with depth and tentatively suggest an increase in plasticity with depth, as observed in other clays (e.g. Bishop et al., 1965). Nevertheless, the dataset is arguably insufficient to confirm these observations and this is acknowledged by the authors. They also note a significant variation in mechanical response between samples taken from within the same one metre interval. Without additional information relating to the test methodology it is not possible to discount experimental artefact, though these findings imply small scale variability within the formation. As such, they recommend expansion of the dataset in relation to the Dutch clay material, in order to increase certainty in estimated values. Based on a linear fit to their shear strength data, the authors suggest values for the undrained coefficient of friction, ranging from 10° - 30° (as effective stress is increased). However, this directly contradicts observations on material from HADES, which has been reported to have an undrained value for ϕ_u of 2° - 4° (TIMODAZ, 2007). No immediate explanation for this discrepancy is apparent, though it could relate to mineralogical/petrological differences within the formation or experimental approach.

Samples from HADES were also tested under both drained and undrained conditions, by Sultan et al. (2010). Experiments included both isotropic compression and triaxial shearing, with the intention of examining the influence of anisotropy and the effects of stress history. Shearing was conducted according to the criteria of Gibson and Henkel (1954), at an axial deformation rate of 0.003 %/min. As with Bouazza et al. (1996), the authors define p - q envelopes for tested samples only at very low pressures (up to p ~0.5 MPa and q ~0.45 MPa). In order to investigate the influence of OCR values on shear strength, Sultan and co-workers also conducted isotropic consolidation of the Boom Clay at a pressure of 9 MPa, before unloading to a range of effective stresses and shearing. The authors observe differences in the yield behaviour of test samples, dependent upon the prior loading history and found that isotropic compression to stresses significantly above the initial yield stress removes the initial sample anisotropy. Nevertheless they do also acknowledge that saturation of the samples at low effective stresses is likely to lead to some alteration of the clay fabric. In conclusion, they provide a formulation which describes the evolution of the yield curve as a function of stress history.

Bésuelle et al. (2013) plot data from triaxial shear testing in p - q space, taking peak stress values (rather than yield values), which appear consistent with previously reported data. They also note the importance of pre-existing inclusions and fissures on the resulting mechanical response of specimens. Deng et al. (2011) provide shear strength data across a wider range of pressures, for samples taken from the Essen borehole (see Section 3.3.3), as well as making comparison with literature data for clay taken from Mol. Samples were hydrated at *in situ* stresses before being unloaded and sheared at a lower stress. Testing was conducted under drained conditions, which may go some way to explain the significant differences between this envelope and the one put forward by Wildenborg et al. (2003). However, drained conditions were assumed, based on the applied shear rate and evolution in pore pressure was not monitored during the course of testing. The resulting shear strength parameters are estimated as 0.1 - 0.2 MPa and 12° - 14° for effective cohesion and friction angle, respectively.

The authors argue that the observation of lower friction angle values than at Mol must be the result of carbonate content. However, there is little evidence to discriminate the influence of carbonate content from other factors, such as differences in initial void ratio from samples recovered across a range of depths. This highlights the importance of handling critical state data in three dimensions (p - q - v), analysing the relationship between differential stress and effective stress within the context of the associated void ratio. Given the spread in data reported for the Boom Clay from HADES, there is not sufficient data to reliably infer differences in mechanical data between the two sites that might not be conceivably explained by variable in burial histories, as opposed to mineralogy.

3.3.6. Critical state scenario analysis for the Dutch Boom Clay concept

As discussed in Section 3.2.2.5, the critical state approach provides a robust methodology for describing the mode and conditions for deformation of a clay, under a range of stress conditions and scenarios. Several workers have reported parameters for the Boom Clay based on critical state concepts. Values from 0.46 to 1 have been reported for the slope of the CSL, M (Bouazza et al., 1996; Deng et al., 2011; Gens and Alonso, 1992; Monfared et al., 2012). As such, there is sufficient data available to construct a reasonably well-constrained critical state envelope for the Boom Clay at Mol.

The critical state soil mechanics model is made of the zero-tension line, the Hvorslev surface and the Roscoe surface. The Hvorslev surface is given by:

$$q = H_c p' + (M - h) \exp \left[\frac{(e_a - e)}{\lambda} \right] \quad \text{Equation 3-22}$$

where H_c is the soil constant = 0.47, M is the slope of the CSL = 0.81 (Horseman et al., 1993), e_a is the intercept of the CSL with $P' = 1$ MPa, λ is the slope of the normal consolidation line = 0.18, and e is void ratio = 0.68. Therefore the Hvorslev surface can be defined as:

$$q = 0.47 P' + 0.34 \exp \left[\frac{(0.88 - e)}{0.18} \right] \quad \text{Equation 3-23}$$

The Roscoe surface can be given by:

$$q = P' M \sqrt{\left[\frac{P'_c}{p} - 1 \right]} \quad \text{Equation 3-24}$$

where P'_c is the preconsolidation stress = 6 MPa.

Whilst **Figure 3-10** represents the best described data for the Boom Clay within the open literature, it represents the CSSM (Critical State Soil Mechanics) model for the Boom Clay at a depth of 223 m; the depth of the Hades URL at Mol. In order to represent the Boom Clay at representative depths in the Netherlands, data was used from Wildenberg et al. (2003). This study gives data for void ratio, over-consolidation ratio, swelling index and compression index for samples at Weelde (313 m depth) and Blija (453 - 561 m depth). Using the Wildenberg et al. (2003) data, **Figure 3-11** shows the CSSM used to describe the Boom Clay in the current study. As can be seen, the Wildenberg data display a similar form to the Horseman data, with an increased preconsolidation stress (the x-axis intercept of the Roscoe surface). This shows that the data are comparable between the two studies.

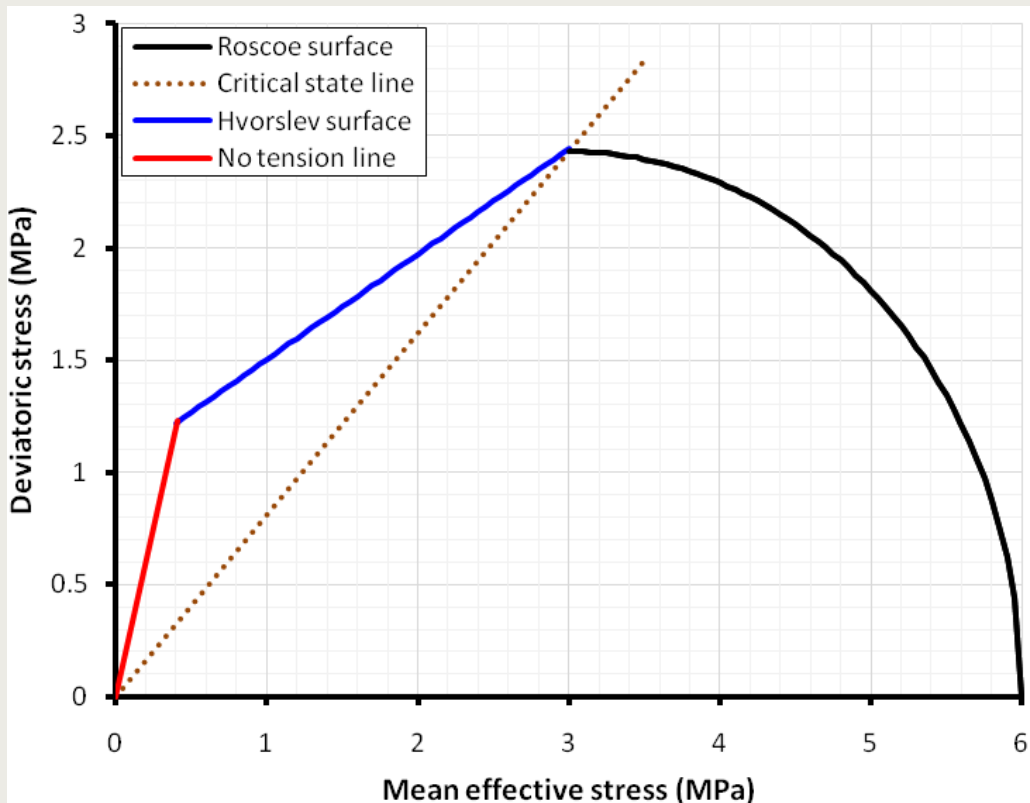


Figure 3-10. The critical state soil mechanics model for the Boom Clay at Mol (Data from Horseman et al., 1993).

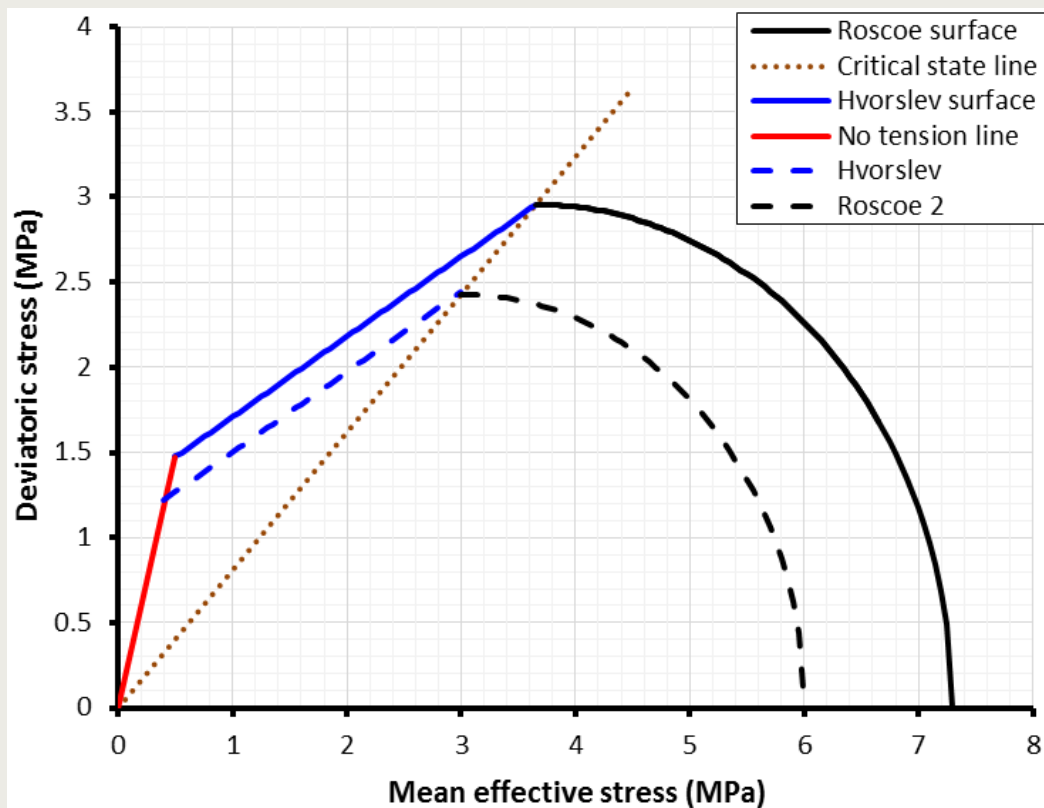


Figure 3-11. The critical state soil mechanics model for the Boom Clay within the Netherlands (data from Wildenberg et al., 2003) compared with Mol (Data from Horseman et al., 1993).

3.3.6.1 Stress state at representative depths

Figure 3-12 shows the stress state expected at representative depths for the Netherlands disposal concept. Data points are plotted for the expected stress state for depths of 400 m, 500 m and 600 m (Section 1.5). The vertical stress (σ_v) was estimated using a density of overlying the Boom Clay of 2.03 g cc^{-1} . Pore pressure was estimated from a hydraulic gradient assuming an overlying density of 1 g cc^{-1} . A minor stress anisotropy has been observed at Mol in Belgium. The horizontal stress components (σ_H and σ_h) have been recorded to be $0.9 \sigma_v$ (Bernier et al., 2007). It has been assumed that this is consistent in the Netherlands. It should be noted that the law of effective stress has been assumed, where effective stress is simply total stress minus the pore water pressure (Section 3.2.1). The stress state at 500 m (plotted as a green cross) is shown with error bars that indicate the variation in effective stress and deviator stress expected over the 400 - 600 m depth range.

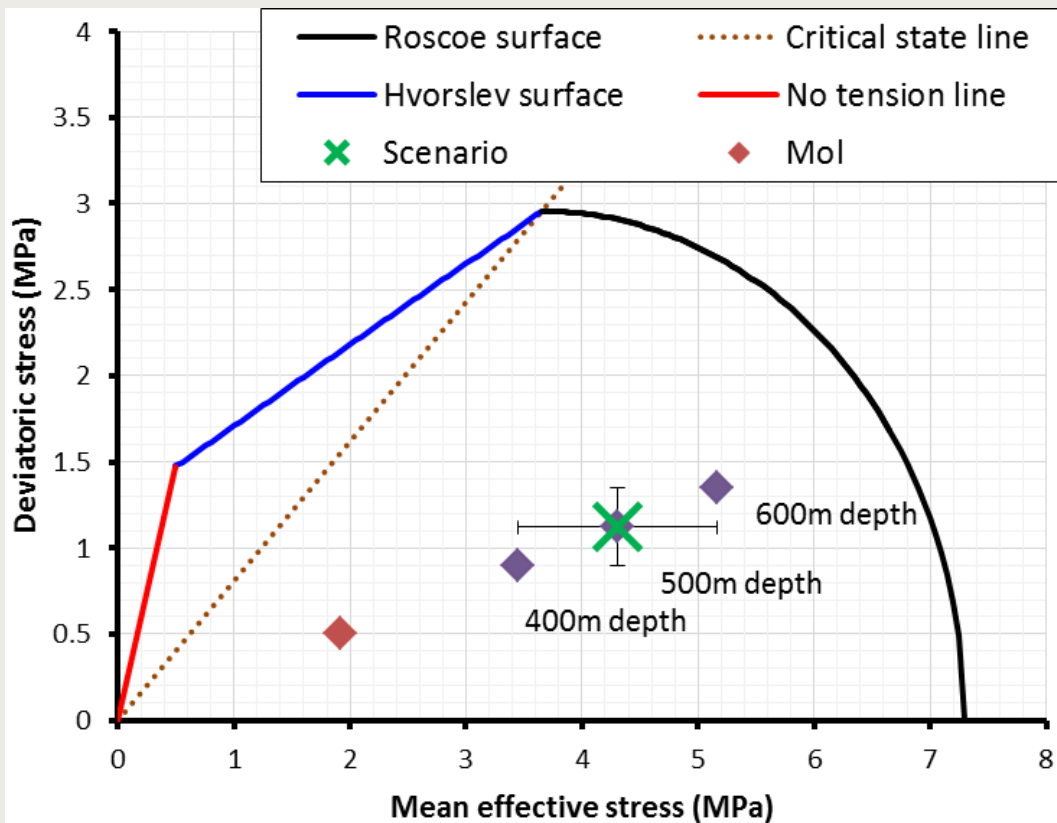


Figure 3-12. The critical state soil mechanics model for the Boom Clay within the Netherlands showing the expected state of effective stress. The location of the effective stresses shows that the Boom Clay is stable at depth and plastic deformation would require a significant change in stress, such as a concentration of stress around a tunnel opening.

Figure 3-12 also gives the stress state at Mol, showing that the increased depth of waste disposal in the Netherlands places the Boom Clay at a more stable stress state (i.e. the stress state is further from the failure envelope). As such, large changes of stress or void ratio are required in order to initiate deformation of the Boom Clay at 500 m depth. A change in stress state, such as a stress concentration created around the periphery of a tunnel opening, is required in order to initiate deformation. Careful repository design and construction can ensure that no such large changes occur as a result of these activities. Nevertheless, it should be noted that the critical state envelope in the Netherlands is based on only one dataset (Wildenborg et al., 2003). Additional testing of high quality core would provide increased certainty in the response of the clay to a range of stress paths.

3.3.7. Swelling behaviour

The volume of a clay-rich material is intrinsically interlinked with the applied stress state. Whilst an increase in the effective stress can result in consolidation (and a reduction in volume), a reduction in stress may likewise lead to sample swelling (characterised by an increase in volume). Chemical changes may also lead to clay swelling and pore fluid composition therefore also acts a direct control on clay volume. As with consolidation, swelling directly impacts the fabric of a clay, potentially affecting physical properties such as hydraulic permeability. Nevertheless, a high swelling capacity encourages closure of voids and fissures and is, therefore, generally seen as a favourable property for a disposal facility host formation. The following sections briefly outline the mechanisms involved in clay swelling, the influence of pore fluid chemistry and the swelling characteristics of the Boom Clay, as described in the literature.

3.3.7.1 Swelling Mechanisms in clay materials

The degree of swelling expected in a clay-rich material is a dependent on: (i) compositional properties that control the swell potential and (ii) environmental factors that control the degree of swelling. Compositional factors include mineralogy, particle size, particle morphology and pore water composition. Environmental controls include the structure and fabric of the material, *in situ* stress conditions (and stress history), density, water content and temperature.

In general, swelling mechanisms can be divided into two forms: mechanical and physico-chemical swelling. Mechanical swelling can be considered as the inverse response to consolidation and is accompanied by dissipation of negative excess pore pressures. Typically, mechanical swelling is the result of stress relief, either by the removal of overburden or elevation of pore fluid pressure.

In contrast, physico-chemical swelling involves a chemical reaction resulting from interaction between water and mineralogical constituents. Physico-chemical swelling relates to the reduction of internal forces within intact clay/rock and is strongly controlled by mineralogy and any associated fabric. In a strongly anisotropic natural material, the swelling response is likely to exhibit an associated anisotropy, resulting from preferential alignment of clay particles.

The microfabric within a high-density clay or compacted argillaceous material can be described in terms of three main features (Figure 3-13): (i) pore spaces, (ii) elementary particle clusters (made up of clay particles or minerals in a parallel configuration) and (iii) particle assemblages. Water is absorbed within the parallel structures formed by (ii) and is termed interlamellar water. This water is bound to clay minerals by a number of mechanisms and is therefore restricted from flow under ambient conditions (Wong, 1998). Arrays of elementary particle clusters in turn form (iii), which constitute the matrix of the material. Any free water is contained within the resulting intramatrix pore space and is able to move in response to a hydraulic gradient at room temperature. In contrast, under normal conditions intracluster water enclosing particle clusters is restricted from flow (Wong, 1998).

This microfabric structure provides the framework within argillaceous materials for two primary forms of internal non-equilibrium swelling to occur: (i) water absorption and (ii) osmotic pressure. The former (i) leads to swelling as a result of hydration of clay surfaces (Low, 1987; Low, 1992). The latter (ii) results in swelling in response to a change in the pore fluid chemistry or a decrease in swelling pressure to below that of the confining stress

(Wong, 1998). Osmosis and water hydration causes swelling of the double layer thickness (Figure 3-14) and expansion at the interlamellar structure, producing intramatrix deformation.

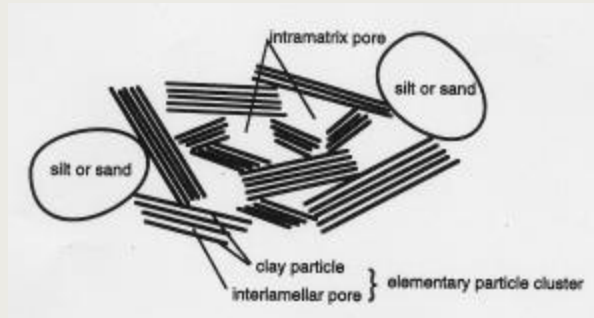


Figure 3-13. Argillaceous material fabric and structure (from Wong and Wang, 1997).

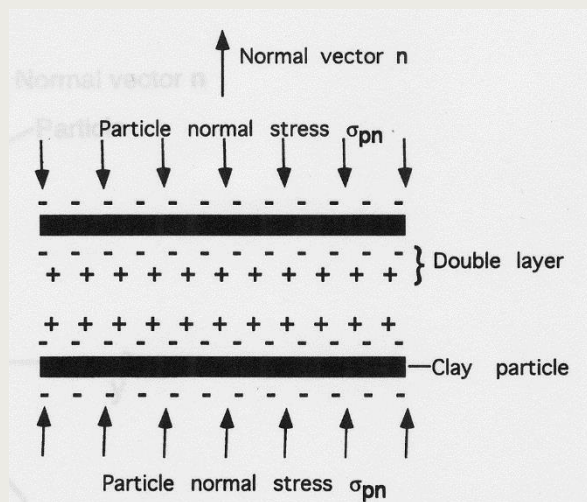


Figure 3-14. Double layers near clay particles (from Wong and Wang, 1997).

3.3.7.2 Swelling properties of the Boom Clay

Methods for determination of swelling properties can be largely split into two approaches; those that determine strain resulting from swelling, and those that measure the required stress to prevent deformation (Hobbs and Jones, 1995). As such, swelling properties for a given material can be characterised in terms of either the swelling potential or the swelling pressure. Swelling potential, $\Delta h/h$, can be described in terms of the change in sample height, Δh , after wetting, in relation to the initial sample height. In contrast, swelling pressure is defined as that required to maintain a constant sample volume during wetting.

A key control on the swelling properties of natural clay is the quantity and mineralogy of those clays present. For example, clays with a high smectite content, are prone to significantly greater swelling than some other clays (Sposito, 1984). In natural materials, and more specifically within the Boom Clay, determination of clay mineralogy can be non-trivial and minerals may not be quantified as separate species, but instead within broader groups (Honty and De Craen, 2011). In addition, the higher the initial dry density of a clay, the greater its propensity to swell in the presence of water. Reported dry density values for the Boom Clay are reasonably typical and range between around 1.45 and 1.75 g/cm³, though most lie between 1.6 and 1.7 g/cm³ (see Appendix Table B0-4). The Atterberg

limits measure for a clay (Appendix Table B0-5) can also be used to predict swelling potential (Lindner, 1976).

Based on reported values (Appendix Table B0-4) the Boom Clay would be classified as having a medium to high swelling potential. These observations are consistent with the clay mineralogy of the Boom Clay and its lightly overconsolidated state, which would suggest a notable capacity for swelling.

Index property	Swelling potential (%)		
	Low	Medium	High
Liquid limit	30-40	40-55	55-90
Plastic limit	15-20	20-30	30-60
Free swell	<60	60-100	> 100

Table 3-1. Classification of clay swelling potential, based on Atterberg limits.

Nevertheless, there are a limited number of studies providing direct measurements of the swelling properties of the Boom Clay. Horseman et al. (1987; 1993) conducted standard 1-D oedometer testing on clay samples retrieved from HADES and measured a resulting swelling pressure of 0.82-0.92 MPa (Horseman et al., 1993). Additional data (though with a higher degree of experimental uncertainty) were also obtained from 1-D consolidation tests, yielding swelling pressure of 0.3, 1.1 and 1.7 MPa. Volckaert et al. (1995) also report a swelling pressure of 0.9 MPa, though the associated experimental data is not provided. A free-swelling approach was taken by Sultan et al. (2010), leading to a slightly lower value of 0.48 MPa. Whilst these findings demonstrate the capacity for the Boom Clay to swell, it should be noted that such pressures are significantly lower than those generated by engineered clay barrier materials such as MX80 bentonite (Graham et al., 2015). However, this does not impact the clay’s propensity to self-seal, which is primarily driven by its exceptional propensity to creep, leading to closure of voids and fissures over very short timescales (see Section 3.4.4).

3.3.7.3 Influence of pore fluid chemistry

The influence of pore fluid chemistry on the swelling capacity of clays is well-established. Generally, characterisation of the physical properties of the Boom Clay in Belgium has been conducted using pore fluid synthesised to be representative of the *in situ* water chemistry. As discussed in Section 2.1, notable differences are expected between the pore fluid chemistry at HADES and that found in a candidate repository location in the Netherlands.

However, there have been very few studies examining the influence of salinity on the physical properties of the Boom Clay. A number of studies demonstrate the potential impacts for highly swelling clays such as bentonite, where the effects are likely to be more pronounced. Experiments on MX80 and FEBEX bentonite show that overall the swelling capacity decreases with increasing salinity (Castellanos et al., 2008; Herbert et al., 2008; Wang et al., 2014). Experiments by Di Maio et al. (2004) compare clays with different smectite clay contents, using a range of pore water compositions in order to investigate the impact of mineral composition on volumetric response. Their results show a clear sensitivity to pore water salinity with increasing smectite content. A decrease in compressibility and consolidation coefficients is also observed with increasing pore water salinity, with the exception of high smectite contents clays under low stress conditions (Di Maio et al., 2004).

Fewer studies are available investigating pore fluid chemistry effects on the hydromechanical properties of the Boom Clay. Deng et al. (2011) compared data from consolidation testing of four Boom Clay samples from Essen (between 226-540 m), hydrated using either synthetic saline fluid or distilled water. They demonstrate that the form of the relationship between void ratio and permeability is relatively unaffected by pore fluid chemistry. However, their findings are not presented in the context of the applied stress state. It is therefore unclear to what degree the swelling state (and hence void ratio) of each sample is impacted by pore fluid chemistry, for a given effective stress. Without this additional data it is not appropriate to assume the influence of pore fluid chemistry on the hydromechanical properties of the clay will be negligible.

The influence of pore fluid salinity on swelling properties was also examined by Nguyen et al. (2013). They conducted 1-D oedometer tests on Boom and Ypresian Clay samples, using pore fluid of increasing Na content. Laboratory observations indicate that changes in Na+ concentration can notably alter the swelling state (Figure 3-15) and the hydromechanical properties of the clay. In particular, increased salt concentration resulted in an increase in the oedometric modulus, E_{oed} , hydraulic permeability and consolidation coefficient. Changes were more pronounced for the Ypresian Clay, most likely resulting from the higher smectite content.

Nevertheless, the data relating to salinity effects appears to be relatively limited for the Boom Clay. Additional testing to ascertain the impact on hydromechanical properties in the Netherlands (using appropriate pore fluid chemistries) would be beneficial.

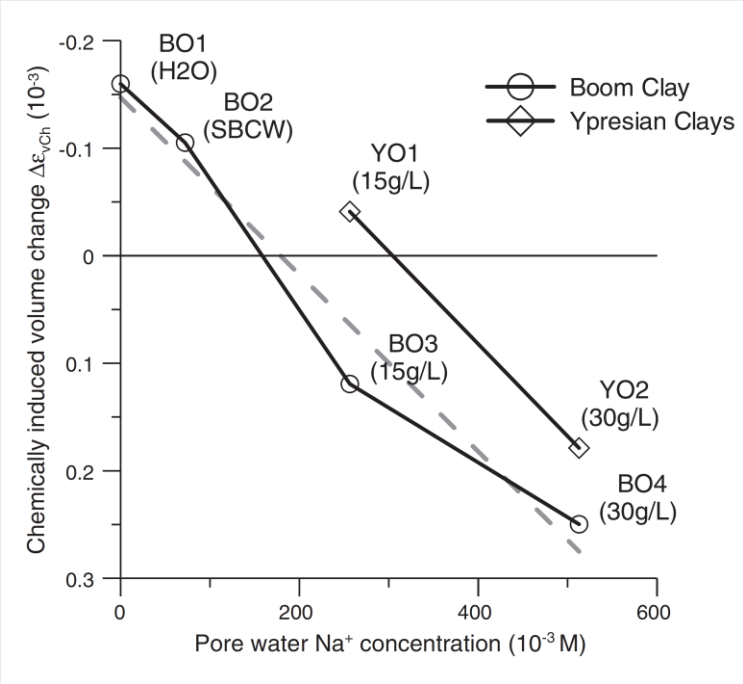


Figure 3-15. After Nguyen et al. (2013). Chemically induced volume change versus pore water Na+ concentration during solution injection.

3.4. Structural characteristics of the Boom Clay

Structural features within the Boom Clay will influence its hydro-mechanical properties on a range of scales. The development of these features is controlled both by the initial physical properties of the clay and environmental effects (e.g, temperature, stress field, etc.). A detailed burial history includes data on the magnitude and orientation of the

stress field that a rock has experienced. This allows us to link the deformation process with the associated stress levels. The potential deformation processes associated with argillaceous media have been discussed in Section 3.1. In this section, structural characteristics of the Boom Clay are briefly discussed.

3.4.1. Sedimentary fabric

The Boom Clay has sub-horizontal laminations, which dip at approximately 1-2° to the north-east. The laminations are highlighted by changes in clay-particle rotation and grain size changes (Dehandschutter et al., 2005a). This fabric is a result of slow deposition in a calm environment (see Chapter 1). Scanning Electron Microscope (SEM) imagery of these laminations show a well-developed preferred alignment of the clay particles parallel to these lamination surfaces. This strongly developed fabric is responsible for the strong anisotropy observed in its mechanical response (Bastiaens et al., 2007, Wemaere and Marivoet, 1997, Bastiaens and Demarche, 2003).

Al Mukhtar et al. (1996) studied fabric development in reconstituted Boom Clay under different applied axial loads. They used a conventional oedometer to consolidate three samples under axial stresses of 1, 5, and 15 MPa, respectively. The specimen loaded to 1 MPa was shown to have a heterogeneous arrangement of porosity, whereas the samples loaded to 5 and 15 MPa can be seen to have a more homogeneous distribution of particle arrangement. The reason for this was attributed to the alteration of pore spaces associated with the higher stresses.

3.4.2. Fracturing and faulting

Dehandschutter et al. (2005a) and Mertens et al. (2003) have carried out detailed studies on the discontinuities present in the Boom Clay. These papers describe discontinuities found both at field exposures and underground at the HADES URL.

Both micro-scale and meso-scale faults have been recognised in the Boom Clay Formation. Meso-scale faults can be seen in the Kruikeke area, south-west of Antwerp in Belgium (**Figure 3-16**). These faults are spaced approximately 5 m apart, are approximately 5 m long and a maximum displacement of about 1 m. An average trend of 120° and a dip of 50° to the north-west (Dehandschutter et al., 2005a) was also noted.

Micro-scale discontinuities comprise of centimetre-scale (3 - 6 cm) slickensides, which are common at Boom Clay exposures. Dehandschutter observed an apparently random distribution for these discontinuities, though suggested they may be more common in clay-rich layers. Two recognised sets of slickensides were noted; those with a dominant strike of approximately 120° and a secondary group, with a strike of around 040°. Both sets were observed to dip at 50 - 60° (Dehandschutter et al., 2005a).

The most abundant discontinuities observed within the formation are Mode I vertical fractures, which are often more apparent after weathering. Nevertheless, they do not generally appear to be associated with excavation and are the result of natural processes (Mertens et al., 2003). The orientation of these fractures is not dissimilar to the previously described meso and micro-scale faults. The primary population display a consistent strike of 130°, whilst a secondary population strikes at around 30°. These joints are consistent throughout the whole of the Boom Clay and can be considered a regional feature (Dehandschutter et al., 2005b). Dehandschutter argued that these extensional features relate to a large-scale extensional event in a nearly NE-SW orientation. Several of the investigated jointed areas are also highlighted by a change in bedding orientation in the vicinity of the jointing (Dehandschutter et al., 2004; 2005a). This change in bedding is

associated with a shear component, the clay particles become aligned by grain-boundary sliding and particle reorientation; this results in localised reductions in porosity.

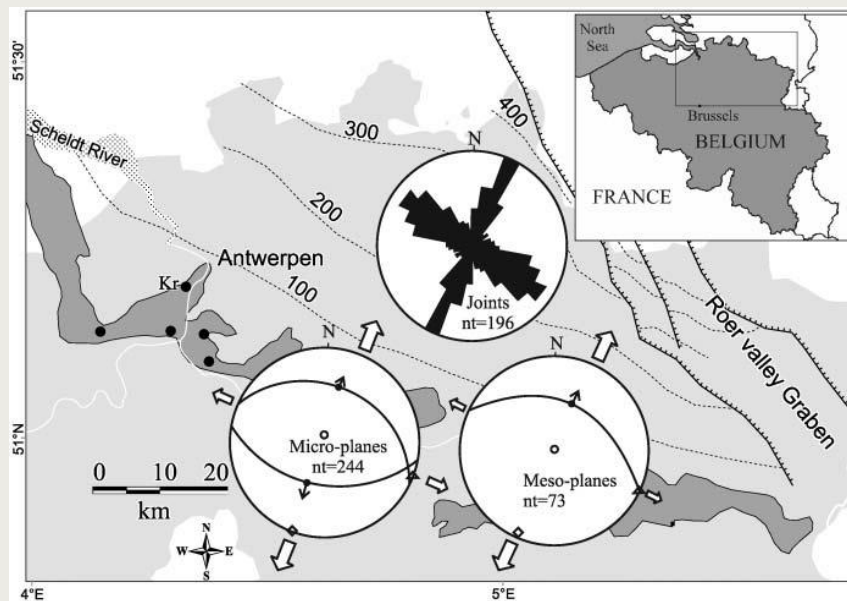


Figure 3-16. Location map of the Boom Clay (grey area). • studied clay-pits. Structure contours of the base of the Boom Formation in metres outlined by dashed lines. Lower inset diagrams: stereographic projections (equal area, lower hemisphere) of the mean orientation of micro shearplane and mesoplane faults (great circles), with striation azimuth indicating shear sense (arrows). Upper inset diagram shows rose diagram of joint planes. Kr, Kruibeke clay pit. From Dehandschutter *et al.* 2005b.

Bulk characteristics of the Boom Clay are clearly dependent on burial and exhumation, but field observations also highlight the formation of localised discontinuities over the clay's history. Dehandschutter *et al.* (2005a) presents observations of these features within a Critical State framework, which can be used as a powerful tool for understanding textural, structural and physical changes in clay fabric as a result of an evolving stress field.

3.4.3. Excavation damage zone

Understanding damage development in the host formation, as a result of excavation processes, is crucial to safety case development for geological disposal facilities. Local perturbations in the effective stress field have the potential to deform the host rock in a number of ways during the excavation and backfill of repository infrastructure. Such damage is likely to alter the hydromechanical properties of the bulk rock, which may continue to evolve with time, impacting its capacity for radionuclide transport.

The construction and development of the Hades URL has enabled a detailed study of the fracture pattern created within the Excavation Damage Zone (EDZ). Mertens *et al.* (2004) report that large shear planes are generated during excavation of horizontal galleries, as a result of stress redistribution, as shown in **Figure 3-17**. The construction of the shaft at Mol displayed a circular pattern of shear planes. A seismic and borehole campaign was initiated to characterise the EDZ along the main gallery at Mol. The large shear planes were observed to have a strike approximately perpendicular to the tunnel axis, with many of the planes becoming steeper further away from the second shaft constructed at Mol. **Figure 3-17** shows the idealised geometry of the large shear planes, with respect to the excavated tunnel (Mertens *et al.*, 2004). The extent of the EDZ is influenced by the

presence of any natural fractures or heterogeneities and is a function of the initial stress field, the bulk material properties, and the geometry of the tunnel (Blumling et al., 2007).

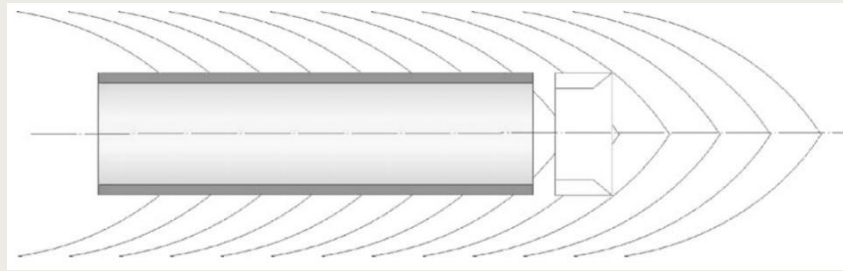


Figure 3-17. Schematic representation of a vertical cross-section through the connecting gallery at Mol showing the typical symmetrical form of the encountered shear planes (from Mertens et al., 2004).

3.4.4. Sealing properties

Whilst the potential to generate an EDZ is well understood, such features are by no means permanent, as clays often display a significant capacity for time dependent sealing. Bastiaens et al. (2006) define sealing as the reduction of fracture permeability by any hydromechanical, hydrochemical, or hydrobiochemical processes. In contrast, healing of discontinuities requires a return of the material to its original mechanical strength (Bastiaens et al., 2006).

The sealing of discontinuities is thought to result from a combination of processes. Bastiaens et al. (2006) quote consolidation and creep to be the main contributors to sealing. Certainly it is clear that the presence and mobility of water (Blumling et al., 2007) is a key governing factor impacting the sealing capacity of the clay.

Shortly after the construction of the connecting gallery at Mol a network of radial piezometers was installed around the gallery to monitor the temporal evolution of the pore pressure distribution, as part of the SELFRAC project. The array of piezometers extended up to 40 m into the clay around the excavated tunnel. Bastiaens et al. (2006) report that at the time of study pore pressure could only be measured 30 cm into the clay, indicating that no unsealed fractures network exists beyond a few decimetres into the host formation.

The SELFRAC project also analysed seismic measurements from an encased borehole. Changes in seismic velocities, frequencies and amplitudes were measured with time, as an indicator of damage and sealing evolution. Over a period of 30 to 50 days the peak amplitudes increased and measured waveforms became more similar. These geophysical changes were attributed to the sealing of the EDZ (Bastiaens et al., 2006), though some inconsistency in observations made interpretation non-trivial.

Sealing of discontinuities within the Boom Clay is known to be exceptionally rapid (Bernier et al., 2007), as shown by micro-computed tomography (μ CT) image analysis of an artificially fractured clay sample (Bastiaens et al., 2006). Figure 3-18 shows the initial fracture and the result after saturation. The second image is taken after 4.5 hours and it appears to have partially sealed. Hydraulic conductivity measurements were made alongside these images and the resulting values were seen to recover to the same order of magnitude as an undisturbed sample, being approximately 10^{-12} m/s (Bastiaens et al., 2006).

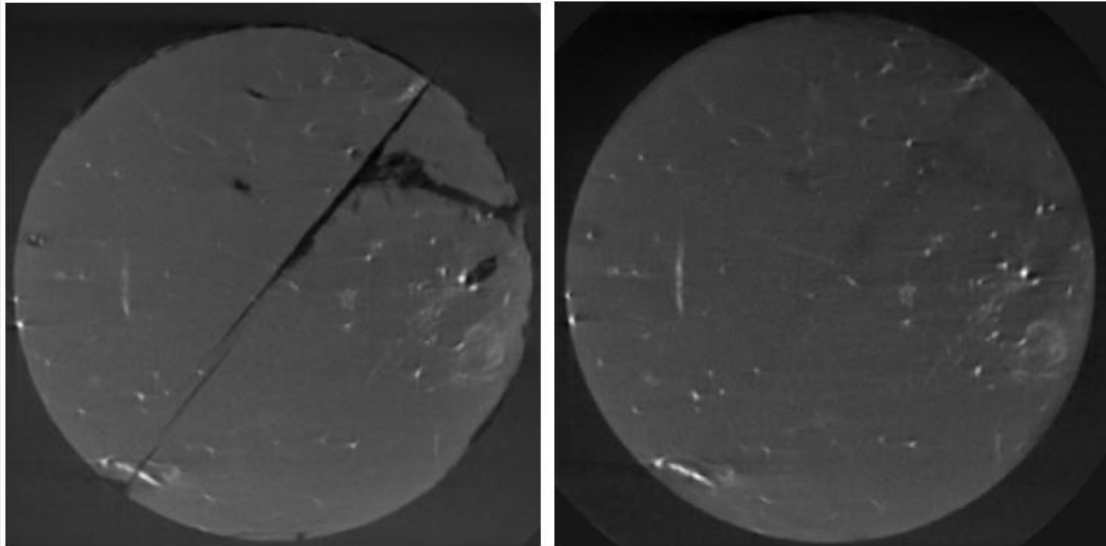


Figure 3-18. SELFRAC Self-sealing experiment. Image on the left shows the initial fracture within the sample, the image on the right shows sealing of the fracture after hydration. From Bastiaens et al. 2006.

Similar work was carried out by Li et al. (2013) as part of the TIMODAZ project. A fractured Boom Clay sample was placed in a constant volume cell for 4-6 days without further hydration. After this period of time the fractures could not be visualised by CT scans. Furthermore, permeability tests were carried out in two orientations and they both showed similar values, suggesting the fractures had already sealed before the test. This test approach was developed further to evaluate the effect of temperature on both intact and fractured samples. The intrinsic permeability remained constant with heating, suggesting the structure of the Boom Clay was not altered with increasing temperatures up to 80 °C (Li et al., 2013). It is not clear whether these findings hold for temperatures above 80 °C without additional testing.

SCK-CEN has investigated several scenarios relating to sealing issues in which the hydraulic conductivity of the galleries was modelled to values three to six orders of magnitude above that of intact Boom Clay. Calculations for these scenarios indicate that even under these extreme variations in conductivity there would only be a limited contribution of such a pathway to the potential for release of radionuclides (Blumling et al., 2007).

A significant body of work exists demonstrating the excellent self-sealing capacity of the Boom Clay. These favourable properties imply a reduced potential for long-term damage to facilitate transport of radionuclides through the EDZ. Intuitively it seems likely that this propensity for self-sealing will remain or be enhanced at a depth of 500 m. However, there is a shortage of data examining the potential for self-sealing in the Boom Clay at higher effective stresses and further testing will be required to support this hypothesis.

3.5. Mechanics summary

The mechanical properties and behaviour of the Boom Clay at HADES have been well-characterised over several decades. No experimental measurements could be found relating to the elastic moduli for the Boom Clay in the Netherlands and there is a paucity of such data for relevant depths in Belgium. However, it is possible to make inferences about other mechanical aspects of the formation in relation to the Dutch Boom Clay concept. In particular, it seems likely that:

- The clay will have a lower OCR and potentially be closer to a normally consolidated state;
- For a lithologically identical clay to that at HADES, a clay void ratio of -0.6 ± 0.05 might be expected;
- The form of the CSSM yield envelope can be estimated;
- The increased depth of waste disposal in the Netherlands places the Boom Clay at a more stable stress state (i.e. the stress state is further from the failure envelope);
- Large changes of stress or void ratio will be required in order to initiate deformation of the Boom Clay at 500 m depth;
- Expansion of the dataset will refine our understanding of the form and location of the yield envelope in p - q space;
- The clay will demonstrate a reasonable capacity to swell, though large swelling pressures are unlikely to be generated;
- Differences in pore fluid chemistry between HADES and a repository location in the Netherlands may result in differences in the hydromechanical properties of the clay.
- A high capacity for self-sealing of the clay is likely, though this has yet to be demonstrated.

Recommendations

- Additional experimental testing of the Boom Clay from HADES (at higher effective stresses) providing an improved understanding of:
 - The elastic response of the clay;
 - The elastic moduli and associated anisotropy;
 - The influence of compaction state on the UCS of the clay;
 - Local variability in the mechanical response (elastic and inelastic) of the clay;
 - The influence of stress history on mechanical anisotropy (elastic and inelastic) of the clay;
 - Anisotropy in the swelling response of the clay;
 - The influence of salinity on mechanical and geotechnical properties;
 - The impact of depth on self-sealing capacity and rheological behaviour of the clay.
- Recovery of well-preserved core from appropriate locations and depths is required to provide an improved understanding of:
 - The burial history of the region and associated impacts on mechanical properties of the clay;
 - Spatial variability of the mechanical properties (elastic and inelastic) of the clay;
 - The influence of lithological differences on geomechanical properties (e.g. the influence of carbonate content on yield behaviour);
 - Existing mechanical anisotropy.

In particular, predictions of yield (especially wet-side deformation scenarios) are currently based on an extremely limited dataset. Uncertainty would be much reduced by consolidation testing of the Boom Clay retrieved from appropriate depths in the Netherlands, allowing better constraint of the preconsolidation stress and, hence, consolidation state, of the clay.

Whilst shear strength data is available to estimate dry-side yield, additional shear strength testing at higher effective stresses would also be beneficial.

4. Transport processes

Fluid flow processes play a key role in the safety assessment of a geological repository; they control processes including (i) rehydration of the host formation, plugs, seals and engineered barriers, (ii) transport of solutes and changes in pore fluid chemistry (iii) canister corrosion processes and (iv) transport of radionuclides away from the waste canisters. Of primary importance is identifying the dominant mechanisms for specific transport scenarios. For example, selection of a low permeability host formation ensures that advective hydraulic transport is limited and diffusional processes predominate. The following sections consider hydraulic processes and properties of the Boom Clay, the role of osmosis and coupled flow, diffusional processes and the migration of gases.

4.1. Hydraulic processes

4.1.1. Intrinsic permeability

Darcy's law states that the volumetric flow (Q) of water in a porous medium is linearly proportional to the hydraulic gradient applied. For a one-dimensional hydraulic flow, Darcy's law can be written as:

$$Q = \kappa A \left(\frac{dh}{dx} \right) = - \frac{\kappa A}{\rho_w g} \left(\frac{dP_p}{dx} \right) \quad \text{Equation 4-1}$$

where κ is the hydraulic conductivity ($\text{m}\cdot\text{s}^{-1}$), A is the cross-sectional area perpendicular to the flow direction (x), h is the hydraulic head (m), ρ_w is the density of water ($\text{kg}\cdot\text{m}^{-3}$) and dP_p is the pore pressure gradient (Pa). The quantity $q = Q/A$ ($\text{m}\cdot\text{s}^{-1}$) is known as the Darcy velocity or specific discharge, which describes the average velocity of the fluid moving through the cross-sectional area A of a porous medium. Hydraulic conductivity is a complex parameter influenced by the scale of the medium (Fallico et al., 2010).

In order to exclude the influence of the transmitted fluid, a fundamental property of the geological medium is defined, known as the intrinsic permeability (or the coefficient of permeability), k_i (m^2). This quantity can be related to the hydraulic conductivity, κ ($\text{m}^2\cdot\text{s}^{-1}$), by:

$$k_i = \frac{\kappa \eta_w}{\rho_w g} \quad \text{Equation 4-2}$$

where η_w and ρ_w are the absolute viscosity and density of water, respectively, and g is the acceleration due to gravity. At 20 °C the absolute viscosity of water is 1.002×10^{-3} Pa.s and density is $0.9982 \text{ Mg}\cdot\text{m}^{-3}$ (De Marsily, 1986). Because of their strong bedding fabric, clays are generally expected to exhibit a significant hydraulic anisotropy. As such, intrinsic permeability in an anisotropic material is more fully defined using a tensor, such that:

$$\mathbf{k} \equiv \begin{bmatrix} k_{11} & k_{12} & k_{13} \\ k_{21} & k_{22} & k_{23} \\ k_{31} & k_{32} & k_{33} \end{bmatrix} \quad \text{Equation 4-3}$$

However, where anisotropy is strongly associated with one plane, as is the case for well-bedded clays, it can be assumed that the material is transversely isotropic. In such a case, permeability can be expressed by one value parallel to bedding, k_{xx} , and one perpendicular

to bedding, k_{zz} . The degree of hydraulic anisotropy of a clay can then be described in terms of the anisotropy ratio, k_{xx}/k_{zz} .

Heterogeneity and the influence of scale must also be considered when defining hydraulic properties of clay formations. In particular, care must be taken to select a suitable Representative Elementary Volume (REV) both in relation to measurement of hydraulic properties and to appropriate parameterisation of numerical simulations.

4.1.2. Specific storage

The specific storage, S_s , of a porous rock is defined as the volume of water a the rock unit releases in response to a unit change in hydraulic head (Hantush, 1960);

$$S_s = \frac{1}{V_a} \frac{dV_w}{dh} = \frac{1}{V_a} \frac{dV_w}{dp} \frac{dp}{dh} = \frac{1}{V_a} \frac{dV_w}{dp} \gamma_w \quad \text{Equation 4-4}$$

where S_s is the volumetric specific storage (m^{-1}), V_a is the bulk volume of that portion of rock from which water is released (m^3), dV_w is the volume of water released from storage (m^3), dp is the decline in pressure (Nm^2), dh is the decline in hydraulic head (L) and γ_w is the specific weight of water (Nm^3).

4.1.3. Experimental determination of hydraulic permeability

The hydraulic conductivity of the Boom Clay has been extensively studied at the HADES URL in Belgium. As described in Equation 4-1, hydraulic conductivity (κ) quantifies the capacity for water to be transmitted through a porous medium. To allow for anisotropy of clay fabric, conductivity may be quantified with respect to flow parallel to bedding or perpendicular to bedding. For a shallow, dipping clay such as the Boom Clay, this is often defined in terms of the orientation in the field; i.e. horizontal conductivity, κ_h , or vertical conductivity, κ_v . Generally, the latter is the most commonly quoted value. Several methodologies exist to determine these properties, both in the laboratory and during *in situ* testing.

In the laboratory, conductivity of a test sample is generally measured using a permeameter cell. For clays and mudrocks, such apparatus must have very low leakage rates and are often specifically designed to measure the small flows involved for low permeability materials. Conductivity is directly related to the interconnected porosity of a given material and, as such, correct measurement requires the potential influence of effective stress to be allowed for (see Section 3.2.1). This is particularly important for testing clays, where testing under the appropriate *in situ* effective stress is crucial to determining conductivity. Testing conducted under atmospheric conditions will likely lead to swelling of the clay (resulting in additional inflow until steady-state is reached) and a likely over-estimation of hydraulic conductivity.

It should also be noted that use of inappropriate pore fluid may result in chemical swelling/consolidation, similarly impacting hydraulic conductivity as a result (Section 3.3.7.3). As such, hydraulic testing should be conducted with pore fluid in chemical equilibrium with the clay being tested. Once samples are subjected to appropriate *in situ* conditions, they are allowed to return to a fully saturated state, before hydraulic testing begins. Generally, porous filter discs are used to distribute flow of water across the sample injection surface. Water is then injected at the upstream inlet, either at a constant flow rate or by applying a constant pressure head. The resulting outflow response is then monitored at the downstream outlet, until a steady-state is reached, at which time flow

into the sample is equal to flow out. Permeability can then be estimated by assuming Darcian flow (Equation 4-1 and Equation 4-2).

More recent laboratory methodologies include pulse transient and oscillating pore pressure methods. Both use the same essential equations to determine hydraulic conductivity, diffusivity and inter-connected porosity. A cylindrical rock sample is saturated with a pore fluid and connected to upstream and downstream reservoirs, which allow the system to be equilibrated to an elevated pore pressure. For the oscillating method the downstream volume has to be as small as practicable. In the pulse test the upstream reservoir pressure is instantaneously elevated above baseline pressure and allowed to decay. The oscillating approach involves continually oscillating the upstream pressure around the baseline value (Elkhoury et al., 2011; Kranz et al., 1990). The pulse test measures a change in hydraulic head over a finite time period, whilst the oscillating test allows measurement of the steady-state pressure amplitude ratio between the reservoirs. As such the physical conduction of fluid through the pore spaces of the material does not occur, but rather an associated pulse in local pore pressure. As with pulse transient methods, such an approach does not, therefore, provide a measure of hydraulic conductivity during steady state-flow and may not elicit the true hydraulic response of the material as a result.

For *in situ* measurements, single point or multi point piezometers may be used. These can be considered as permeameters, especially when they are used to measure flow. Piezometers can be used to cover a wide area of interest and produce permeability information on a construction or regional scale (Bernier et al., 2007; Gedeon et al., 2012). Bernier et al. (2007) describes single-point steady-state measurements performed using piezometers installed radially to the test drift in the HADES URL. They describe this method as reliable and accurate technique to measure hydraulic permeability.

4.1.4. Hydraulic properties

As discussed in Chapter 2, the regional burial history of the Boom Clay strongly influences its porosity, fabric and, in turn, its permeability. As such, hydraulic data should always be considered in the context of the associated depth interval and location from which it has been retrieved. A summary of some of the reported hydraulic properties for the Boom Clay is given in **Appendix Table B-06**, along with the associated depth and void ratio data (so as to provide this additional context). The majority of hydraulic data present in the literature relates to material taken from HADES, which has been very well-characterised. For the Boom Clay at these depths, these data give an average void ratio, hydraulic conductivity perpendicular to bedding, hydraulic conductivity parallel to bedding and hydraulic anisotropy of 0.619, $1.7 \times 10^{-12} \text{ m}^2$, $4.1 \times 10^{-12} \text{ m}^2$ and 2.5, respectively. However, it is important to recognise that variations in the mineralogical content of a given sample are likely to impact the measured hydraulic properties.

A significant body of work exists quantifying hydraulic behaviour of the clay at Mol. Much of this work results from a series of EC-funded research projects in the 1990's, including the MEGAS, PEGASUS and PROGRESS projects (Horseman and Harrington, 1994; Volckaert et al., 1995; Haijtink and Roswell, 1998; Harrington and Horseman, 1999). Project findings from laboratory testing at BGS and SCK-CEN are reported in **Appendix Table B-06**, though these values do not fully reflect the large number of samples tested. These studies also provide the majority of the laboratory observations for specific storage at the Mol site, which range between $\sim 8 \times 10^{-6}$ to $9 \times 10^{-5} \text{ m}^{-1}$. Findings from these studies (and additional observations shown in **Appendix Table B-06**) indicate that hydraulic data from Mol are reasonably consistent and imply the formation has relatively homogenous properties for a given depth interval. *In situ* test results from HADES also suggest that laboratory

measurements scale reasonably well to field scale (**Appendix Table B-06**; Volckaert et al., 1995; Yu et al., 2013).

4.1.5. Key factors influencing hydraulic properties

An in-depth review of research conducted on the hydraulic properties of the Boom Clay in Belgium is given by Yu et al. (2011; 2013). They discuss a range of potential influencing factors and, based on observations from a range of test programmes, they argue that sample size, applied hydraulic gradient and pre-existing sample damage have limited impact on reported values. These observations are also consistent with findings from a number of earlier reports (Volckaert et al., 1995; Haijink et al., 1998). Review findings by Yu et al. (2011; 2013) lead to estimated geometric mean values for κ_v and κ_H (at HADES) of 1.7×10^{-12} and 4.4×10^{-12} m/s, respectively, with a vertical anisotropy of about 2.5. These values are almost identical to those calculated in this report (**Appendix Table B-06**), highlighting the relatively high level of certainty for the properties at the Mol site. The authors also note that higher κ values are observed in the more silty zones, above and below the Putte and Terhagen Members, but quoted values can still be considered as relatively low (10^{-12} to 10^{-10} m.s⁻¹). Whilst the hydraulic properties of the Boom Clay at Mol are clearly well-constrained, in the following section we describe potential factors which may lead to differences in these properties in a potential repository in the Netherlands.

In particular, there are three primary questions which must be considered when attempting to extrapolate hydraulic properties measured at Mol to the context of a Dutch repository: (i) how spatially variable are the hydraulic properties of the clay? (ii) what is the likely impact on hydraulic properties at greater depth of burial? (iii) what might the impacts be of any differences in burial history? In this section, we attempt to address some of the key certainties and uncertainties associated with these questions, before suggesting recommendations for the future.

A number of studies in recent years have focussed on assessment of the degree of homogeneity within the Boom Clay formation both laterally (on a regional scale) and stratigraphically. Aertsens et al. (2004) investigated this latter aspect by measuring transport properties in a large number of cores, taken from throughout the clay formation at a Mol borehole. Samples were tested under two experimental arrangements; (i) pulse injection experiments and (ii) constant head permeametry. Their findings display a high level of consistency in hydraulic conductivity throughout the upper 90 m of the formation, indicating a relatively high degree of homogeneity within the Boom Clay succession.

It should be noted, however, that for both test methodologies hydraulic experiments were not conducted under *in situ* conditions, but instead samples were unconfined. This is acknowledged by the authors who argue that the resulting measurements are not dissimilar to previous values for laboratory testing of Mol material. Nevertheless, the influence of effective stress on hydraulic conductivity within the Boom Clay is well-recognised (see below). Testing in the absence of *in situ* pressures is likely to be most severe on deeper samples, where swelling will lead to an over-estimation of permeability. In addition, the constant head tests were conducted using de-ionised water, rather than pore water in chemical equilibrium with the clay, which may lead to a further over-estimation of conductivity.

Whilst some variations in hydraulic conductivity can be linked to stratigraphy, the above methodological factors indicate that absolute conductivity values may be less reliable. Effects resulting from the absence of lithostatic pressures and use of de-ionised water are likely to be more significant in samples with a higher clay content. It is therefore also non-trivial to differentiate between lithological controls on conductivity, as opposed to clay content impacting sample response under test conditions. Nevertheless, measured values

do indicate a reassuringly low degree of variation in conductivity throughout the drilled succession.

In order to investigate regional variability within the formation, Wemaere et al. (2008) used a similar approach to examine the hydraulic conductivity of the Boom Clay at four borehole locations across Belgium (Doel, Zoersel, Weelde and Mol). Minimal additives were applied to drilling fluids in order to maintain sample integrity and a careful storage procedure ensured good preservation of sample material. Permeability testing was conducted using a standard constant head approach and, as with Aerstens et al. (2004), samples were injected with de-ionised water. Their findings indicate that the hydraulic conductivity of the Boom Clay can be considered as homogenous at a formation scale, with the Putte and Terhagen members being the most homogeneous and least pervious within the formation. They also demonstrate a clear association between grain size and hydraulic conductivity, the one increasing with the other, and propose a site-specific relationship between these two parameters.

However, it should be noted that testing was not conducted under *in situ* stress conditions and the authors acknowledge that this is likely to have resulted in an over-estimation of measured conductivities, suggesting that absolute values may not be as reliable as the observed form of the relationship. They also highlight that the comparison of conductivities between some borehole locations (Doel and Mol) cannot be reconciled by grain size alone and attribute this discrepancy to differences in compaction state of the clay, which is evidenced by porosity measurements. Whilst current depth may be of importance, they note that prior geochemical and burial history will also play a role in determining the resulting physical properties of the clay.

Based on data collected from throughout the literature, Yu et al. (2013) provide a statistical analysis which again highlights the importance of both burial history and lithological variations in grain-size. However, they state that examination of other potential influencing factors (e.g. mineralogy, carbonate content, etc.) could not be conducted because of the current paucity of data. Nevertheless, the authors conclude that hydraulic conductivity values are remarkably consistent (particularly within the Putte and Terhagen members), in spite of the relatively large geographical area under consideration. These findings suggest that the Boom Clay at a Netherlands location, will likely display broadly similar hydraulic properties to that at Mol. Lithological differences are likely to lead to smaller magnitude differences in these properties, though well-preserved core is required to determine such impacts with certainty.

Aside from differences caused by lithological variability at the regional scale, higher effective stress conditions and distinct burial histories will also impact the hydraulic properties of the clay. Anisotropy of the clay fabric is intuitively likely to increase with depth. The impact of bedding orientation on hydraulic flow in the Boom Clay has been quantified in a number of studies (Horseman et al., 1993; Horseman and Harrington, 1994; Volckaert et al., 1995; Harrington and Horseman, 1999; Hildenbrand et al., 2002). Reported values for hydraulic anisotropy can be relatively significant and generally range from around 1 to 3, with an average value ~2.5 (**Appendix Table B-06**).

Wemaere et al. (2008) present laboratory measurements for samples taken from different depths and locations within the formation and give both vertical and hydraulic conductivities. However, calculating the resulting hydraulic anisotropy values from their presented data it is clear that the need to uncouple the effects of lithological variation from burial history does not allow for reliable statements to be made relating to the controls on anisotropy without further study. Whilst most data within the literature relates to clay recovered at the depth of HADES, it seems likely that the ratio between horizontal

and vertical conductivities will be more pronounced (>2.5) at greater depths, because of the impact of the overburden on the clay bedding fabric. However, additional test data relating hydraulic anisotropy to relevant burial depths is needed to provide more detailed estimates.

As has previously been discussed, void ratio within the Boom Clay is relatively sensitive to burial history. Given that a significant reduction in void ratio is observed on compaction, it is intuitive to expect a similar reduction in permeability. This is backed up by statistical analysis of borehole observations in the Boom Clay, conducted by Yu et al. (2013). The authors noted a strong stratigraphic trend which could be related to grain-size characteristics, yet they also attributed additional regional variation to differences in porosity (Figure 4-1) resulting from burial of the clay.

Many studies examining the influence of effective stress on conductivity of the Boom Clay were reported during the late 1980's and throughout the 1990's. Early work by Horseman et al. (1987) demonstrated that hydraulic conductivity of the clay decreased with increasing effective stress, following an approximately linear relationship between k and the logarithm of effective stress (Figure 4-2).

Later studies (Horseman and Harrington, 1994; Volckaert et al., 1995; Harrington and Horseman, 1999; Rodwell et al., 2000) demonstrated that, as might be expected, this relationship is hysterisic for the Boom Clay and follows a similar form to that for void ratio (Figure 4-3), indicating that conductivity is never fully recovered on unloading. As with void ratio, there is a paucity of hydraulic conductivity data relating to the Dutch Boom Clay under appropriate effective stress conditions. However, it is possible to infer the likely range of conductivities, based on laboratory data examining this relationship.

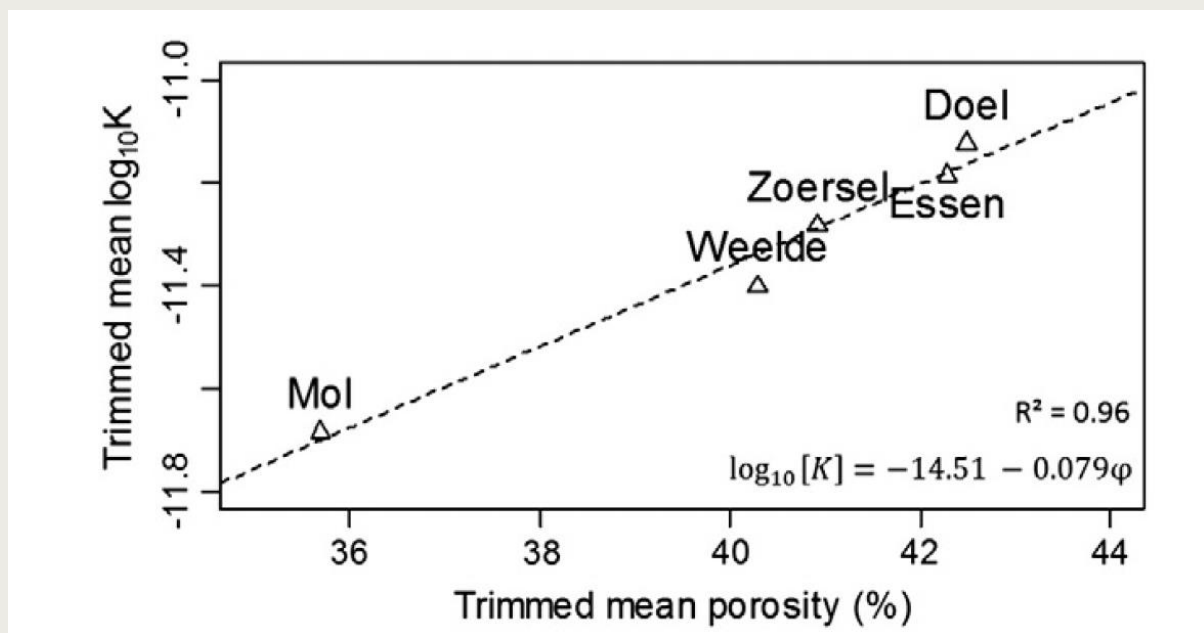


Figure 4-1. 50% trimmed mean porosity versus 50% trimmed mean logarithmic hydraulic conductivity for the different boreholes, from Yu et al. (2013).

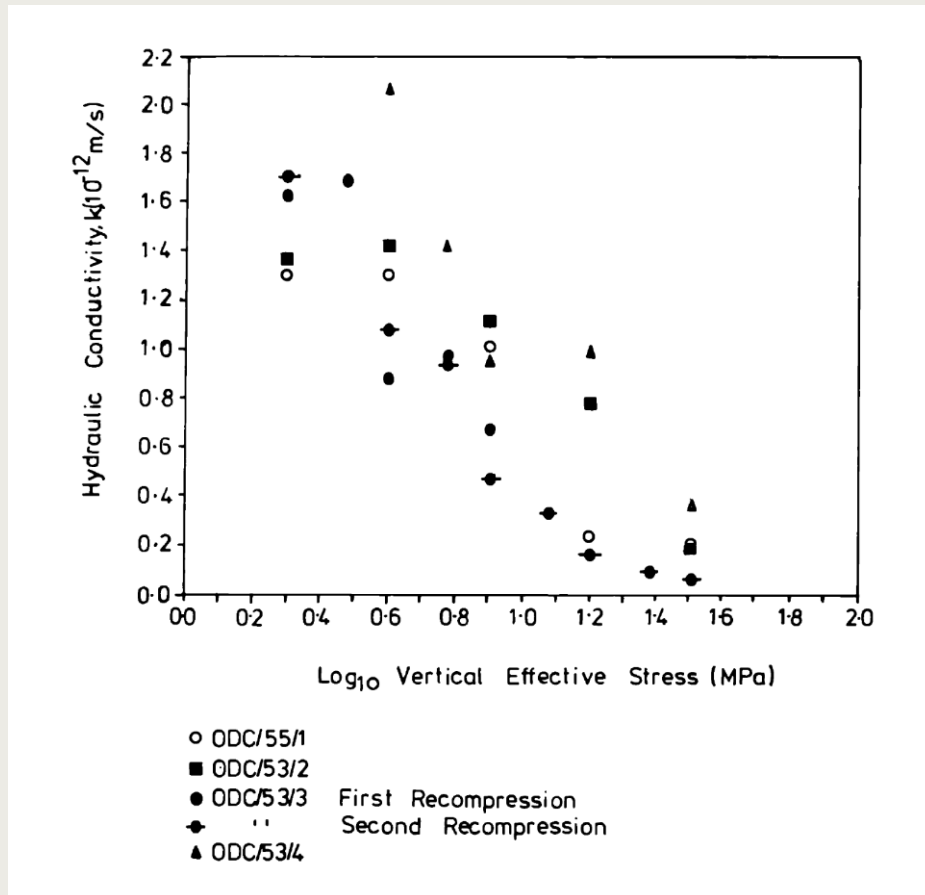


Figure 4-2. Relationship between hydraulic conductivity plotted and the logarithm of the vertical effective stress, as observed by Horseman et al. (1987).

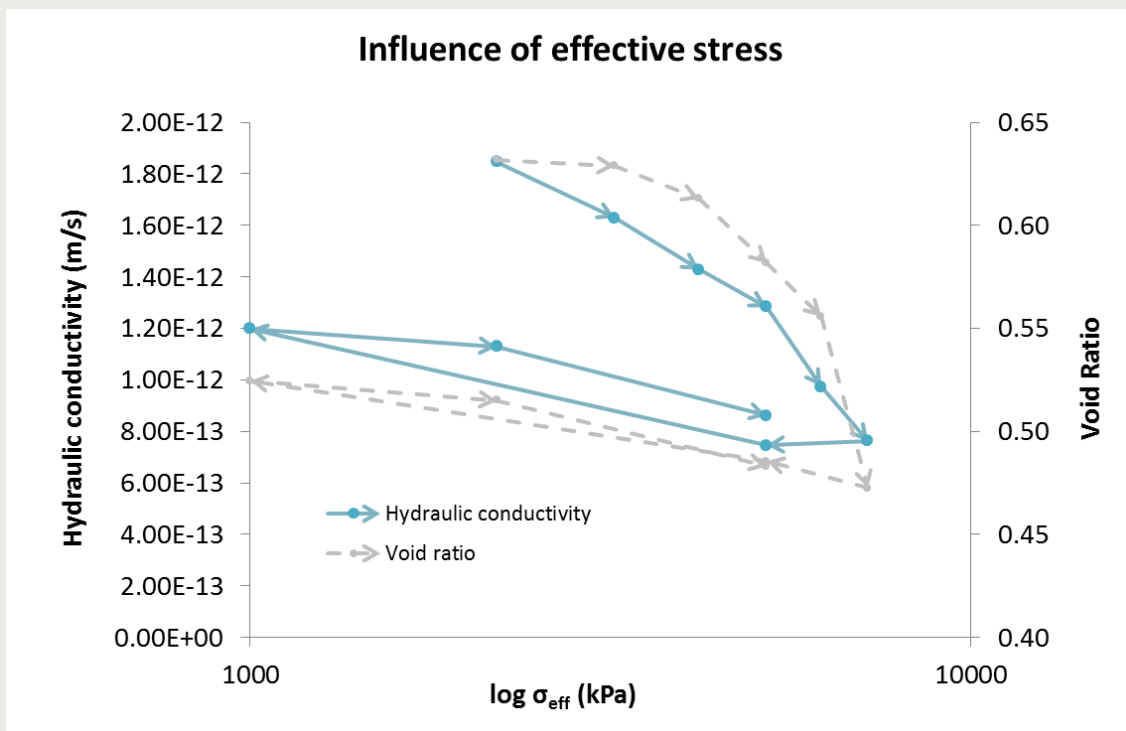


Figure 4-3. Experimental data from a Boom Clay sample tested by Harrington and co-workers as part of the MEGAS project (Volckaert et al. (1995), BGS). Observations clearly demonstrate the

hysteretic response of conductivity to loading and unloading, associated with the reduction in void ratio on compression.

Figure 4-4 shows hydraulic conductivity for a Boom Clay test sample (Volckaert et al., 1995, BGS) as a function of effective stress, alongside stress conditions at HADES and for the Dutch repository concept (as outlined in Section 1.5). In addition, the measured preconsolidation stress for the Boom Clay at Mol, P_c' Mol, and an estimated preconsolidation stress for the Boom Clay at 500 m depth in the Netherlands, P_c' NL, (based on the observations of Wildenberg et al., 2003) are highlighted by the red and blue dashed lines. The discrepancy between P_c' NL and the expected effective stress conditions at 500 m depth, indicates that the clay has experienced ~160 m uplift since its maximum point of burial (based on a pressure difference ~3.2 MPa and an overburden with a density ~2.03 g cc⁻¹). This compares to an equivalent estimate of ~210 m uplift for the HADES URL and suggests that the formation could have undergone ~50 m less uplift at Blija than at Mol. However, such estimates should be treated with extreme caution, given the scarcity of preconsolidation data for clay in the Netherlands and the potential for local variability. In addition, it has proven non-trivial to reconcile geological observations with this estimate for uplift at Mol, which may in part be impacted by ‘pseudo-consolidation’ of the clay resulting from diagenetic effects (Horseman et al., 1993).

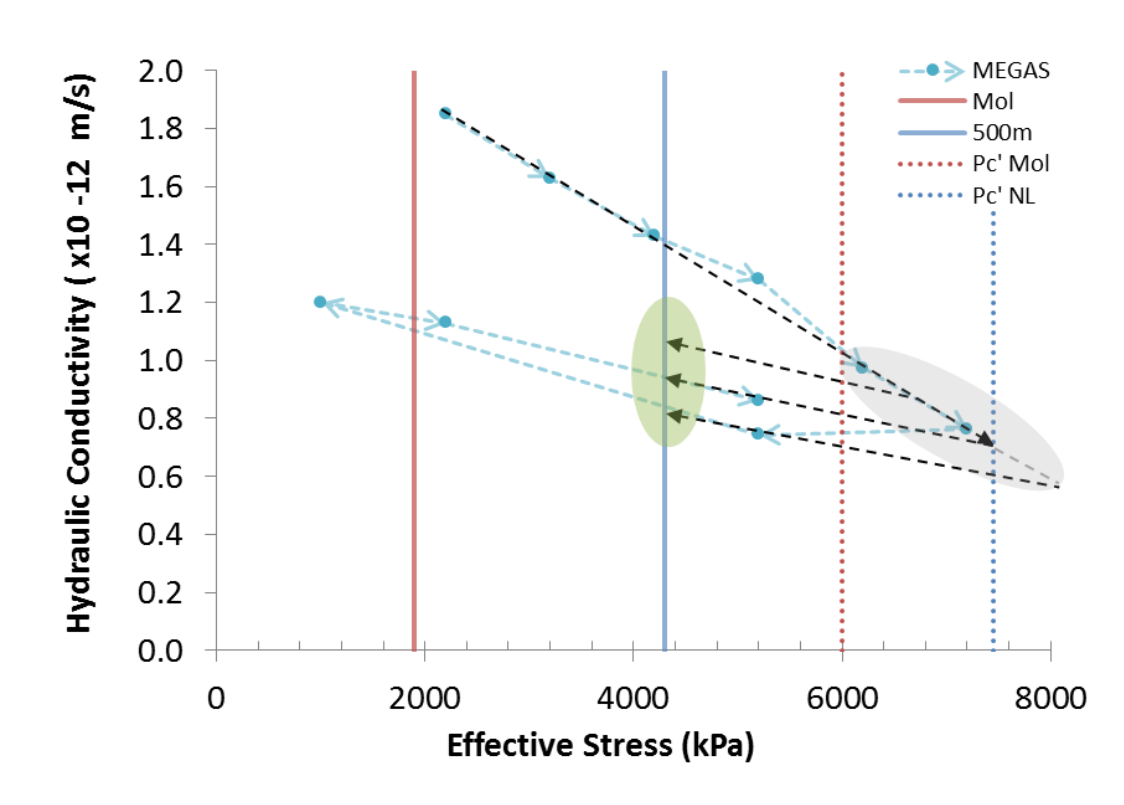


Figure 4-4. Experimental data from the Boom Clay tested by Harrington and co-workers as part of the MEGAS project. The grey ellipse approximates the potential range of starting preconsolidation values for a site in the Netherlands. The uncertainty in this value is reflected by the example unloading responses that may result from a reduction in effective stress (dashed black lines). The green ellipse approximates the potential range of hydraulic conductivities likely after unloading from maximum burial depth. These values are highly sensitive to initial hydraulic conductivity of the sample before loading takes place.

As a result of the uncertainty in the likely preconsolidation stress for clay at a Dutch repository (reflected by the grey ellipse), it is only possible to infer a likely range of

hydraulic conductivities (highlighted in green), since the clay may have followed a number of possible unloading paths (dashed black lines). In the absence of better constrained data, it seems likely that prior unloading to effective stress conditions at 500 m would lead to a reduction in virgin conductivity ~30 to 60%. Based on an average conductivity value for the Boom Clay taken from the literature (**Appendix Table B-06**), this would result in a probable hydraulic conductivity (perpendicular to bedding) in the range of 1.2×10^{-12} to 6.8×10^{-13} m/s.

However, it should be noted that these values are highly sensitive to initial void ratio (and associated hydraulic conductivity). Nevertheless, given the relative lack of variability observed in conductivity at the Mol site, such values may provide a reasonable ‘first estimate’. Since the data used relates to material from Mol, this estimate does not necessarily account for the influence of any lithological variation or differences in diagenetic history between the two sites. Recovery of well-preserved core will be necessary to further-constrain hydraulic properties of the clay at relevant locations in the Netherlands.

4.2. Diffusion and Fick’s law

Diffusion-driven transport in the Boom Clay (assumed to be saturated and homogeneous) is classically evaluated using Fick’s Law for one-dimensional flow, adapted to account for sorption effects;

$$J = -D_e \frac{dC}{dx} \quad \text{Equation 4-5}$$

where J is the flux of solutes ($\text{mol}\cdot\text{s}^{-1}\cdot\text{m}^{-2}$), D_e is the ‘effective’ diffusion coefficient and dC/dx is the concentration gradient (C , $\text{mol}\cdot\text{m}^{-3}$).

Diffusion is the spontaneous process of matter transportation from one part of system to another, resulting from random molecular (Brownian) motions. It is a net transport of chemical species and it is called tracer diffusion when one chemical species diffuses into another (Shackelford and Moore, 2013). In the context of gas generation within a repository environment, estimation of diffusion properties is complicated by the potential involvement of a number of gases (H_2 , CH_4 , CO_2 , etc.). As such, uncertainty in the likely source term can lead to additional uncertainty in the resulting diffusive response as gas is generated.

4.3. Tortuosity

For a porous material, flow properties are strongly controlled by the path along which fluid must pass, whether by advective or diffusive processes. The complexity of this path can be described in terms of the tortuosity (τ) for a given material. This parameter is very closely linked to porosity and can be defined as the average ratio of the microscopic path length (L) to the macroscopic path length (x) in the medium, or:

$$\tau = \frac{L}{x} \quad \text{Equation 4-6}$$

However, quantification of τ is non-trivial and, as a result, a number of models for indirect estimation of τ , as a function of porosity, have been developed. Shen and Chen (2007) and Sun et al. (2013) discuss different approaches (see examples, **Table 4-1**).

However, there is a lack of tortuosity estimates published for the Boom Clay. Using a Boom Clay porosity of 28.75% (Dehandschutter et al., 2004), and the three equations outlined in Table 4-1, yields tortuosity values of 1.61, 1.51 and 1.57. All three equations predict that a lower porosity (at higher compaction states) causes a higher tortuosity. Care has to be taken though, as only the effective porosity should be used to predict tortuosity, as it represents the available porosity.

Tortuosity equation	Determination	Reference
$\tau = 1 - 0.49 \ln \phi$	Experimental	Barrande <i>et al.</i> (2007) Mauret and Renaud (1997)
$\tau = \frac{1}{\phi^{0.33}}$	Empirical	Bear (1972) Dullien (1975)
$\tau = 1 + 0.8(1 - \phi)$	Lattice-Gas, cellular-automaton method	Koponen <i>et al.</i> (1996)

Table 4-1. Tortuosity relationships for porous media (τ = tortuosity; ϕ = porosity)

4.4. Osmosis and coupled flow phenomena

The validity of Darcy's law applied to clays has been questioned since the 1960's (Oakes, 1960; Hansbo, 1960, 1973; Kutelek, 1969) and the existence of possible 'thresholds' proposed as an explanation for departures between observation and theory (Miller and Low, 1963). However, Mitchell (1976) suggests such departures result from a number of factors including experimental errors, internal consolidation/swelling effects, particulate migration, and bacterial growth. Mitchell cites work by, amongst others, Olsen, (1965, 1969), Gray and Mitchell (1967) and Chan and Kenney (1973) as proof for the general validity of Darcy's Law. Mitchell suggests apparent departures may stem from particle migration, electrokinetic and osmotic effects not included in the formulation of Darcy's Law. Indeed, clays, mudrocks and shales exhibit a number of important differences from other porous media including the sub-microscopic nature of the pore space, large surface area of the mineral phases, strong physico-chemical interactions, deformable matrix, low tensile strength and pronounced coupling between the hydraulic and mechanical responses. These differences mean that flow by simple filtration, driven by a difference in hydraulic pressure, may not be the only transport process operating within these materials.

There is now substantial evidence in the literature that argillaceous rocks act as semipermeable membranes capable of supporting an osmotic flux of groundwater (Hanshaw, 1962; Kemper and Evans, 1963; Young and Low, 1965; Kemper and Rollins, 1966; Fritz and Marine, 1983; Fritz, 1986; Neuzil, 1994; Wong and Heidug, 1994 and Van Oort, 1994). The main uncertainty concerning osmosis under field conditions is whether or not the membrane is rendered ineffective by the presence of fractures (Hanor, 1984). However, a series of long-term field experiments reported by Neuzil (1994, 2000) examining the osmotic movement of water in the Pierre Shale, indicate osmotic pumping between the borehole and the formation occurs.

However, in the context of clays, mudrocks and shale, coupled flow phenomena refers to processes in which flow of any kind (i.e. fluid, heat, solute or electrical current) occurs as a result of the application of a gradient not normally associated with that flow. In mathematical terms such flows are said to be dependent on a non-conjugate force. From reversible thermodynamics (Katchalsky and Curran, 1967), a flow J_i is usually assumed to be linearly related to the gradient X_i such that;

$$J_i = -\sum_{k=1}^n L_{ik} X_k \quad \text{where} \quad i=1, 2, 3\dots n \quad \text{Equation 4-7}$$

where i and k represent the different types of flow and driving gradient respectively and L_{ik} are phenomenological coefficients (Bear, 1972). In this way we can define a coupled flow matrix, Table 4-2.

	Potential Gradient (X_i)			
Flow (J_i)	Hydraulic	Temperature	Electrical	Chemical
Fluid	Advection <i>Darcy's Law</i>	Thermo-osmosis	Electro-osmosis	Chemico-osmosis
Heat	Isothermal heat transfer	Thermal conduction <i>Fourier's Law</i>	Peltier effect	Dufour effect
Current	Streaming current	Thermo-electricity	Electrical conduction <i>Ohm's Law</i>	Diffusion and membrane potentials
Ion	Streaming current	Soret effect (thermo-diffusion of electrolyte)	Electro-phoresis	Diffusion <i>Ficks's Law</i>

Table 4-2. Flow matrix showing direct (on-diagonal) and coupled (off-diagonal) flow processes, the latter often referred to as Onsagerian coupled-flow processes after the eminent chemist and physicist Lars Onsager.

Horseman et al. (1996) provide a detailed description, including mathematical formulation, for each flow processes. They describe work undertaken by a number of researchers examining the individual processes and their application to natural and engineered clay-based systems, including concepts of ideal and non-ideal clay membrane behaviour. Since the pores of most clay membranes are of sufficient diameter to allow the movement of even the largest hydrated ions, Horseman et al. (1996) suggest that chemico-osmosis and the process of salt exclusion is primarily linked to electrical restrictions operating within the narrow pore structures of the clays. However, back-diffusion of solutes through micro fractures or zones containing low clay content material, can lower membrane efficiencies (Horseman et al., 2007). This results in a differential pressure across the membrane that is lower than that predicted by theory alone.

From a theoretical perspective, the phenomenological coefficients, L_{ik} , are assumed to follow the Onsager reciprocal relations such that $L_{ik}=L_{ki}$ for $i \neq k$. The diagonal coefficients, L_{ii} , can be identified with the usual uncoupled equations of flow such as Darcy's Law for pore water movement and Fick's Law for solute diffusion. Bader and Kooi (2005) consider flow and solute transport in a single solute semi-permeable system to derive the single off-diagonal coupling coefficient for this pair of equations. Their equations are;

$$q = -\frac{k}{\mu} \nabla p + \lambda \rho_f \nabla \omega \quad \text{Equation 4-8}$$

$$J_s^d = \zeta \rho_f \omega \frac{k}{\mu} \nabla p - \zeta \rho_f \omega \lambda \rho_f \nabla \omega - D \rho_f \nabla \omega \quad \text{Equation 4-9}$$

where q is the pore water flow rate, J_s^d is the solute mass flux, k is the permeability, μ is the fluid viscosity, p is the fluid pressure, ρ_f is the fluid density, ω is the solute mass fraction, ζ is the osmotic reflection coefficient, D is the diffusion coefficient, and λ is given by;

$$\lambda = \frac{\zeta k}{\mu M_s} nRT \quad \text{Equation 4-10}$$

where M_s is the molar mass of the solute, n is the number of ions in the solute, R is the gas constant, and T is the absolute temperature.

Malusis and Shackelford (2002) and Malusis et al. (2012) analyse the more general system comprising fluid flow, solute transport and electrical current equations, including the case of multiple charged solutes, building on the work of Yeung (1990) and Yeung and Mitchell (1993). They compare the approach of using a single compound solute equation with using separate equations for each constituent ion.

Goncalves and Tremosa (2010) instead consider flow coupled to a thermal gradient and derive the coupling coefficient by scaling up microscopic processes, based on the work of Derjaguin et al. (1987). The final form of their equations is;

$$\mathbf{q} = -\frac{k}{\mu} \nabla p - \frac{k \Delta H}{\mu T} \nabla T \quad \text{Equation 4-11}$$

$$J_H - \mathbf{q}H = -\frac{k \Delta H}{\mu} \nabla p - \lambda \nabla T \quad \text{Equation 4-12}$$

where J_H is the heat flux, H is the pore water specific enthalpy, ΔH is the macroscopic volume-averaged excess specific enthalpy due to fluid-solid interactions, and λ is the thermal conductivity of the porous medium. Goncalves et al. (2012) develop an expression for ΔH based on the change in hydrogen bonding adjacent to clay surfaces.

For the Boom Clay, Heister et al. (2006) directly measured the membrane potential of reconstituted clay discs. While clearly demonstrating the presence of osmotically driven flow in Boom Clay, they also highlighted the importance of electro-osmosis which accounts for a significant portion of total flow. The induced membrane potential was found to relate to the salt concentration gradient across the discs which decreased over time as a result of the backflow of ions arising from the semipermeable nature of the membrane. Osmotic efficiency was also found to be dependent on the mineralogical composition of the samples with higher efficiencies reported for bentonite than the Boom Clay. However, the authors were unable to directly estimate membrane efficiency as their experimental apparatus was unable to measure the intrinsic permeability of the clay discs.

In contrast, laboratory experiments performed on intact samples of a Jurassic marine shale Opalinus Clay (a potential host formation in Switzerland) reported by Horseman et al. (2007), measured membrane efficiencies ranging from 1% to 6% (mean around 4%). However, the high compressibility coefficient and low membrane efficiency revealed by these experiments can be explained by a number of factors from sample damage to chemically induced swelling. However, while membrane efficiency is low, the results clearly demonstrate Opalinus Clay is capable of supporting an osmotic flow of water. Of greater importance is the impact of these results on the specification, operation and interpretation of borehole tests aimed at hydrogeological characterisation. Horseman et al. (2007) suggest an osmotic coupling term should be included in the effective diffusion

coefficient when interpreting such data and seems reasonable to conclude this may also be the same for the Boom Clay.

Garavito et al. (2007) report a field experiment performed in the Boom Clay at the Hades URL. Similar to Heister et al. (2006), the authors report a decrease in membrane efficiency from 41% for 0.01 NaHCO₃ to 7% for 0.14 NaHCO₃ and suggest that membrane efficiencies are high in undisturbed sections of the Boom Clay. Data from Garavito et al. (2007) show a small but rapid build-up in pressure (peaking at around 12 hours which is then followed by a protracted negative transient (months in duration) probably related to the diffusion of ions from the test reservoir into the Boom Clay Formation. While the authors indicate the development of osmotically driven hydraulic fractures is not possible under the conditions of their tests, the semi-permeable membrane behaviour of the Boom Clay is of relevance to radioactive waste disposal. Indeed, they suggest additional experiments with appropriate fluid chemistries matching those likely to be generated by the decay of wastes should be undertaken.

Given the sensitivity of coupled flow processes to both the composition and compaction state of the clay, it seems probable that osmotic efficiency is likely to increase in a repository sited at 500 m depth. It is therefore important from both long term performance assessment and from hydrogeological characterisation that coupled flow processes are directly measured under appropriate *in situ* and geochemical conditions.

4.5. Gas migration

In a clay-hosted repository four primary phenomenological models can be defined to describe gas migration (Figure 4-5) (Cuss et al., 2014; Marschall et al., 2005): (i) gas movement by solution and/or diffusion, governed by Henry's and Fick's Laws respectively, within interstitial fluids migrating along prevailing hydraulic gradients; (ii) gas flow in the original porosity of the fabric governed by a generalised form of Darcy's Law, commonly referred to as visco-capillary flow; (iii) gas flow along transient, localised dilatant pathways (micro-fissuring), the permeability of which is dependent on the interplay between local gas pressure and the effective stress state; and (iv) gas flow along macro fractures (such as those observed in hydrofracture activities during hydrocarbon reservoir stimulation), where fracture propagation is the result of gas pressure exceeding the sum of the minor principle stress and tensile strength. In radioactive waste disposal most interest is focussed on understanding the processes and mechanisms governing the advective transport of gas (mechanisms ii through iv).

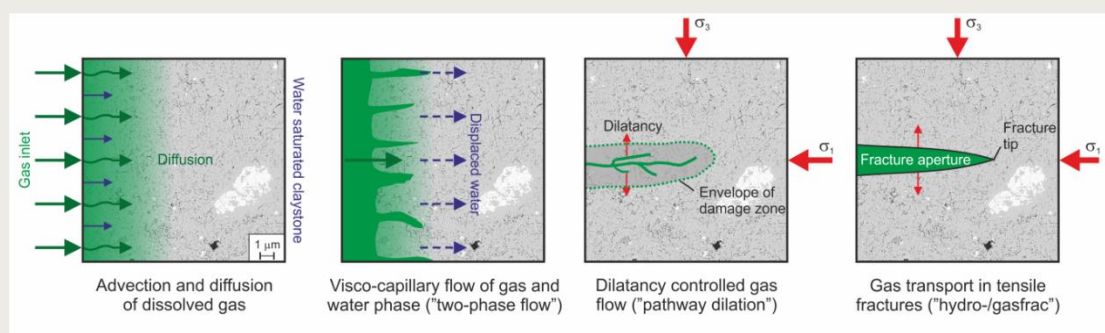


Figure 4-5. Possible gas flow processes in argillaceous materials.

4.5.1. Gas transport by diffusion

Experimental determination of the diffusive properties of gas within clay is exceptionally challenging and such data for the Boom Clay is, therefore, limited. This has led to a high

level of uncertainty in relevant parameters, directly impacting numerical simulation of gas transport processes. In order to anticipate the likely pressures which may be reached during gas generation at a waste canister (and the potential to reach conditions likely to lead to advective transport of a free gas-phase), a well-defined rate of diffusion is crucial.

Efforts were made to determine gas diffusion parameters for hydrogen in the Boom Clay as part of the MEGAS project. Researchers at SCK-CEN utilised two experimental methodologies; through-diffusion testing and in-diffusion testing (Volckaert et al., 1995). Observations during the experimental programme were hampered by leakage problems and the impacts of sample-degassing, but they were able to estimate a diffusion coefficient for H₂ of between $4.2 \times 10^{-12} \text{ m}^2 \cdot \text{s}^{-1}$ and $1.6 \times 10^{-10} \text{ m}^2 \cdot \text{s}^{-1}$. Nevertheless, Weetjens and Sillen (2006) demonstrated that a greater degree of certainty was required in order to exclude the possibility of a free gas phase occurring as a result of gas generation.

More recent work conducted by SCK-CEN has attempted to address this through the development of a new experimental methodology termed a 'double through-diffusion' test (Jacops et al., 2013a). In this approach, two dissolved gases are allowed to diffusive through opposite ends of a Boom Clay sample, at the same time. The clay is placed between two vessels, each containing one of the two diffusants only (in this case He and CH₄). Evolving concentrations within each vessel are then measured by regular sampling throughout the duration of testing. Based on these observations, Jacops et al. (2013a) estimated apparent diffusion coefficients for dissolved He and CH₄ of 12.2×10^{-10} and $2.42 \times 10^{-10} \text{ m}^2 \cdot \text{s}^{-1}$ respectively. The authors suggest that the remaining uncertainty on these values is ~10%.

The same methodology was also used by Jacops et al. (2015) using Argon and 5% H₂ in Argon (called 'Hytec') as diffusants. In addition, the authors included a number of measures (sterilisation by chemical agents, heat and gamma radiation) to ensure findings were not impacted by microbial activity within the test material. Blank samples (tested with Argon alone) were also used, in order to ensure diffusion properties were not impacted by sterilisation techniques. The authors report that reproducible results could only be achieved by use of several sterilisation techniques. They report a diffusion coefficient for H₂ of $D_e = 2.64 \times 10^{-10} \text{ m}^2 \cdot \text{s}^{-1}$ for transport perpendicular to bedding. Two values for transport parallel to bedding were also measured as $D_e = 7.25 \times 10^{-10} \text{ m}^2 \cdot \text{s}^{-1}$ and $D_e = 5.51 \times 10^{-10} \text{ m}^2 \cdot \text{s}^{-1}$.

Whilst the reduced uncertainty in these properties provides a step forward for modelling of diffusive gas flow through the Boom Clay, no such measurements could be found for material taken from greater depth intervals (more appropriate to the Dutch Boom Clay concept). Other than assuming that these values represent an upper value for diffusivity in a Dutch repository within the Boom Clay, it is not possible to make further statements about likely diffusion coefficients in such a context.

4.5.2. Advective and dispersive transport

The movement of gases through argillaceous host rocks will occur through the combined processes of molecular diffusion (governed by Fick's Law) and bulk advection. In many natural and engineered applications the processes of gas generation can exceed the diffusional capacity of the system (Horseman et al., 1999; Sillen and Leupin, 2013), leading to the potential for migration of a free-gas phase if the required pressure conditions are reached. Understanding the advective flow of two or more fluid phases within porous media is important in a number of fields of science and engineering, from radioactive waste disposal to hydrocarbon exploitation.

4.5.2.1 Two phase flow

Traditional theoretical development has assumed that the porous medium only experiences small bulk deformations and this appears to be appropriate for relatively permeable formations. However recent experimental work with gas migration in very low permeability materials has found that discrete pathway creation by dilation must be considered for these materials (Harrington et al., 1999; Angeli et al., 2009; Skurtveit et al., 2012; Cuss et al., 2014; Cuss and Harrington, 2011; 2012).

Multiphase fluid flow is modelled by combining the continuity equation for each phase with the generalised form of Darcy's law and constitutive equations for relative permeabilities and capillary pressures between phases (Parker, 1989). The continuity equation for each phase may be written as;

$$\frac{\partial}{\partial t}(\varphi \rho_i S_i) + \nabla \cdot (\rho_i \mathbf{q}_i) = \gamma_i \quad \text{Equation 4-13}$$

where φ is the porosity, ρ_i is the phase density for phase i , S_i is the saturation of phase i , \mathbf{q}_i is the Darcy velocity vector for phase i , and γ_i is a source-sink term for mass transfer between the phases and any external sources. Darcy's law for phase i may be written as;

$$\mathbf{q}_i = -\frac{k_{ri}k}{\mu_i} \nabla(P_i + \rho_i g z) \quad \text{Equation 4-14}$$

where k_{ri} is the relative permeability of phase i , k is the intrinsic permeability tensor, η_i is the viscosity of phase i , P_i is the pressure in phase i , and g is the acceleration due to gravity. To complete the description of the system it is necessary to define the relative permeabilities and capillary pressures as functions of the phase saturations. These may be defined either with tabulated data or explicit functional forms such as van Genuchten (1980) and may also incorporate hysteretic effects (Kool and Parker, 1987).

The functional forms chosen for the capillary pressures are generally empirical in nature and reflect the fact that as the wetting phase saturation decreases the non-wetting phase invades smaller pores within the formation and consequently the capillary pressure between the phases increases. One of the most commonly used functions is that given by van Genuchten (1980) and may be written as;

$$P_c = P_0 ([S^*]^{-1/m} - 1)^{1-m} \quad \text{Equation 4-15}$$

where P_0 and m are parameters used to fit to the experimental data, P_c is the capillary pressure difference between non-wetting and wetting phases, and S^* is the effective wetting phase saturation given by;

$$S^* = \frac{(S_w - S_{rw})}{(1 - S_{rw})} \quad \text{Equation 4-16}$$

where S_w is the wetting phase saturation S_{rw} is the residual wetting phase saturation.

Functions for relative permeability have been derived from analysis of network models of the porous medium. Thus van Genuchten (1980) obtained, for the wetting phase, k_{rw} , the following expression:

$$k_{rw} = \sqrt{S^*} \left\{ 1 - \left(1 - [S^*]^{1/m} \right)^m \right\}^2$$

Equation 4-17

Alternatively, more empirical correlations may be used such as the generalized form of the functions obtained by Corey (1954);

$$k_{rw} = k_{rw-max} [S^*]^{n_w}$$

Equation 4-18

for the wetting phase and for the non-wetting phase:

$$k_{rg} = k_{rg-max} \left[\frac{S_g - S_{rg}}{1 - S_{rg} - S_{rw}} \right]^{n_g}$$

Equation 4-19

Here n_w , n_g , k_{rw-max} , and k_{rg-max} are parameters for fitting to the experimental data and S_{rg} is the residual non-wetting phase saturation.

To date, the authors are unaware of experimental research that conclusively affirms the validity of visco-capillary flow through the Boom Clay.

4.5.2.2 Dilatant flow

In initially saturated mudrocks with extremely narrow interparticle spaces, the capillary threshold pressure required to initiate gas flow is simply too large for the gas to be able to penetrate and desaturate the clay (Harrington and Horseman, 1999). Indeed, Hedberg (1974) in a paper examining the role of gas in the overpressure of oilfield shales quotes a translation from Tissot and Pelet (1971) in which they state “The displacement of an oil or gas phase from the centre of a finely grained argillaceous matrix goes against the laws of capillarity and is in principle impossible. The barrier can, however, be broken in one way. The pressure within the fluids formed in the pores of the source-rock increases constantly as products of the evolution of kerogene are formed. If this pressure comes to exceed the mechanical resistance of the rock, microfissures will be produced which are many orders of size greater than the natural (pore) channel of the rock. These microfissures will permit the escape of an oil or gas phase, until the pressure has fallen below the threshold which allows the fissures to be filled and a new cycle commences.”

This approach to the conceptualisation of immiscible gas flow succinctly sums up modern thinking on the topic and is of potential relevance to all storage and extraction industries dealing with low permeability clay based systems. Indeed, Mandl and Harkness (1987) support this hypothesis and suggest that hydrocarbon migration can only occur through thick, continuous water wet rocks of low permeability via the process of fracturing, forming what they refer to as ‘dykelets’.

In 1994 a study reported by Horseman and Harrington examining the movement of repository gases through isotropically stressed samples of the Boom Clay, attributed the migration of gas to the formation of pressure induced dilatant pathways. Volckaert et al. (1995) provided additional evidence in support of this hypothesis including images of localised gas discharge from clay sample surfaces.

A typical example of the Boom Clay response to gas flow is presented in **Figure 4-6**. In these tests, Horseman and Harrington (1994) note that no measurable quantities of gas discharged from the downstream end of the sample were detected during the initial gas compression phase. Breakthrough was marked by a short period of gradually increasing

downstream flow, followed by a sudden increase in flow rate. The pressure build-up curve terminated in a well-defined peak which occurred after the original breakthrough event. This was followed by a spontaneous negative pressure transient to a near steady-state condition.

A number of tests exhibited a small upward trend in gas pressure during the latter part of the transient (Figure 4-6), which Harrington and Horseman (1999) attribute to the underlying system dynamics controlling gas flow. The apparent capillary threshold pressure was obtained by the cessation of pumping, allowing the injection pressure to decay through the samples, denoted by C=0 (where C is a measure of the rate of gas compression, in $\mu\text{l/h}$). When gas pumping was reinstated pressure was observed to climb to a broad secondary peak somewhat lower than the primary peak. This was again followed by a second spontaneous negative pressure transient. Harrington and Horseman (1994) note that flow out of the clay continued through the second pressurisation event, suggestive of incomplete pathway sealing. As gas pressure continued to increase, a second broad peak was observed at a lower value than the original pressure peak. The second post-peak steady-state gas flow was significantly higher than the original, which may be related to work-hardening of the clay around flow pathways (Graham and Harrington, 2014). The test in Figure 4-6 was completed with a second shut-in stage in which the pressure declined towards an equilibrium value close to the original.

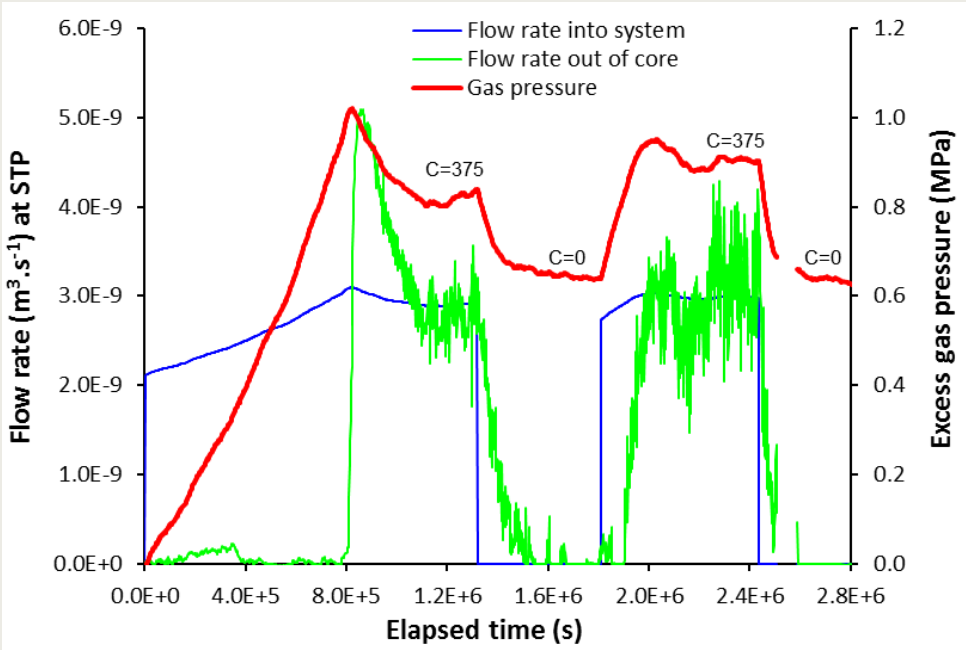


Figure 4-6. Experimental history T3S1 on the Boom Clay (Harrington and Horseman, 1999). This is a typical response for gas flow parallel to bedding in this overconsolidated clay, with ‘C’ denoting the rate of gas compression in $\mu\text{l/h}$. Breakthrough is marked by a short period of gradually increasing outflow, followed by a sudden increase in flow rate. C=0 represents a shut-in stage when gas pressure is allowed to decay, the asymptote of which provides a measure of the apparent capillary threshold pressure. The secondary peak is broader and somewhat lower than the primary peak.

Based on a series of detailed experiments, Horseman and Harrington (1994) related the resistance to gas flow to the total potential of the soil water reflecting the summation of physico-chemical forces operating within the clay. Gas flow was linked to total stress through a force balance first proposed by Lambe (1960). This approach recognised the importance of ‘water’ within the system and the ability of thin water films to conduct stress when strongly associated with the clay substrate. Horseman and Harrington (1994)

also reported intermittent or ‘burst’ type flow during gas migration experiments (Horseman and Harrington, 1998). This combined with minimal desaturation of test samples conformed to the conceptual model proposed by Tissot and Pelet (1971), indicating that the processes first identified for oilfield shales also apply to less indurated materials such as the Boom Clay.

These concepts were further developed in Volckaert et al. (1995), Horseman et al. (1996), Ortiz et al. (1996), and Sen et al. (1996). Laboratory data compiled by Horseman and Harrington (2000) is presented in **Appendix Table B-7**.

Fitting a power-law function through subsets of data from Horseman and Harrington (1994) and Volckaert et al. (1995) it is possible to relate the gas breakthrough pressure of the Boom Clay to either the hydraulic conductivity or intrinsic permeability (Davies, 1991). In this way we can define two relationships, one derived from tests performed under a constant head boundary condition;

$$P_b = 4.71 \times 10^{-4} \kappa^{-0.312} \quad \text{Equation 4-20}$$

where P_b is the breakthrough pressure (MPa) and κ is the hydraulic conductivity ($\text{m}\cdot\text{s}^{-1}$). The second relationship is derived from constant flow rate tests and relates breakthrough pressure to intrinsic permeability, k_i (m^2):

$$P_b = 4.71 \times 10^{-4} k_i^{-0.312} \quad \text{Equation 4-21}$$

These relationships are valid for flow normal and parallel to bedding so long as the appropriate values for hydraulic conductivity or intrinsic permeability are used.

The concept of preferential pathway flow was further explored by Ortiz et al. (2002), who report a long-term field test examining the mechanisms governing gas flow and their long-term impact on hydraulic behaviour. The authors discuss the invalidity of the generalised Darcy Law applied to the Boom Clay and show that gas flow through the clay has negligible impact on the hydraulic behaviour under field conditions. They reaffirm the hypothesis for cyclic gas flow, first proposed by Horseman and Harrington (1994).

Indirect evidence for the creation of pressure-induced gas pathways was found by Horseman and Harrington (2000) in a test on the Boom Clay, undertaken using a ‘ K_0 ’ geometry (i.e. where radial expansion of the sample is constrained). **Figure 4-7** is a cross plot of data subsets from **Appendix Table B-7** comparing steady-state flows and differential pressures for tests performed under isotropic and K_0 boundary conditions. While the confining stress applied to each core is different, **Figure 4-7** clearly shows a much steeper gradient for isotropic tests than those for the K_0 geometry, even though the latter were performed at a much higher confining stress. These results suggest pathway closure is much less efficient under K_0 conditions, and that the nature of the stress field and boundary conditions are key factors in the processes governing the migration of gas through the Boom Clay.

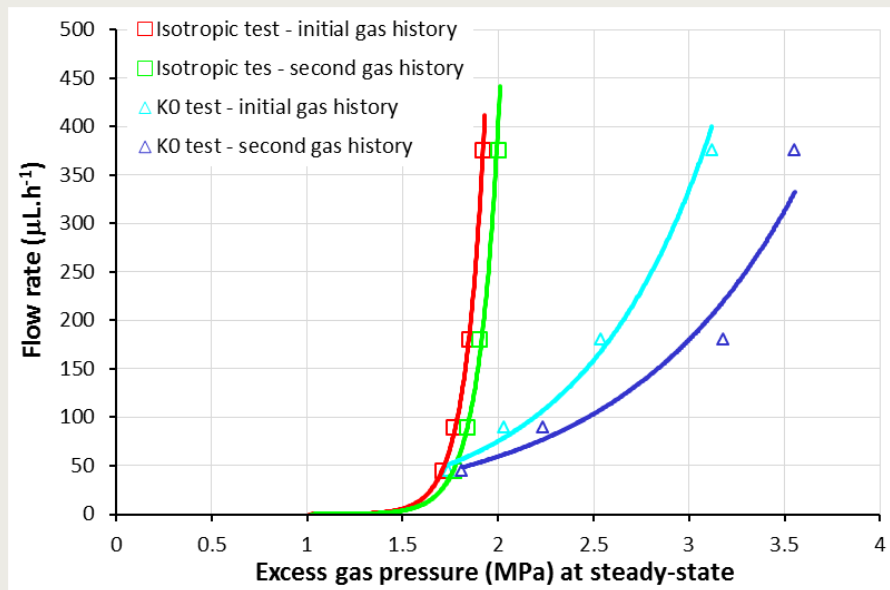


Figure 4-7. Cross-plot of steady state gas flow data from Horseman and Harrington (2000) for comparable flow rates from both isotropic and K_0 tests.

Earlier experiments undertaken on samples of compact bentonite by Pusch and Forsberg (1983) reported water saturations close to unity, suggesting gas must have passed through a relatively small number of discrete pathways. Pusch et al. (1985) also reported water saturations close to unity and observed a critical pressure for gas flow of a similar order of magnitude to that of the swelling pressure. Detailed studies by Horseman et al. (1997) and Horseman and Harrington (1997) reported a series of experiments and theoretical analyses in which gas flow was accompanied by dilation of the clay fabric. Initial gas breakthrough pressures were found to be equal to or slightly in excess of total stress and, again, no measureable desaturation of the material was observed (even after prolonged injection times). Horseman and Harrington (1997) suggested that gas did not migrate through the original pore space of the water-saturated bentonite and that gas permeability was a dependent variable, rather than a material property, linked to the number, width and aperture distributions of dilatant features. This hypothesis was further developed by Harrington and Horseman (1999) which summarised a series of observations on the Boom Clay and engineered materials.

A significant body of evidence is now available demonstrating similar behaviour in a range of clay rich materials. Studies on subsea hydrocarbon seepages suggest capillary displacement pressures are often so large, that gas pressure required to initiate flow can approach or even exceed the total stress (Clayton and Hay, 1994; Judd and Sim, 1998). Work by Donohew et al. (2000) examined gas migration behaviour through clay pastes of varying moisture content and mineralogy. In all experiments gas flow was accompanied by the creation of dilatant, preferential pathways, the morphology of which was related to the plasticity and density of the clay. Hovland et al. (2005) examined pockmark formation in the Nyegga area of the North Sea and concluded that the observed features were formed by sudden 'catastrophic' fluid flow. Post failure, micro seepages were also noted, suggesting only partial self-sealing of the initial pockmark pathway occurred. The development of dilatant pathways is a well-recognised phenomenon in hydrate studies and their impact on seabed sediments is commonly referred to as 'grain displacing hydrate formation' (Holland et al., 2008). Holland et al. presented a series of X-ray images showing filamental hydrate structures traversing sediment cores recovered from the Godavari Basin, India. Similar to the processes described by Donohew et al. (2000), gas flow and

subsequent hydrate formation in these weak sediments occurred through the creation of new porosity and was not associated with flow within the original fabric of the sediment.

Further work on laboratory samples of compact bentonite (Harrington and Horseman, 2003a) clearly showed advective gas flow was associated with the development of multiple dilatant pathways. These features were shown to vary temporally and spatially within the clay with gas pressure, total stress and pore water pressure integrally linked once the gas entry pressure had been reached. Observations at the field scale (Harrington et al., 2007; Cuss and Harrington, 2011; Cuss et al., 2010) from an underground research facility in Sweden confirmed these results showing clear hydromechanical coupling during gas flow. Graham et al. (2012) presented a review of these results and their implications for numerical modelling.

In recent years, significant effort has been placed on examining gas and water flow in more lithified mudrocks which have been to greater depths of burial (Angeli et al., 2009; Cuss and Harrington, 2011; Cuss et al., 2014; Gerard et al., 2014; Harrington et al., 2003; Harrington et al., 2009; Harrington et al., 2012a; Marschall et al., 2005; Rodwell et al., 1999; Romero et al., 2012; Skurtveit et al., 2010; Skurtveit et al., 2012). Marschall et al. (2005) presented borehole data from a gas injection test within the Opalinus Clay which exhibited a hydromechanical response during gas injection testing. Later work by Romero et al. (2012) on laboratory scale Opalinus Clay samples confirmed dilation occurred during gas flow, leading to the development of a void ratio dependent permeability expression (Senger et al., 2014).

Data from a series of long-term laboratory experiments examining gas flow in Callovo-Oxfordian (COx) claystone clearly showed flow was accompanied by dilation of the original fabric at gas pressures below that of the minimum principal stress (Harrington et al., 2012a, 2014; Cuss et al., 2014; Cuss and Harrington 2011, 2012). **Figure 4-8 (left)** is from a triaxial test performed on COx under *in situ* conditions. The data clearly shows that gas flow is accompanied by a small, but well defined volume increase of the sample which cannot be explained by poroelastic compressibility. As outflow evolves towards steady-state, dilation increases indicating gas permeability is a dependent variable, integrally linked to the number, location and aperture distributions of conductive pathways (Harrington and Horseman, 1999), in this example, manifest as a change in volumetric strain. Cuss et al. (2014) note that the observed increase in radial strain is non-uniform suggesting localised flow occurs within the sample. Post-test measurements of sample weight and volume indicate no discernible desaturation, similar to observations by other researchers including Pusch and Forsberg (1983), Pusch et al. (1985), Horseman and Harrington (1994, 1997), Horseman et al. (2004) and Harrington and Horseman (1999, 2003a, 2004) investigating clay-rich materials.

Visual observations of COx samples submerged in glycerol and gently heated to promote degassing (Harrington et al., 2014), **Figure 4-8 (left)**, indicate gas flow occurs through a localised network of pathways, bypassing much of the clay matrix. Within COx, Harrington et al. (2012a, 2014) and Cuss et al. (2014) suggest the coupling of gas flow and mechanical variables results in the development of significant time-dependent effects, impacting many aspects of COx behaviour, from gas breakthrough time to the control of deformation processes. In contrast to the modelling approach adopted by Senger et al. (2014), Gerard et al. (2014) described gas flow through COx using an embedded fracture model. While the solution to this model is somewhat arbitrary (dependent on the initial parameterisation of the fracture(s)) a better fit to the laboratory data was obtained compared to that obtained using a standard visco-capillary approach.

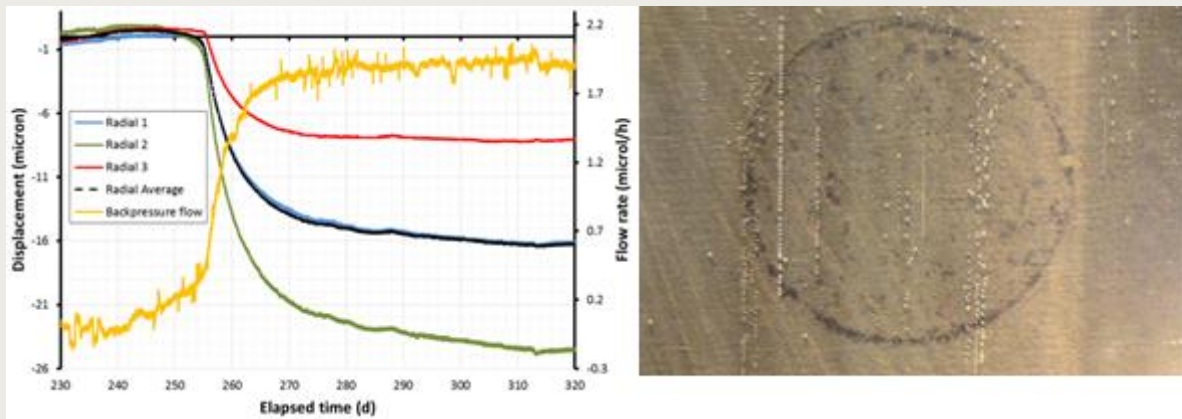


Figure 4-8. (Left) Strain data from triaxial test undertaken on a sample of Callovo-Oxfordian clay showing coupling correlation between sample volume and gas outflow (permeability). Negative strain indicates dilation of the sample. (Right) Post-test degassing of a COx sample submerged and gently heated in glycerol, indicating localised gas flow through the claystone.

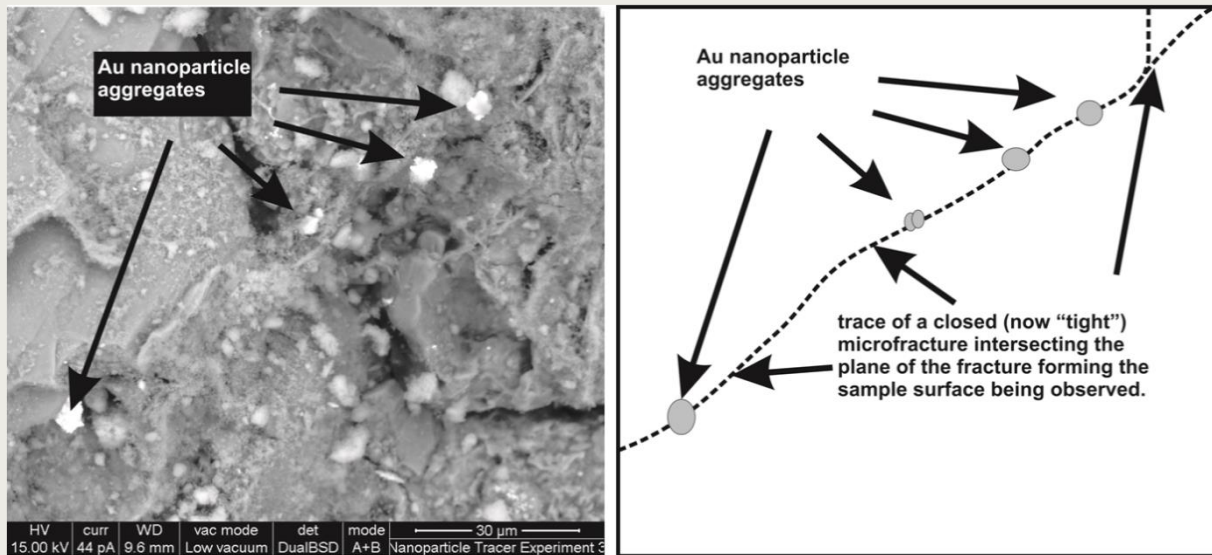


Figure 4-9. Mixed SE and BSE image showing a trail of aggregated gold nanoparticles trapped within the trace of a now closed pathway. The Au particles are trapped along what appears to be a sealed pathway that is sub-orthogonal to the plane of the fracture surface (Harrington et al., 2012b).

Recent work examining caprock integrity from a number of North Sea hydrocarbon fields (Angeli et al., 2009; Harrington et al., 2009; Skurtveit et al., 2010, 2012) indicate dilatancy may be a common mechanism associated with caprock failure. Laboratory experiments injecting carbon dioxide through samples of Draupne shale show a clear increase in axial and radial volume during gas flow (Angeli et al., 2009; Skurtveit et al., 2010, 2012). Simultaneous measurements of P and S wave velocity show a change in behaviour as CO₂ moves through the sample. Laboratory tests on Nordland shale samples from the Sleipner CO₂ inject site were described and numerically modelled by Harrington et al. (2009). Their analysis suggested anisotropy to gas flow was greater than that of water and that gas movement primarily occurred through the development of pressure-induced pathways.

Indeed, images showing the traces of previous 'dilatant' features were presented by Harrington et al. (2012b) in which a mixture of gold and titanium oxide nano powders were injected (within a carrier gas) through the Boom Clay. Post-test scanning electron

microscopy imaging showed layers of clay material draped around aggregates of nano powder as well as a line of aggregates left along the trace of a sealed fracture (**Figure 4-9**). The dimension and shape of the aggregates along with the morphology of the ‘pore’ conclusively demonstrated that the Boom Clay must have dilated to accommodate the gas flow.

There is, therefore, a substantial body of evidence illustrating the importance of gas-induced dilation as a primary fluid flow mechanism in clay-rich materials. At repository depths of interest to the disposal concept investigated in OPERA, such behaviour seems highly probable, given the greater consolidation state of the Boom Clay and the resulting increase in capillary restriction (Chapter 2).

4.5.3. Continuum approach to gas flow

In 1994, Horseman and Harrington assumed continuum gas flow properties in their analysis of controlled flow rate experimental data, using the basic flow equation;

$$Q_{st} = \frac{v_{st} k_g A_s}{2RT\eta_g L_s} (P_{gi}^2 - P_{go}^2) \quad \text{Equation 4-22}$$

where Q_{st} is the volumetric flow rate ($\text{m}^3 \cdot \text{s}^{-1}$) under standard temperature and pressure (STP) conditions, v_{st} ($=0.024 \text{ m}^3$) is the molar volume of gas at STP, k_g (m^2) is the gas permeability, R ($8.314 \text{ J} \cdot \text{mol}^{-1} \cdot \text{K}^{-1}$) is the gas constant, T (k) is the temperature, η_g ($\text{Pa} \cdot \text{s}$) is the viscosity of gas, P_{gi} (Pa) is the pressure of the gas just inside the sample at the upstream end of the core, and P_{go} (Pa) is the pressure of gas just inside the downstream end of the sample.

While the gas pressure P_{go} could not be directly measured in the laboratory, Horseman and Harrington (1994) related this parameter to the sum of the backpressure, P_{wo} , and the apparent capillary pressure, P_{co} (which they referred to as the ‘shut-in’ pressure), where:

$$P_{go} = P_{wo} + P_{co} \quad \text{Equation 4-23}$$

Further analysis by Horseman and Harrington presented in Ortiz et al. (1997) and Rodwell et al. (2000) suggested the assumption of continuum gas flow behaviour did not present a serious limitation, since the basic flow law could be re-couched in terms of flow along one or more preferential pathway(s). By analysing the behaviour of the test system used by Horseman and Harrington, Sen et al. (1996) developed a differential equation for the rate of change of upstream gas pressure, which could be solved for gas migration behaviour across a range of test stages from post-peak to shut-in. While this model was based on a somewhat restrictive assumption of constant gas permeability, it appeared to provide a reasonable fit to certain subsets of data (Ortiz et al., 1997; Rodwell, 2000).

Ortiz et al. (1997) provide a numerical solution to the basic flow law for an equivalent capillary bundle;

$$k_g = \frac{NA_c R_H^2}{\chi \tau^2} \quad \text{Equation 4-24}$$

where N , A_c , R_H , U and x are the number of capillaries per unit cross-section, cross-sectional area (m^2), hydraulic radius (m), shape factor (dimensionless) and tortuosity

(dimensionless) of each capillary. By substituting this equation into the basic flow equation gives:

$$Q_{st} = \frac{v_{st} N A_c R_H^2 A_s}{2 R U \eta_g \chi \tau^2 L_s} (P_{gi}^2 - P_{go}^2)$$

Equation 4-25

Ortiz et al. also quote a solution for flow along a single gas-induced fracture as;

$$Q_{st} = \frac{v_{st} W_c \delta^3}{48 R T \eta_g L_s} (P_{gi}^2 - P_{go}^2)$$

Equation 4-26

where the flow of gas is dependent on the aperture, δ , and width, W_c , of the gas filled fracture. In this expression the flow of gas is now decoupled from the cross-sectional area of the sample.

4.5.4. Scale-dependence and its impact on gas flow

Ortiz et al. (1997) provide a commentary of Horseman and Harrington, arguing that the treatment of permeability as a continuum can be considered appropriate, provided that the "representative elementary volume" (REV) is defined so as to be large enough to contain very many pathways. However, as the authors point out, if the gas exploits the weakest pathway from source to sink, then the concept of a "continuum" or "equivalent porous medium" gas permeability is no longer valid. An illustration of this argument is presented by considering the effect of doubling the cross-sectional area of the sample of a laboratory experiment. Assuming the sample is large enough to be considered to be an REV for gas flow, then the volumetric flow rate of gas for a fixed pressure gradient will be twice as large in the big sample than it is in the small one. However, if each sample contains only a single gas pathway, then the volumetric flow through the two samples will be more or less the same, regardless of their cross-sectional area. If the data is then interpreted for "weakest link flow" assuming continuum behaviour, the gas permeability of the big sample would be calculated to be half that of the small sample.

Horseman and Harrington suggest that at the time of writing (i.e. 1997) both laboratory and field test data would seem to support the "weakest link" concept of gas migration in the Boom Clay, although this had yet to be proven. This remains the case for the Boom Clay. While work by Harrington et al. (2012b) using gold nano-particles alluded to the localisation of gas flow and proved the importance of dilatancy as a mechanism for gas migration, there is little direct physical evidence of pathway development (e.g., from gas tracer studies or the use of tomographic imaging techniques). Work by Donohew et al. (2000) on a range of clay pastes observed the migration of gas was always accompanied by the development of localised dilatant pathways. **Figure 4-8 (right)**, also suggests localisation of gas flow. However, dedicated gas migration experiments are needed to confirm these concepts. If 'weakest link concept' is valid, however, it has important implications in the development of mathematical models of near-field gas movement.

4.5.5. Impact of burial history on gas flow

Information on the burial history of the Boom Clay is scarce and little information is available within the open literature (Section 1.3). Fortunately, a significant number of studies have been undertaken examining the consolidation behaviour of the Boom Clay (Section 3.3.3). These studies show that the Boom Clay undergoes significant volume

change during compression, which impacts both hydraulic permeability and specific storage. A cross plot of data presented by Ortiz et al. (1997), indicates a significant reduction in conductivity occurs during the compression of the Boom Clay (Figure 4-10). It is likely that at the repository depths of interest to the Netherlands, hydraulic conductivity will be $\sim 10^{-13} \text{ m.s}^{-1}$ and below; an order of magnitude lower than the values observed at Mol.

Very little information on the impact of burial stress on the gas migration behaviour of the Boom Clay exists. Horseman and Harrington (1994) report an early test on the Boom Clay (designated T2S1-G) in which the dependence of peak gas pressure to the effective stress was briefly examined. Here simultaneous increments in backpressure and confining stress were applied to the sample (Figure 4-11 stages 1 through 3) and the resultant change in differential pressure and gas in/out flow were measured. On this basis, Horseman and Harrington proposed a simple relationship linking peak gas pressure, P_{gp} , to effective stress, σ_{eff} , as:

$$P_{gp} \approx 0.85\sigma_{eff} \quad \text{Equation 4-27}$$

While the authors note the expression is only valid for the specific sample tested, the data indicates gas migration is functionally dependent on the stress state acting on the clay. This was further explored within the same test by applying an additional increment in total stress (Figure 4-11 stage 4). This raised peak gas pressures by 0.24 MPa changing the numeric value from 0.85 to 0.81. This supports the assertion that peak gas pressure (which for the majority of the test coincided with the gas breakthrough pressure), is dependent upon the effective stress. However, the form of this relationship with respect to the Boom Clay in general cannot be ascertained from the data presented and further work is required.

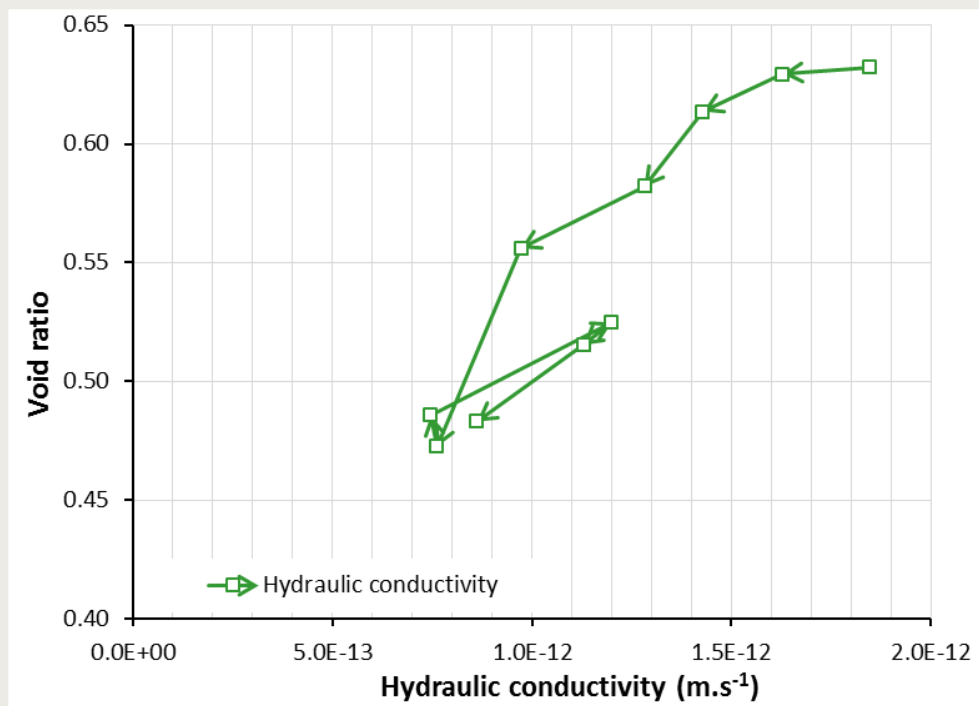


Figure 4-10. Cross plot of void ratio against hydraulic conductivity for the Boom Clay from the Mol URL taken from data presented by Ortiz et al. (1997). Data clearly shows permeability decreases (around 60%) for a change in void ratio of 0.63 to 0.47.

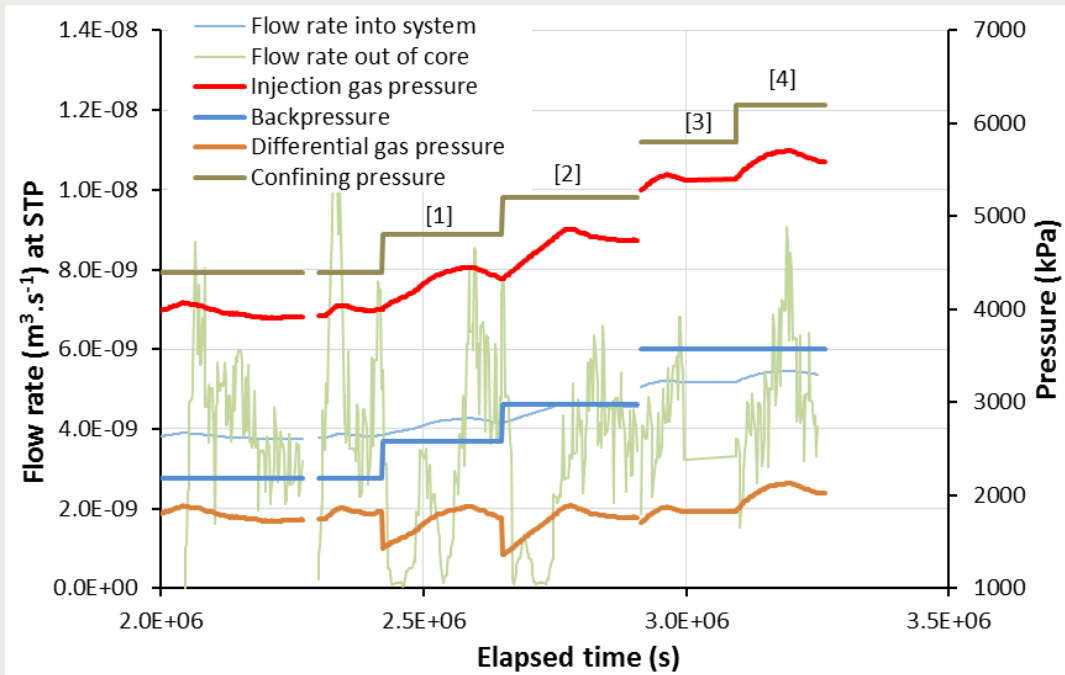


Figure 4-11. Reprocessed data from Horseman and Harrington (1994) showing the sensitivity of gas pressure to changes in confining stress for sample T2S1.

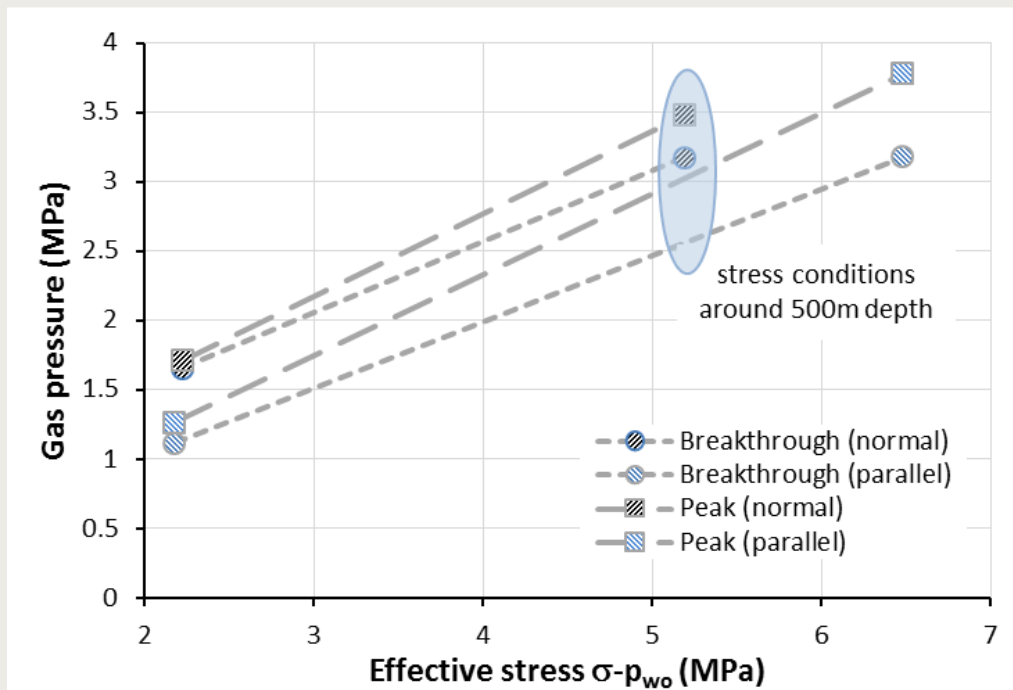


Figure 4-12. Cross plot of data presented in Horseman and Harrington (2000) showing average breakthrough and peak gas pressures against effective stress for samples normal and parallel to bedding. Effective stress conditions for a repository at a depth of 500 m are marked (blue ellipse).

Horseman and Harrington (2000) tabulate breakthrough and peak gas pressures for a matrix of tests performed on the Boom Clay specimens orientated both parallel and normal to bedding (Appendix Table B-7). Given the variability in parameters it seems prudent to calculate average values for breakthrough and peak gas pressures based on sample

orientation. A cross-plot of these values against effective stress, **Figure 4-12**, provides approximate trends with which to estimate breakthrough and peak gas pressures at a repository depth of 500 m. While this approach is somewhat crude, breakthrough and peak gas pressure are estimated to range between 3 and 3.5 MPa respectively for flow normal to bedding and 2.5 to 3.0 MPa parallel to bedding. These values will require verification through further laboratory and field scale experiments.

4.5.6. Impact of gas migration on hydraulic properties

To examine the impact of gas migration on the hydraulic properties of the Boom Clay, Harrington and Horseman (1997) undertook a small study on a single sample of the Boom Clay, measuring the hydraulic conductivity and specific storage both before and after gas testing (**Appendix Table B-8**). Inspection of the data indicates a small but measurable drop in hydraulic conductivity as a direct result of gas injection. The authors report that the path followed by the clay in conductivity-effective stress space moves down and to the left as a result of gas injection. Harrington and Horseman report a systematic increase in like-for-like specific storage values after gas injection, suggesting this can be attributed to the compressibility of residual gas left along previous migration paths. A similar observation was made for tests performed on CO_x by Harrington et al. (2014) who observed a small reduction in permeability and an increase in specific storage. Field experiments undertaken by Ortiz et al. (2002b), examining the impact of gas flow on hydraulic behaviour, suggest that after ten weeks of water re-injection the preferential pathway generated during gas injection no longer represents a preferential pathway for aqueous borne radionuclides.

4.5.7. Gas driven radionuclide migration

The potential for gas to mobilise and transport aqueous borne radionuclides must be considered in repository performance. As part of the FORGE (Fate Of Repository GasEs) project, SCK-CEN undertook a detailed study examining the mobility of iodine (selected as the sorption of iodine under normal Boom Clay conditions is negligible) during gas injection experiments (Jacops et al. 2013b). To mitigate the effects of background iodine diffusion, tests were undertaken quickly with gas breakthrough often induced within 4 days of injection. However, results from this study suggest less than 1% of the iodine is mobilised as a direct result of gas flow. The study also reports very low desaturation rates during gas injection, with values uniformly below 1% for the Boom Clay. These values are in general agreement with those reported by Volckaert et al. (1995) and indicate rapid gas pressurisation of the Boom Clay has minimal impact on the rate of desaturation.

However, the mobility and fate of gas borne radionuclides remains an open question, as does the capacity of gas to mobilise aqueous borne radionuclides in accumulations of free water which may be present in silt/sand horizons within the Boom Clay formation.

4.6. Transport summary

It is possible to estimate a likely range of hydraulic conductivities ($\sim 2 \times 10^{-13} - 1 \times 10^{-12} \text{ m.s}^{-1}$) expected within the Boom Clay formation at depths of 500m. However, such estimates exclude the potential for lithological variation and are limited by a paucity of data in relation to burial history, preconsolidation pressure and expected void ratio, leading to a remaining degree of uncertainty. Hydraulic properties will also exhibit significant anisotropy (with a ratio > 2 being highly likely), though additional testing is required in order to constrain this further. Coupled flow behaviour is even more poorly constrained at appropriate *in situ* conditions, although significant effects are expected. Whilst there is a limited amount of data relating to diffusion of gases for the Boom Clay at

HADES, no such measurements could be found for material taken from greater depth intervals. Other than to assume that these values represent an upper value for diffusivity in a Dutch repository within the Boom Clay, further statements about likely diffusion coefficients are not possible.

In relation to advective gas flow, there is now a growing body of evidence demonstrating that such migration in clays, mudrocks and shales is commonly associated with the development of pressure-induced dilatant pathways whose aperture, width and distribution functions dictate the conditions at which gas becomes mobile and the apparent gas permeability values. The case for such behaviour in the Boom Clay is particularly sound. Under these conditions, standard visco-capillary models of two-phase flow (Aziz and Settari, 1979; De Marsily, 1986) based on concepts of phase displacement provide a poor representation of the underlying physics governing flow. In the absence of appropriate phenomenologically based models, outputs from these codes should be treated with caution, in particular, when used in a predictive manner.

Further work on the Boom Clay is required to better define the coupling between gas flow and stress, the role of REV in sample selection, and the impact of heterogeneity and anisotropy on the process and mechanisms governing gas flow.

Recommendations

- **Additional experimental testing of the Boom Clay from HADES (at higher effective stresses) providing an improved understanding of:**
 - The influence of depth of burial on hydraulic anisotropy;
 - The influence of salinity on hydraulic properties (permeability and specific storage);
 - Coupled flow phenomena, in particular osmosis and electro-osmosis coupling coefficients and geochemical conditions for representative near-field chemical conditions;
 - Diffusion rates for relevant repository gases;
 - The pressures at which a free gas phase will become mobile and the evolution to peak pressure (validation of estimates);
 - The influence of compaction state and anisotropy on dilatant pathway formation and evolution;
 - The distribution, evolution and longevity of dilatant gas pathways.
- **Recovery of well-preserved core from appropriate NL locations and depths is required to provide an improved understanding of:**
 - Lithological controls on void ratio, hydraulic permeability, gas entry, peak and shut-in pressures (e.g., sand/clay fraction and carbonate content);
 - Lithological controls on the function dependence of gas permeability to stress state;
 - The burial history of the region, expected void ratios and associated impacts on hydraulic permeability and specific storage;
 - Spatial variability of hydraulic properties;
 - Existing hydraulic anisotropy.

In particular, predictions of hydraulic properties are based on an assumed preconsolidation stress. However, these estimates are limited by the uncertainty in this value which may be impacted by differences in the burial history and mineralogy of the clay in the Netherlands. Uncertainty would be significantly reduced by consolidation testing of the Boom Clay retrieved from appropriate depths in the Netherlands, providing data on void ratio and better constraint on the

5. Thermal effects

Experimental testing of clays, both in the laboratory and *in situ*, has shown that elevated temperatures can affect pore water pressure (Chen et al., 2011; Cui et al., 2009; François et al., 2009; Li, 2013; Monfared et al., 2012), mean effective stress (Chen et al., 2011; François et al., 2009; Monfared et al., 2012), pore structure (Li, 2013), pore water viscosity (Monfared et al., 2012), friction angle and shear strength (Cui and Tang, 2013; Monfared et al., 2012), and unit volume (Cui and Tang, 2013; Cui et al., 2009; François et al., 2009). As such, a Dutch repository design must allow for the potential impacts of heat emission of the wasteform on the host formation.

The size of the zone of thermal influence within a repository will be dependent on various factors, including:

- Thermal exposure of the waste (i.e. duration);
- Heat dissipation;
- Maximum temperature.

These factors can be controlled, to some extent, by the size of the waste canisters placed in the repository, their spacing and the thickness of buffer material used. Such aspects of repository design will in turn influence its footprint and larger-scale features (Horseman and McEwen, 1996). Current proposals for a Dutch repository in the Boom Clay involve defining the canister spacing to limit the temperature (below 100 °C) in the surrounding host rock and engineered barrier (Verhoef et al., 2011). A thorough understanding of the long-term thermal impacts on host formation properties is therefore crucial for the development of a repository concept and the associated disposal safety case.

The following sections describe the thermal properties of the Boom Clay from Belgium, as well as some potential impacts resulting from long-term exposure to elevated temperature conditions.

5.1. Thermal parameters

Heat emitted from high level waste is likely to affect both the host formation and the engineered backfill/buffer in a repository. The size of the thermal zone of influence will depend upon the rate of heat dissipation, which is intrinsically linked to the thermal conductivity of the material. The degree of influence will depend on the thermal expansion coefficient of the material, as well as that of the pore water. Thermal conductivity is a transport property and is characteristic for a specific material. For an isotropic material the thermal conductivity in one direction is defined as (Incropera et al., 2007);

$$\kappa_T = \kappa_{Tw} \kappa_{Ts}^{(1-w)} \quad \text{Equation 5-1}$$

where w is the water content, κ_{Tw} is the thermal conductivity of water (0.60 W/m°C) and κ_{Ts} is the thermal conductivity of the sample matrix, i.e. the solid (Midttømme et al., 1998). However, it should be noted that conventionally thermal conductivity is denoted as 'k' and will therefore be described as such for the remainder of the chapter. Elsewhere within the report 'k' has been used to denote intrinsic permeability, as described in the listed symbols and abbreviations.

As might be expected, the thermal conductivity of solids is, in general, larger than that of liquids and gases. Anisotropy of thermal conductivity is defined as the ratio between thermal conductivity parallel and perpendicular to bedding. Some example values of thermal conductivity for clays and shales are given in (**Appendix Table B-9**). Direct measurements of the thermal conductivity of the Boom Clay are rare and values are generally estimated based on fitting to laboratory or field data. Values reported for the Boom Clay in the literature tend to range from around 1.6 to 1.7 W/m°C; these are relatively typical for a lightly overconsolidated clay and compare well to other candidate repository host formations, such as the Callovo-Oxfordian Clay (France, 1.57 W/m°C) and the Opalinus Clay (Switzerland, 1.7 W/m°C).

However, it should be noted that these values do not account for anisotropy and are not quoted in combination with an orientation in relation to the clay fabric. Midttømme et al. (1998) measured anisotropy ratios for thermal conductivity in several UK clays, which ranged from around 1.05-1.75. Given the well-established anisotropy of other Boom Clay physical properties, it seems likely that a significant difference in conductivity with orientation to bedding may likewise be present, though no data relating to this could be found within the literature.

Also of importance are the thermal expansion coefficients, a thermodynamic property of the material which connects the change of temperature with linear or volumetric expansion (Benazzouz and Zaoui, 2012). Thermal expansion coefficients are not constant and vary with temperature and pressure. For a homogeneous material the linear expansion coefficient, α , and volumetric expansion coefficient, β , are defined below;

$$\alpha = \frac{1}{L} \left(\frac{\partial L}{\partial T} \right)_P \quad \text{Equation 5-2}$$

$$\beta = \frac{1}{V} \left(\frac{\partial V}{\partial T} \right)_P \quad \text{Equation 5-3}$$

where T is the temperature, L is the length (in the direction of expansion), V is the volume, ρ is the density and derivatives are taken at constant pressure P (Benazzouz and Zaoui, 2012; Sillen and Marivoet, 2007). For an isotropic material the volumetric expansion coefficient is precisely three times larger than the linear expansion coefficient (Vardon et al., 2016). A comparison of linear and volumetric thermal expansion coefficients for different clays is given in **Appendix Table B-10** and **Appendix Table B-11**. As with mechanical properties, the thermal expansion behaviour of clay will be highly dependent on its drainage state and reported values for α in the Boom Clay are more than double when heating takes place in undrained, as opposed to drained, conditions.

It should also be noted that elevated temperatures can also impact clay mineralogy, instigating phase changes in some materials. The Boom Clay has a clay fraction of ~30 % which is composed of smectite; a 2:1 clay. When exposed to elevated temperatures smectite can become unstable and transform to illite, a more stable silicate phase (Wersin et al., 2007). Evidence from geological analogue systems indicates that this transformation is very slow and is the result of temperature exposure > 150 °C (Wersin et al., 2007). Therefore, assuming a repository footprint is designed to limit temperatures to < 100 °C, it seems likely that illitisation will not be an ongoing process within a Boom Clay-hosted repository.

5.2. Elevated temperature testing

A significant body of work exists examining the influence of elevated temperatures on the Boom Clay. The focus is primarily on the thermo-hydro-mechanical response of the material on heating and cooling, as well as the permanence/transience of any resulting changes in the physical properties of the clay. Experimental investigation has included several decades of *in situ* testing at the HADES underground laboratory at Mol, with tests programmes often lasting for several years. Some key field tests and associated findings are described in further detail in Section 5.6. Field scale testing has also been accompanied by a number of laboratory studies, focussed on qualifying and quantifying key effects.

A number of heating methodologies are available in the laboratory and include:

- (i) submersion of the sample cell in heated oil;
- (ii) the use of electrical heaters surrounding the cell;
- (iii) the use of a water-filled copper spiral around the cell;
- (iv) the use of a pressure cell entirely contained within a heated oven or incubator.

Standard methodologies for mechanical and fluid flow testing are then employed, in order to examine the impact of heating on material response. The impact of the thermal expansion of experimental apparatus must be carefully considered when analysing test observations and many studies involve the inclusion of rigorous calibration for such effects though, where disassembly is required between tests, these can never be fully negated. Selection of the appropriate drainage condition is also crucial, since the clay response to thermal loading is significantly altered if pore pressures are unable to dissipate.

A range of elevated temperature experiments can be found in the literature, for various clay-rich materials, examining thermal properties and processes under relevant applied conditions. Key studies and findings are introduced in the following sections (Sections 5.3-5.6). As with mechanical and hydraulic testing, the majority of clay samples have been derived from the HADES underground laboratory at Mol (unless otherwise stated) and are therefore taken from a depth of around 220 m. **Appendix Table B-12** gives a summary of some key laboratory approaches to investigating thermo-hydro-mechanical coupling effects for different clays.

5.3. Mechanical response and impacts

Based on the thermal expansion coefficients (**Appendix Table B-11**), it is clear that exposure to elevated temperatures will result in differing responses in the liquid (pore water) and solid (soil skeleton) phases within a porous material. In a low permeability clay, these differences result in a complex material response to thermal loading, which is strongly influenced by boundary conditions and can include the generation of significant thermal strains and the rapid development of excess pore pressures (Baldi et al., 1991; Chen et al., 2011; Cui et al., 2009; François et al., 2009; Monfared et al., 2012).

Early work investigating the thermal properties of the Boom Clay was conducted in the 1980's and 1990's, much of which occurred as part of European research collaborations. Primary focus was on mechanical aspects of the clay response. Baldi et al. (1988) conducted heating tests on three clays (Italian Pontida, Boom and Kaolin), in order to examine the differential volumetric strains generated by elevated temperatures on the clay-skeleton and the clay-water system. Experiments involved subjecting clays to constant effective stress and constant isotropic consolidation under drained conditions and various temperatures. Testing was conducted using a triaxial cell fitted with one radial and two axial heaters. Baldi and co-workers observed that, whilst under constant stress conditions, heating of the clay samples led to consolidation with similar outflow behaviour to that

seen during mechanical consolidation. In order to investigate the influence of consolidation state on the reversibility of induced strains, test samples were subjected to isothermal loading followed by isobaric heating, then isothermal unloading and isobaric cooling, at which stage the clay was allowed to return to its original temperature and pressure conditions. The findings indicate that, when overconsolidated, the response of the Boom Clay is thermoelastic (strains are reversible) whilst normally consolidated the Boom Clay responds in an inelastic fashion (strains are not fully reversible).

Further testing on the Pontida silty clay also suggests that thermal strains are dependent on both temperature and effective stress. Findings suggest a significantly higher thermal expansion coefficient exists for free water than for water absorbed on clay minerals. As a result, the clay skeleton may undergo contraction or expansion on heating, depending upon the effective pressure. The authors report that volumetric strain was dilatant for low isotropic stress and compactive at higher stresses (a tendency which was seen to be compounded at higher temperatures). At intermediate effective stresses (0.5 - 1.0 MPa), this sensitivity to temperature is a key control with compaction and dilation occurring at higher and lower temperatures respectively. Finally, Baldi and co-workers put forward a phenomenological method to calculate the effective thermal expansion of water in fine pores. They also use their experimental data to develop an approach for evaluating the reduction in the elastic domain, in response to elevated temperatures, and the associated impact on the yield limit.

Hueckel and Pelligrini (1992) describe experiments applying heating and cooling cycles to samples of clay under constant total stress and undrained conditions. Testing was conducted on the Boom Clay from Mol (at 240 m depth), as well as Pasquasia clay from Italy (at 160 m depth). Both normally consolidated and over-consolidated specimens of the Boom Clay were used. They observed a large increase in pore water pressure on heating, resulting in large irreversible strains and possible mechanical failure. Conversely, subsequent cooling led to a drop in pore water pressure. Their observations indicated that the material response to heating and cooling could be satisfactorily explained using the standard effective stress principle, assuming shear strength and consolidation are described in terms of a thermally-controlled plastic yield limit.

Horseman and co-workers (Horseman et al., 1987; Horseman et al., 1993) conducted shear testing on undrained Boom Clay samples under room and elevated (80°C) temperature conditions. Clay samples were heated using an electrical heating jacket, clipped around the vessel. The authors report that both the undrained Young's modulus, E_u , and the peak shear strength at failure for the high temperature tests were observed to be not dissimilar to measured values at room temperature, when extrapolated to the same effective stress conditions ($P_{eff} = 2.24$ MPa, as *in situ* at Mol). These observations are used by Horseman and co-workers to 'tentatively suggest' that heating in this temperature range is not sufficient to cause significantly adverse effects on the clay's mechanical properties, providing any thermally-induced excess pore pressures are allowed to dissipate.

Measurements of the change in pore pressure and the associated volumetric strains during thermal consolidation of the two heated samples are shown in **Figure 5-1** and **Figure 5-2**. The authors suggest that for *in situ* stress conditions at Mol, excess pore pressures of the order of 1 MPa may be generated during heating from ambient to 80 °C. In addition, a notably larger strain response and higher resulting excess pore pressure were observed for the sample held at a higher total stress level, indicating that mechanical preconsolidation can exacerbate pore pressure build-up. These findings may result from the reduction in pore water mobility in more consolidated clay and suggest that greater levels of pore pressure build-up may occur in clay with a higher OCR.

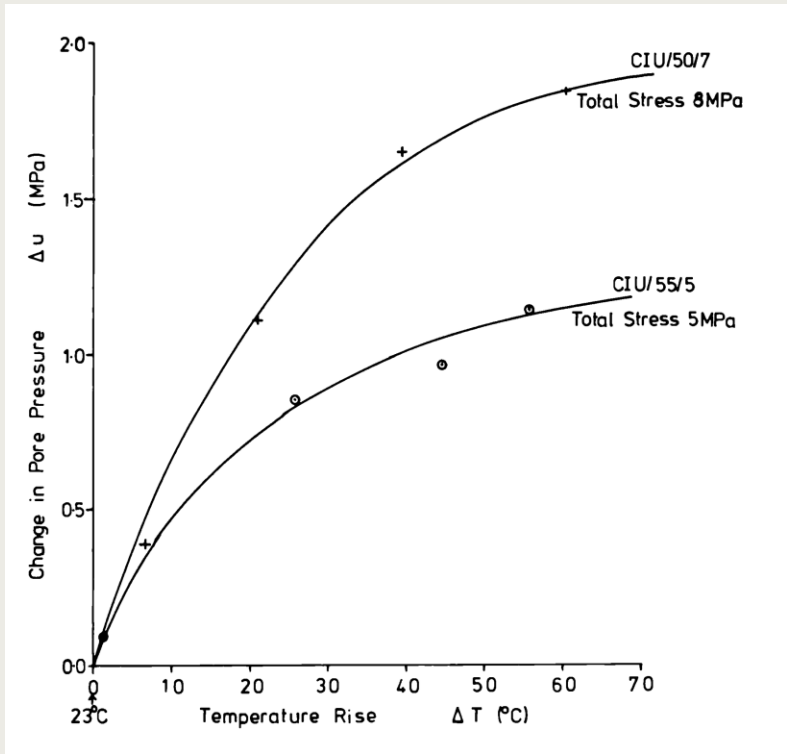


Figure 5-1. Change in pore pressure plotted against temperature rise above ambient for two Boom Clay samples held at constant total stress (isotropic). After Horseman *et al.* (1987; 1993).

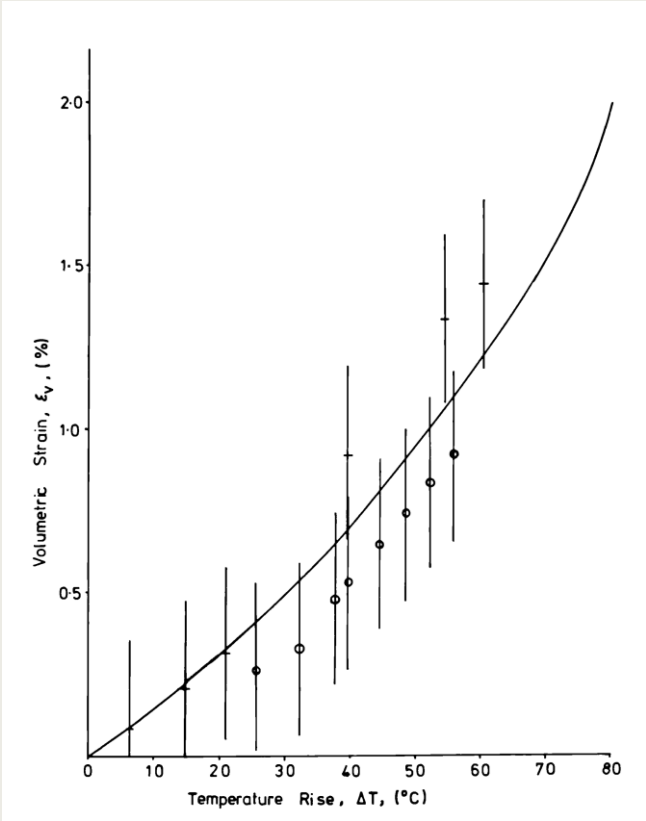


Figure 5-2. Volumetric strain (with error bars) plotted against temperature rise above ambient. Test data relate to the Boom Clay samples subjected to an isotropic loading of 8 MPa (dashes) and 5 MPa (circles). A polynomial model is fitted to the test data. After Horseman *et al.* (1987; 1993).

The influence of temperature and confining pressure on clay response was investigated by De Bruyn and Thimus (1996). They carried out a suite of laboratory experiments on eleven samples of the Boom Clay, examining the influence of temperature (at 20°, 50°, 75° and 80 °C) and confining pressure (2.1, 3.1 and 4.1 MPa). In order to minimise sample variability, all material was pre-prepared from the same block of clay which was sourced at the HADES laboratory at a depth of ~223 m. One sample had previously been subjected to undrained, unconsolidated testing (UU), whilst the others had been subjected to undrained, isotropic consolidation, though findings from this stage of testing were not described in this study. Samples were first fully saturated, then allowed to consolidate at a constant confining pressure, whilst an applied backpressure was maintained at (0.1 MPa). Specimens were only allowed to consolidate for two days; given the low permeability of the Boom Clay it is therefore unlikely that they would have reached their final state by this time. The same heating rate (0.5 °C/min) as that used by Horseman et al. (1987) was then applied. After the selected test temperature was reached, held and allowed to stabilise, samples were then sheared until yield.

During the heating phase of testing, sample pore pressure was seen to rise in response for all samples. However, the magnitude of pore pressure elevation was observed to be much more significant for test samples heated to 80 °C than for those heated to 50 °C. During shear testing the form of the observed stress-strain evolution was unaffected (as compared to room temperature) when heated to 50 °C, although the peak stress reached before yield was notably reduced. A further reduction in strength was observed for samples heated to 80 °C. However, the reduction in peak strength was observed to be more pronounced between room temperature and 50 °C, than between 50 °C and 80 °C. Fitting a Mohr-Coulomb envelope to test data indicated a drop in values for cohesion (τ_0) and friction angle (ϕ) from 0.89 and 10.0° (at room temperature) to 1.03 and 4.6° (at 50 °C). As with Horseman et al. (1993), no clear change in the critical state M coefficient was observed. In contrast, Hueckel and Pellegrini (1989) report a drop in M from 1.0 to 0.8 when temperature increased from 20°C to 80 °C.

Baldi et al. (1991) also reported a slight decrease of friction angle at critical state with increasing temperature for samples of the Boom Clay. Their findings are described in brief by Francois et al. (2009). Following on from the conclusions of Baldi et al. (1988), the authors observed a transition between an expansive and a contractive response to thermal loading, which appears dependent on the OCR of the clay. Assuming a pre-existing preconsolidation stress for clay from Mol of 6 MPa, results from thermal loading indicate that the transition occurs between OCR = 6 and OCR = 2, with contraction observed at OCR = 1 and OCR = 2 (Figure 5-3).

Delage et al. (2004) also examined sample volume change under drained conditions and a slowly increasing thermal load. Experiments were conducted using an isotropic confinement vessel, with a heating coil placed around the outside wall of the cell. Changes in sample volume were measured based on inflow to the confining system. Whilst the effects of compressibility of the apparatus were carefully calibrated for, changes in system compressibility resulting from reassembly for each new test sample cannot be excluded. Achieving accurate results with this method of strain measurement is non-trivial, although it is often adopted for thermal loading tests, as measuring inflow/outflow from the sample is complicated by the differing thermal responses of water and solids.

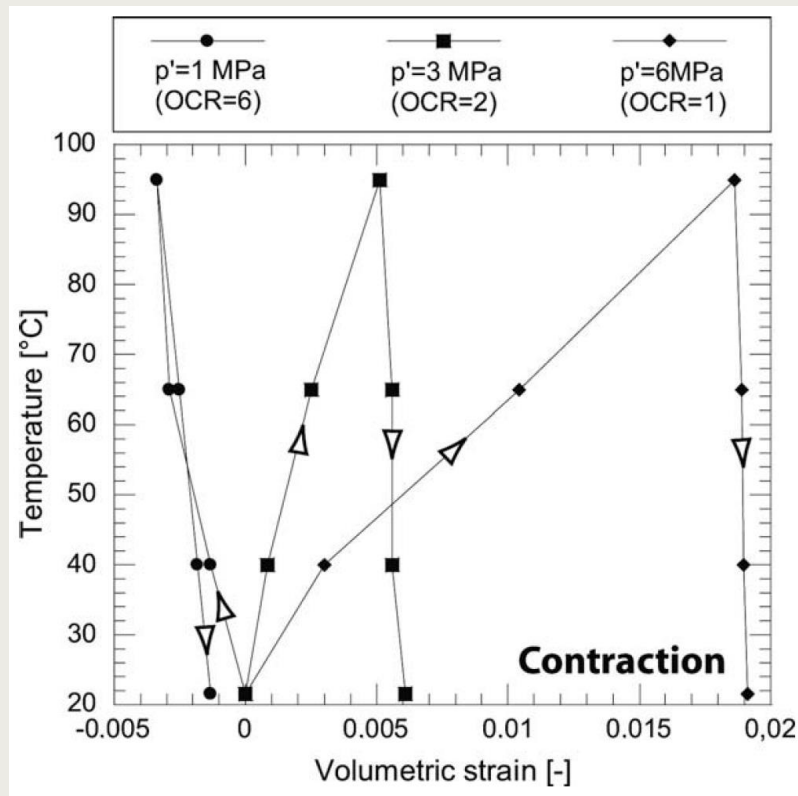


Figure 5-3. The Boom Clay volumetric response to thermal loading at three different OCRs. P' = confining pressure. Results indicated a transition from contraction to expansion between OCR = 2 and 6. From Francois et al. (2009), after Baldi et al. (1991).

Testing was initiated by first saturating a clay sample at an applied water pressure of 1 MPa and under an isotropic confinement of 1.03 MPa, resulting in an effective stress of 30 kPa. This procedure would have resulted in some swelling of the sample, as hydration did not take place under original *in situ* conditions (unless later reconstituted), though this effect is not discussed. The sample was then loaded to a pressure of 4 MPa before being unloaded to a pressure of 2 MPa, with the purpose of consolidating the sample to an OCR \approx 2. It is presumed that the initial hydration procedure was applied in order to remove the influence of the clays prior preconsolidation history ($P_c' \sim 5 - 6$ MPa, Section 3.3.3), which would instead result in an OCR of around 2.5 to 3. However, this is not discussed and no evidence is provided to demonstrate the success of such a procedure.

After mechanical consolidation, the sample was subjected to a series of temperature increments, starting at room temperature and resulting in the thermal consolidation of the clay. The authors report that an expansion was observed under low temperature loading (between 23 and 50 °C), whilst exposure to higher temperatures (50 - 60, 60 - 70 and 80 - 95 °C) resulted in a contraction of the clay. Where consolidation occurred, the authors noted an initial smaller magnitude expansion which was shortly followed by a larger magnitude contraction. Nevertheless, the ultimate response in these cases was a reduction in sample volume. It was also highlighted that once contraction begins, the form of the consolidation curve is highly similar to that induced by mechanical loading, indicating that volume decrease is likewise related to dissipation of excess pore pressure. The authors use an analytical approach to demonstrate that a negligible amount of water is drained during the heating phase, leading to an initial increase in volume as a result of the undrained thermal expansion of both mineral constituents and water. Once the temperature distribution is uniform, contraction akin to mechanical consolidation at constant temperature then takes place. The consolidation coefficient is also calculated based on

thermal consolidation curves with the only notable change occurring between 60 and 70 °C. This is attributed to the competition between increased permeability and decreasing void ratio (as a result of elevated temperature), though the authors argue that the resulting change in this coefficient is not sufficient to be considered significant.

Sultan et al. (2002) also conducted laboratory experiments on the Boom Clay samples taken from HADES, in order to examine thermo-mechanical coupling. In particular, the test programme was designed to investigate the effect of temperature on preconsolidation stress and, conversely to examine the influence of the overconsolidation ratio of the clay on consequent thermal volume changes. Testing was conducted under isotropic confinement and elevated temperatures were applied by way of a heating coil placed around the outside wall of the pressure cell.

The authors present data relating volumetric strain to temperature for different cooling rates, which appears to show that the degree of thermal straining is rate dependent. It is therefore argued that some earlier work exhibiting expansive behaviour during cooling may be the result of inappropriate selection of cooling rates, which should be as slow as possible. Nevertheless, the evidence for this dependency is only given for one sample and is not placed within the context of the test programme, with very little information provided on test history; in particular the heating history of the test sample.

During thermal consolidation testing, the chosen heating/cooling rate was selected based on observations of sample volume change resulting from cooling increments of 0.1 °C. However, the associated cumulative strains shown appear to be more than two orders of magnitude larger than those shown when discussing cooling rate dependency. Furthermore, as with some other test programmes, samples were initially saturated under exceptionally low effective stress conditions (0.05 MPa) which are likely to notably impact the pre-existing properties of the clay. Test data from thermal loading does appear to impact the preconsolidation pressure of the clay, though additional information relating to the experimental history would help clarify the significance of the results. The authors also present additional data relating to the influence of OCR on the volumetric strain behaviour of the Boom Clay during loading, which is described in further detail by Delage et al. (2004).

Delage and co-workers state that normally consolidated samples displayed contraction on heating, independent of the applied effective stress and that thermal contraction increases with decreasing OCR, leading to its dominance at OCR = 1. They also note that the temperature at which thermal contraction begins to dominate increases with increasing OCR. However, the effective stress conditions applied to generate the required OCRs are unclear and, whilst the prior burial history of the clay samples is not relevant at effective stresses above 5 - 6 MPa, at lower OCRs an explanation is not given as to why this history can be neglected. This may, in part, explain the differences observed in the volumetric strain response for thermal loading at OCR = 2, as compared to the findings of Baldi et al. (1991).

The influence of OCR and the time-dependent behaviour of the Boom Clay were also investigated by Cui et al. (2009). Testing was conducted in a triaxial cell with a heating coil placed on the outer cell wall, in order to induce elevated temperature conditions. The clay specimens were first allowed to hydrate at close to *in situ* effective stress conditions, with confining and pore pressure slowly incremented until a target $P_c = 3.5$ MPa and $P_p = 1$ MPa was reached. After saturation, samples were thermally or mechanically loaded (either at a constant rate or by stepped increments), by increasing heater temperature or applied confining stress. Observations from mechanical consolidation (from $\sigma_{eff} = 2.5$ to 10 MPa) at a range of isothermal states (ranging from 25 to 76 °C) demonstrate that resultant strain

rates are greater at higher temperatures, suggesting a faster response to changing stresses at elevated T.

The impact of thermal loading (from 25 to 80 °C) was also examined under isobaric conditions (ranging from $\sigma_{eff} = 2.5$ to 4.0 MPa). The authors found that under elevated temperatures the clay displayed either a volume increase or a volume decrease, depending on the OCR value and temperature range. Thermal consolidation occurred under small OCR conditions (at $\sigma_{eff} = 2.5$ MPa) and lower temperatures (39.4, 40 and 55°C), whereas thermal expansion occurred under large-OCR conditions (at $\sigma_{eff} = 3.5$ and 4 MPa). The authors suggest a transition between these two behaviours is therefore likely to occur between an OCR of around 1.4 and 2.0, consistent with the findings of Baldi (1988; 1991). A rate dependency was also observed, as with mechanical consolidation, such that larger volumetric strain rates were observed at higher applied temperatures.

5.4. Impact on hydraulic properties

There is a significant body of work indicating that when subjected to thermal loading the Boom Clay undergoes volumetric changes not dissimilar to those induced during mechanical consolidation. Since an associated reduction in permeability is well-established for the mechanical case, the potential for a similar effect on the hydraulic properties of heated Boom Clay should be considered.

Nevertheless, only a small number of studies examining this aspect of THM behaviour are available. Delage et al. (2000) conducted constant head tests on laboratory samples at temperatures of 20, 60, 70, 80 and 90°C and found no evidence to suggest any impact on permeability as a result of thermal loading.

As part of the TIMODAZ project, SCK-CEN conducted constant volume permeameter tests in order to investigate the thermo-hydraulic behaviour of intact and fractured Boom Clay (Li et al. 2013; **Figure 5-4**). During heating of both fractured and intact samples (up to 80°C), hydraulic conductivity was seen to remain reasonably constant, with no significant evidence of hysteresis on cooling. These findings are consistent with similar laboratory observations made in bentonite (Harrington et al., 2014; Zihms et al., 2015) and the authors conclude that it is likely the pore structure of the clay matrix is not significantly affected by elevated temperatures, although the reversible influence of changes in the viscosity of water should not be neglected.

Additional thermal test programmes within TIMODAZ included work conducted by Monafared et al. (2012), who examined the influence of thermal loading (1 °C/h; 25 - 65 °C) on undrained, fractured samples subjected to deviatoric loading. They showed that the generation of excess pore water pressure, and the associated decrease in effective stress, can result in failure along existing shear bands. In spite of the presence or creation of such discontinuities, hydraulic permeability seemed to be unaffected, highlighting the exceptional self-sealing properties of the Boom Clay.

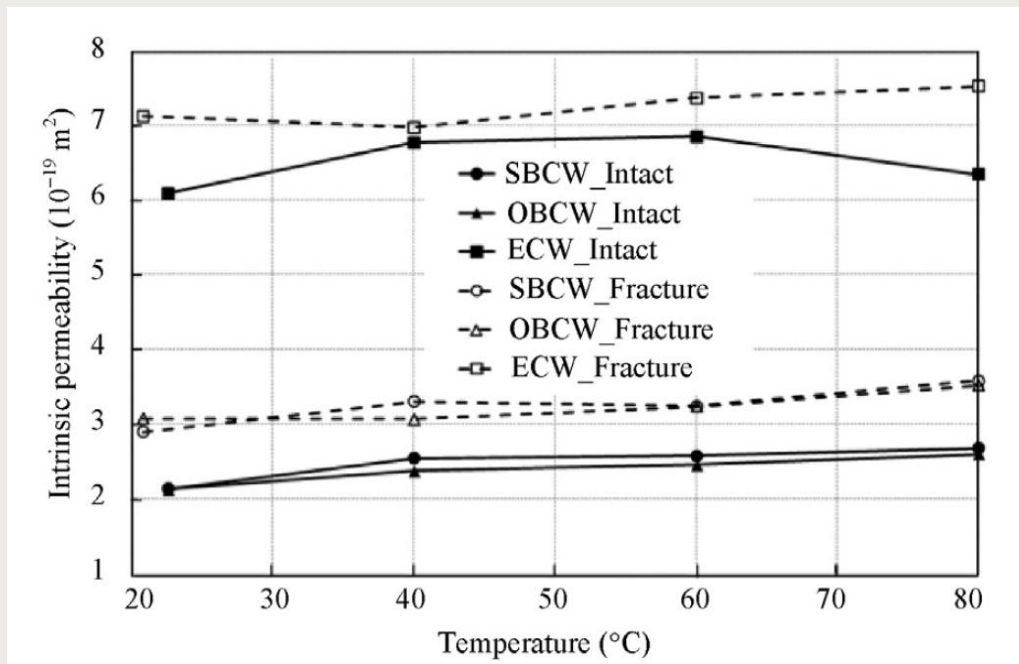


Figure 5-4. Influence of temperature on intrinsic permeability of the Boom Clay. After Li et al. (2013).

5.5. Impact of temperature on gas migration

Triaxial experiments undertaken by ISMES (Istituto Sperimentale Modelli E Structure), reported in Volckaert et al. (1995), were undertaken on samples of Boom and Pontida Clay. Temperatures were varied from 22 °C to 96 °C to examine their impact on gas breakthrough pressure. Two tests on the Boom Clay were also performed with water saturations of 0.83 and 0.88. Tests performed on saturated samples of the Boom Clay and Pontida Clay both exhibited a general increase in breakthrough pressure as a function of temperature. Scaling the data presented in Volckaert et al. for the Boom Clay (Figure 5-5), it is possible to define an approximate relationship between gas breakthrough pressure, P_b (kPa), and temperature, T (°C), as:

$$p_b = 9.47T + 958$$

Inspection of Figure 5-5 shows breakthrough pressure is somewhat sensitive to changes in temperature and increases as temperature rises. ISMES (also reported in Volckaert et al., 1995) examined the impact of temperature on ‘specific discharge’ i.e. gas flow rate out of the cores. Data presented also shows a reduction in outflow for a given pressure gradient as temperature increases. This indicates gas migration becomes more difficult with increasing temperature and implies that the Boom Clay undergoes thermal contraction during heating. Further work is required to explore this behaviour and assess its impact at depth.

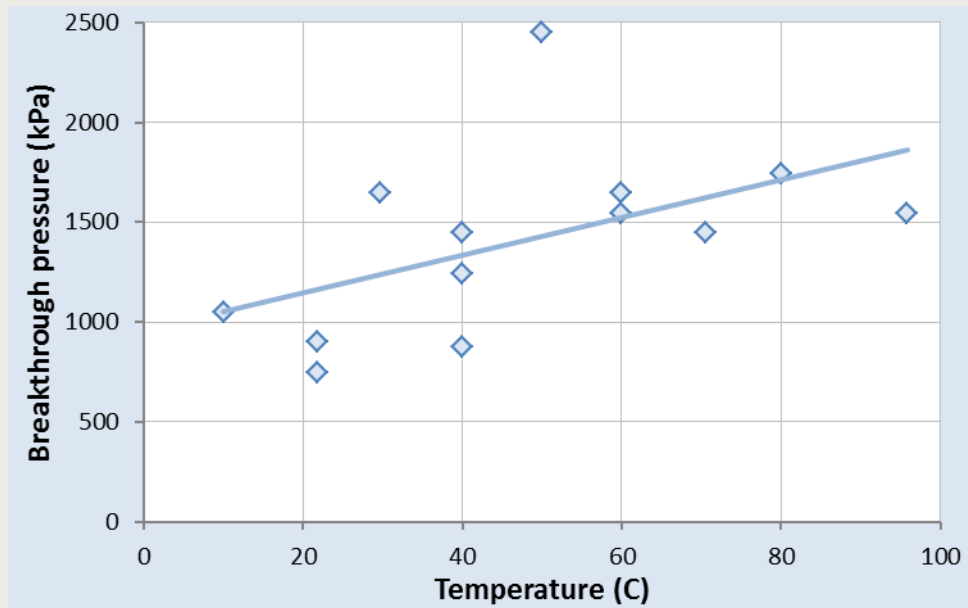


Figure 5-5. Breakthrough pressure against temperature for triaxial data on saturated samples of the Boom Clay, taken from Volckaert et al. (1995).

5.6. THM *in situ* studies

The HADES Laboratory has provided the opportunity for many *in situ* THM experiments to be conducted on the Boom Clay over the past three decades; mostly as part of EC-funded research programmes. This has resulted in the generation of a substantial amount of data relating to the large-scale response of the Boom Clay to elevated temperature conditions. This section briefly describes some key *in situ* experiments and associated observations.

A summary of three THM experiments, conducted *in situ* at HADES, is given by Bernier and Neerdael (1996). In all three tests a thermal load was applied and the physical evolution of the system monitored during either one or several heating and cooling cycles. Monitored parameters included: temperature, density, water content, permeability, total and effective stress, pore water pressure, and displacement.

The BACCHUS (Backfilling Control Experiment for High-level wastes in Underground Storage) test involved compacted Boom Clay emplaced around a heater, in turn emplaced in the host formation. This design allowed the THM behaviour of the Boom Clay to be examined in response to a constant thermal load of 100 °C at the interface between the heater and the engineered barrier. Heating began in March 1989 and ended later that year in August. Thermal loading took around two months to reach maximum temperatures and, as at the laboratory scale, resulted in an associated pore pressure pulse into the clay. After the heaters were switched off and cooling began, it took an additional three weeks for excess pore pressures to fully dissipate.

The CERBERUS (Control Experiment with Radiation of the Belgian Repository for Underground Storage) experiment was set-up to investigate both the impact of thermal loading (using heating elements) and radiation (simulated with 60°C) in combination. During testing, heating elements gave a constant working power of 730 W on the wall of the casing. This led to an elevated temperature in excess of 120°C, though a number of power failures led to several short-term temperature drops during testing. These shut-down phases were used to estimate a thermal conductivity for the clay of 1.6 W/m°C and a thermal diffusivity of 25.0 m²/y. It is not made clear, however, whether these values

take into account the anisotropy of the clay. Pore pressure evolution for this test is more complex and the authors attribute this, in part, to possible fracturing during the early stages of thermal loading. At the same time an increase in the local permeability coefficient by a factor of 1.6 was noted, despite allowing for the impact of the temperature-dependency of pore water viscosity. Likewise, the pore pressure response during power-failures is more complex to interpret and appears location dependent. It is also highlighted that pore water pressure at each location appears to be more sensitive than temperature during short-term variations in heating conditions. Furthermore, a reduction in permeability with heating was observed, which is attributed to thermal consolidation. The influence of heating on geomechanical measurements could not be reported in detail, since the monitoring sensors were damaged by the radiation generated during the experiment.

The CACTUS (Characterisation of Clay under Thermal loading for Underground Storage) experiments involved the emplacement of a 3.6 m long heater into a 14 m long borehole at HADES. The gap between the clay wall and the heater was filled with Boom Clay powder mixed with water. Heating started in September 1990, initially beginning with a one month power ramp (from 400 W to 1200 W), before being held at constant power (1200 W) until January 1992. For an additional cycle (CACTUS 2), power was kept constant during heating. The authors note that similar results were obtained for both tests. From cooling data, a thermal conductivity and diffusivity of $1.7 \text{ W/m}^\circ\text{C}$ and $6.10^{-7} \text{ m}^2/\text{s}$ were derived.

As with laboratory testing, a steep increase in pore water pressure was observed in response to heating, before dissipation could take effect and pressures began to stabilise towards initial values. Water content was also observed to decrease during the heating phase. Cooling then led to a decrease in measured pore pressures to values significantly below the initial state, before gradually re-equilibrating. At the same time, a gradual increase in the water content was observed. As with pore water pressure, the monitored total stresses initially display a steep increase (of a similar magnitude) during heating, but they then settle to a constant level until cooling begins, resulting in a fast decline followed by gradual stabilisation. The measured density of the clay was also seen to increase and decrease with heating and cooling, respectively, and the authors attribute this to the thermal consolidation and expansion of the clay.

Bernier and Needel (1996) conclude that there is a high degree of consistency in relation to the clay response, when comparing all three field tests. As in the laboratory, thermal loading of the clay is seen to generate similar behaviour as might be generated by an increase in the total stress regime. Loading is accompanied by a decrease in permeability and pore water content and a coincident increase in clay density; much like for mechanical consolidation. However, it is also highlighted that the observations at the time of publication could not allow for conclusions to be drawn relating to the irreversibility of these changes, even at a relatively low thermal load.

Continuation of EC-funded thermal field testing at HADES led to the installation of the THM test called ATLAS (Admissible Thermal Loading for Argillaceous Storage). The ATLAS test was designed in order to examine the THM behaviour of the Boom Clay (De Bruyn and Labat, 2002). Four electric heaters (8 m in total length) were emplaced at the end of a main 19 m long borehole, drilled from the main gallery. Two additional boreholes running parallel with the central borehole were instrumented in order to monitor evolution of the clay in response to heating. Testing began with heaters running at half the maximum power (900W) for a duration of three years, before thermal loading was increased to full power (1800W) for a further year. Heaters were then switched off and the clay allowed to cool. At the end of the test programme clay samples were cored close to the central borehole, where they had been exposed to temperatures up to 70°C during heating.

Primary findings from ATLAS are consistent with those from previous field tests. De Bruyn and Labat (2002) report an increase in total stress in response to heating at 900 W, peaking after one year and persisting once the clay temperature stabilised at around 73 °C, only declining by 0.1 MPa over two years. At the same time, the development over a period of 5 months of excess pore pressure is reported, with only a slightly larger decline resulting from dissipation on stabilisation of temperature (≈ 0.2 MPa). At the initiation of the second phase of heating at 1800 W, total stress and pore pressure were both observed to elevate much more quickly than before, peaking after 2-3 months. This was followed by a decrease in both of these, with magnitude significantly greater than in the first phase. The authors attribute this difference in behaviour to the higher pressure gradient present in the second phase of heating. Between the first and second heating phases, ATLAS was allowed to cool, during which time a steep decline in pore pressure and total stress to below initial conditions was observed in both cases. Measured total stresses then gradually returned to the original state and stabilised, whilst pore pressures were close to, though not fully equilibrated, at the time De Bruyn and Labat (2002) published their findings.

De Bruyn and Labat (2002) also report findings from the geomechanical testing of clay samples recovered from both the ATLAS experiment (heated to ~ 65 °C) and from CERBERUS (heated to a maximum of 90 °C). No obvious deviation was apparent beyond that of general sample variability between the geotechnical properties of the heated clays, as compared to standard Boom Clay samples from HADES. Shear testing was also conducted on test samples, using the same methodology as previously described for De Bruyn and Thimus (1996), in order to examine the effects of heating on the geomechanical properties of the clay. Test findings indicate no distinct deviation in the behaviour of the heated samples, as compared to standard test results, and the authors estimate a resulting shear strength of 0.8 MPa and an internal friction angle of 4°. The authors therefore conclude that the mechanical properties of the clay are not impacted by a history of thermal loading, within the confines of expected sample variability.

Francois et al. (2009) also reported observations and interpretation of data from ATLAS, supported by numerical modelling. They note that after the second heating phase was initiated, temperature significantly increased in the near-field, though the zone of influence was not dissimilar to the first phase. This implies that thermal power does not directly affect the size of the elevated temperature zone, at least within the confines of the temperature range considered and time allowed for testing. Nevertheless, pore pressure measurements indicate that the excess pressure zones generated extended beyond the elevated temperature region. Changes in pore pressure were observed up to 20 m away from the main boreholes, whilst temperature variations were only seen within a radius of 8 m. The authors also note that effective stresses never fully returned to the initial state in spite of the total dissipation of excess pore pressures at the test end. This effect is attributed to thermo-plasticity, leading to irreversible volumetric strain which in turn permanently redistributes the effective stress state of the clay. As observed in laboratory testing, thermal hardening during heating appears to have resulted in an increase in the apparent preconsolidation pressure of the clay. These observations indicate that the response of the clay to thermal loading is not fully reversible, resulting in a permanent increase in the elastic domain. However, such observations appear to directly contradict findings from laboratory shear testing of post-test samples from ATLAS (De Bruyn and Labat, 2002), though this may be explained in part by the volume of clay and the timescales involved.

More recently the PRACLAY (Preliminary demonstration test for clay disposal of highly radioactive waste) test was initiated at HADES in 2014, with the intention of running for a significantly longer timescale of the order of 10 years. As such, the test programme is

currently in its early stages, but information relating to the aims and design of the experiments is detailed by Li et al. (2010).

5.7. Thermal summary with reference to the Dutch concept

Potential differences in the mechanical and hydraulic behaviour of the Boom Clay at suggested depths for a Dutch disposal facility have been discussed in previous Chapters. Of primary importance will be the impacts of higher effective and differential stresses, including physical changes to the initial conditions of the clay (e.g., higher OCR, lower void ratio and lower permeability). Many aspects of the clay's response to thermal loading under these conditions will not vary from those expected at shallower depths. For example, there are currently no observations to suggest that the hydraulic permeability of the clay is likely to be significantly affected by elevated temperature conditions, irrespective of consolidation state, though additional experimental evidence would be beneficial. The development of excess pore pressures on heating can be expected in both cases, followed by their rapid decline and eventual equilibration on cooling. However, at greater depths any slight reduction in permeability of the clay will limit drainage rates further and is expected to therefore exacerbate pore pressure build-up (Horseman et al., 1993). The shortage of thermal loading tests conducted at appropriate effective stress conditions, however, makes it non-trivial to assess the degree to which this effect is likely to impact pore pressure evolution.

A greater uncertainty relates to the volumetric response of the clay on thermal loading, because of the poorly constrained preconsolidation pressure for the Boom Clay in the Netherlands and a lack of certainty about the transition point between expansive and contractive behaviour. Laboratory and *in situ* test data generally indicate a contractive response for the clay on heating under the effective stresses at HADES, which is consistent with an estimated OCR of greater than 2 (Baldi et al., 1991). However, assuming a preconsolidation stress of ~ 7.45 MPa (Wildenborg et al., 2003) for a Dutch repository, the resulting OCR of 1.7 MPa leads to a high degree of uncertainty in relation to the behaviour of the clay, which may potentially involve an expansive component to its volumetric response. Some experimental findings do, however, suggest that thermally generated strains are not likely to be of a significantly larger magnitude than those observed for clay subjected to *in situ* conditions at HADES (Cui et al., 2009). Nevertheless, further constraint of the expected preconsolidation stress for the Boom Clay in the Netherlands is required and this must be coupled with additional testing to better elucidate the nature and recoverability of volumetric strains induced by thermal loading under higher effective stresses.

Significant efforts have also been made to incorporate the influence of thermal loading into standard failure models for clays. Efforts have been to some extent hampered in the past by somewhat contradictory evidence within the literature. As noted in Sections 5.3 and 5.6, there is some debate as to the effect of temperature on shear strength and the critical state parameter M (Hueckel and Pellegrini, 1989; Horseman et al., 1993; De Bruyn and Thimus, 1996). Hueckel et al. (2009) attribute conflicting experimental observations, in part, to material-specific response and a lack of emphasis on thermal and mechanical history before failure. They provide a detailed account of the mechanisms for, and conditions leading to, thermal failure in saturated clays. The influence of heating/cooling conditions on critical state parameters is discussed and specific examples given, examining the importance of stress and thermal history on clay response and providing a framework for assessment of the potential for failure. Previous work for the Boom Clay in Belgium will need to be adapted in order to allow for the differing initial conditions of the clay in the Dutch concept. It should be noted that additional experimental data providing an improved

understanding of the THM response of the clay at higher OCRs will likely be required in order to do so.

Recommendations

- Additional experimental testing of the Boom Clay from HADES (at higher effective stresses) providing an improved understanding of:
 - The influence of OCR, dry density and availability of free water on the volumetric response to thermal loading. In particular, evidence indicating the point of transition between expansive and contractive regimes is unclear;
 - The influence of compaction state on pore pressure build-up and decline;
 - The impact of thermal loading on the mechanical strength of the Boom Clay; The thermal dependency of critical state parameters in the Boom Clay;
 - The influence of thermal loading on gas migration behaviour and influence of depth on these processes.
- Recovery of well-preserved core from appropriate locations and depths would provide valuable additional information (e.g., preconsolidation stress and current void ratio) to inform targeted experimental investigations of the THM behaviour of the Boom Clay at relevant stress conditions.

6. Microbiology

6.1. Evidence for the occurrence of micro-organisms

There is an increasing awareness that microbes are present and active in most subsurface environments. This is a concern for the implementation of radioactive waste disposal because microbial activity could influence degradation and corrosion of materials used in engineered barriers, alter fluid flow and transport of radionuclides and affect the generation and consumption of gases in a repository environment (Humpreys et al., 2010). Specifically, it has been established that they will be present in the Boom Clay with similar history and mineralogy to that examined at the HADES underground research facility at Mol (e.g. Boivin-Jahns and Ruimy, 1996; Deniau et al., 2001; De Craen et al., 1999; Zhang et al., 2008), as well as in other clay materials (e.g. Pedersen et al., 2000; Fukunaga et al., 2005; Mauclaire et al., 2007; Stroes-Gascoyne et al., 2007, 2010; Urios et al., 2012).

Multiple techniques have been applied to demonstrate microbial presence or activity within clays. At HADES, these include, evidence of sulphate reducing and other bacteria using SEM (De Craen, 1999; Deniau et al., 2001; Wouters et al., 2013), cultivation of bacteria from samples collected using a sterile technique (Boivin-Jahns and Ruimy, 1996; Wouters et al., 2013), detection of bacterial DNA by polymerase chain reaction (PCR) (Boivin-Jahns and Ruimy, 1996; Wouters et al., 2013) and modelling (Zhang et al., 2008).

6.2. The diversity of microorganisms likely to be present

In addition to the data on the microbiology of the Boom Clay, evidence from other clay types provides a useful indication of the conditions required for microbial survival and the kinds of microbial communities and behaviour that might be expected in the Boom Clay. Two studies have investigated the bacterial diversity in the Boom Clay at HADES. The earliest study acknowledged issues surrounding the recovery of DNA from indigenous microorganisms, but nonetheless identified the presence of an active bacterial community within the clay (Boivin-Jahns and Ruimy, 1996). A more recent investigation into the bacterial community present in borehole water identified a diverse bacterial community dominated by Proteobacteria, which also contained significant proportions of Actinobacteria, Bacteroidetes and Firmicutes (Wouters et al., 2013). A range of aerobic and anaerobic bacteria with metabolic activity including nitrate- and sulphate- reduction were identified. Evidence from groundwater microbiology indicates that typically the planktonic community in borehole water is likely to have a different composition to the community attached to surfaces (e.g. Holm et al., 1992; Lehman, 2007; Flynn et al., 2008). It is therefore important to recognise the context from which communities are extracted. A more focussed approach to identify the sulphate reducing bacteria (SRB) present at this site detected *Acidithiobacillus*, *Desulfovibrio* and *Desulfomaculum* species in the clay or clay water in samples with elevated sulphate close to the gallery wall (Aerts et al., 2009). In Opalinus Clay, biochemical methods were employed to investigate the microbial diversity. Analysis of recoverable cell membrane compounds revealed a community dominated by Gram negative bacteria (including SRB, which culture methods showed to be viable) (Mauclaire et al., 2007). This study also showed that a small proportion of fungi was present. A multi-laboratory investigation into the viable populations within Opalinus Clay produced mixed results for microbial detection with some laboratories unable to detect microbes (Stroes-Gascoyne et al., 2007). This indicates that any microbial community present in this environment is near or below the detection limit for some techniques. Archaea may make up a significant proportion of microbial communities in clay environments (Wouters et al., 2013) but so far have not been the target of investigation. Given their potential role in methanogenesis (amongst other things), they are important in understanding the influence of biological processes on biogeochemical gas production.

6.3. Conditions necessary for the presence and survival of microorganisms

To some extent it is surprising that microbes exist at all within the clays because the typical pore sizes are considerably smaller than typical bacterial sizes. Although viable microbes will almost certainly be found within clay host rock, generally their numbers will be low; typically in the order of 10^1 - 10^3 cells per ml clay (Boivin-Jahns and Ruimy, 1996; Stroes-Gascoyne et al., 2007). The small pore size is probably an important factor that determines these low population densities. It has been speculated that organisms found in clays represent those that became trapped during deposition and were able to survive within the clay (Boivin-Jahns and Ruimy, 1996). In these hostile conditions, it is thought that the ability to enter a dormant state through the production of spores (a characteristic of sulphate reducing bacteria as well as many other types bacteria) is important for survival (Pedersen, 2000; Stroes-Gascoyne et al., 2010). Spores have elevated resistance to radiation, desiccation and elevated temperatures and *in situ* experiments found that only spore forming organisms were able to survive 15 month clay incubation experiments (Pedersen et al., 2000). When the temperature was increased (to 50-70°C) only one of the three SRB species used survived. Despite the increased survival rates, there is a slow but significant death rate of spores and reintroduction from survivors is unlikely because of the small pore spaces in the clay (Pedersen, 2000).

What is clear from the work so far carried out is that disturbance caused by excavation increases microbial activity near the excavation zone, as it provides the necessary conditions for aerobic growth. At HADES, bacterial numbers were observed to decrease with increasing sampling distance from the gallery and, beyond 80 cm into the clay, numbers dropped from 105 colony forming units (CFU) at the gallery surface to just a few CFU per ml clay and the microbial respiration rate measured by carbon dioxide production decreased dramatically from 92 nmol CO₂ l⁻¹ h⁻¹ to 0.2 nmol CO₂ l⁻¹ h⁻¹ (Boivin-Jahns and Ruimy, 1996). However, low numbers of viable cells were still detected at the maximum sampling depth of 7 m. A similar observation has been made in bentonite clay; the amount of biomass dropped from 107g DW⁻¹ (dry weight) for aerobes and 103 - 106 DW⁻¹ for anaerobes on the tunnel wall to less than 102g DW⁻¹ for both at 1 m depth (Fukunaga et al., 2005). Swelling of (bentonite) clays reduces viable numbers and almost inactivates SRB activity upon full compaction. The maximum density in which SRB survive appears to be around 1800-2000 kg/m² (Pedersen, 2000; Stroes-Gascoyne et al., 1997). Microbial viability in clay is also dependent upon sufficient water content, with the equivalent of around 30% water in bentonite clay being the minimum requirement (Motamedi et al., 1996; Stroes-Gascoyne et al., 1997).

If the disturbance caused by excavation and operation of the repository allows the development of an active community to develop and persist in the near field following closure, it is possible that hydrogenotrophic growth could relieve the elevated pressures caused by hydrogen generation from canister corrosion and reduce the risk of gas or water flow through preferential pathways created by elevated pressure conditions (Ortiz et al., 2002b). Thermal, hydrological, biological and chemical (THBC) modelling of heating and radiation effects carried out at HADES suggested that microbial activity will occur during the gas generation period. The model could only be made to fit the experimental data if the activity of thermophilic iron- and sulphate- reducing bacteria was postulated. The activity of these organisms in the presence of organic matter counteracted oxidizing conditions caused by heat and radiation and prevented the oxidation of pyrite and resulted in the production of sulphide (Zhang et al., 2008). Microbial growth and activity in the clay surrounding waste could have implications for microbially-influenced corrosion of canisters, adsorption of radionuclides, biomineralisation and smectite-illite conversion. Microbially induced alteration of clays has been demonstrated and is important as it can lead to

dissolution of minerals and silicates (Esnault et al., 2013; Kostka et al., 1999; Stroes-Gascoyne et al., 2007). This process could have implications for the physical properties of the clay and consequences for repository performance.

6.4. Microbiology summary

When considered together, this data points to a small viable indigenous population within clays, which is likely to mainly comprise dormant cells and spores from SRB and Gram-positive organisms. Disturbances that increase water content, nutrients and space (e.g. repository excavation) could revive these dormant populations and lead to sulphate reduction and accompanying changes in pCO₂, alkalinity, pH and Eh (Stroes-Gascoyne et al., 2010; Stroes-Gascoyne et al., 2007; Wersin et al., 2011). The limitations of pore size and water content are likely to minimise the metabolic activity of this community, but experimental and model data suggests that there could be significant impact of microbial activity on repository performance.

It might be expected that microbial activity would be reduced in a repository at greater depths than HADES. The increased compaction and lower water availability within the clay that would likely be encountered with increasing depth may mean that lower survival rates and activity of microorganisms could be encountered at the Netherlands site. However it would be premature to assume that microbial survival is not possible, or that microorganisms will not have an influence on repository performance. The extent of this influence will need to be investigated through field sampling and laboratory experimentation. Another factor to consider when thinking about differences to the microbiology encountered at HADES is the influence in pore water composition and salinity. It is widely acknowledged that both influence microbial community composition and activity, however without detailed characterisation of the pore water the effect of this on microbial processes cannot be predicted.

Recommendations

- **Assess the abundance, diversity and activity of microorganisms present in clay deposits at appropriate depths and locations within the formation and in the open repository environment:**
 - **A range of DNA/RNA based techniques (e.g. DNA pyrosequencing, metagenomics, quantitative PCR) should be carried out to understand the composition and activity of bacterial, archaeal and fungal communities present in the clay. This information will provide a baseline for understanding range of microbial metabolisms present in the repository and the potential for different microbial groups to affect radionuclide migration and fluid flow around the repository. Potential contribution to corrosion or degradation of the engineered components of the repository could also be established.**
- **Thermodynamic modelling (combined with the microbial diversity analysis) would allow the likely biogeochemical processes under anticipated scenarios to be predicted. This would be particularly useful for identifying the circumstances under which microbial gases such as hydrogen, methane and hydrogen sulphide will be produced or consumed;**
- **An experimental programme will be required to understand microbial survival post-closure (e.g. clay squeezing experiments to understand the ability of microbes to survive under predicted pressures and hydration states). This data will complement the modelling work and will establish the physical limits to survival and activity key microbial groups in this environment.**

7. Conclusions

The Boom Clay Formation has many features that lend itself to being considered as a candidate host formation for the geological disposal of radioactive waste in the Netherlands. In particular, its low permeability, radionuclide retardation capacity, low hydraulic gradients and propensity for rapid self-sealing are all beneficial characteristics. In addition the formation has been extensively characterised, given its role as the reference formation for the Belgium national programme for radioactive waste disposal. As such, much understanding in relation to the thermo-hydro-mechanical behaviour of the clay can be directly transferred to the Dutch national programme. In particular, it is possible to tentatively estimate a likely range of transport and mechanical properties for the clay at a proposed depth of 500 m. Many statements can also be made about the expected mechanical and transport behaviour of the clay under such conditions, though less so in the case of thermal response. Much uncertainty can be reduced and predictions validated by further experimental work conducted with clay derived from the Belgian test facility HADES. In many cases, however, the recovery of core from appropriate depths and locations will be required in order to reduce uncertainty, validate predictions and account for the influence of regional differences in lithology and burial history.

8. References

- Aertsens, M, Wemaere, I, Wouters, L, *Spatial variability of transport parameters in the Boom Clay*. Applied Clay Science, 26 (2004) 37-45.
- Al-Mukhtar, M, Belanteur, N, Tessier, D, Vanapalli, S, *The fabric of a clay soil under controlled mechanical and hydraulic stress states*, Applied Clay Science 11 (1996) 99-115.
- Angeli, M, Soldal, M, Skurtveit, E, Aker, E, *Experimental percolation of supercritical CO₂ through a caprock*, Energy Procedia, 1 (2009) 3351-3358.
- Athy, LF, *Density, porosity and compaction of sedimentary rocks*, AAPG bulletin (1930) 1-24.
- Aziz, K, Settari, A, *Petroleum reservoir simulation*, Applied Science Publishers London (1979) 476.
- Bader, S, Kooi, H, *Modelling of solute and water transport in semi-permeable clay membranes: Comparison with experiments*, Advances in Water Resources 28 (2005) 203-214.
- Baldi, G, Hueckel, T, Pellegrini, R, *Thermal volume changes of the mineral-water system in low-porosity clay soils*, Canadian Geotechnical Journal 25 4 (1988) 807-825.
- Baldi, G, Hueckel, T, Peano, A, Pellegrini, R, *Developments in modelling of thermo-hydro-geomechanical behaviour of Boom clay and clay-based buffer materials* (Volume 1), Commission of the European Communities, Luxembourg, (1991a).
- Baldi, G, Hueckel, T, Peano, A, Pellegrini, R, *Developments in modelling of thermo-hydro-geomechanical behaviour of Boom clay and clay-based materials* (Volume 2), Commission of the European Communities, Luxembourg, (1991b).
- Barnichon, J, Volckaert, G, *Observations and predictions of hydromechanical coupling effects in the Boom Clay*, Mol Underground Research Laboratory, Belgium, Hydrogeology Journal 11 (2003) 193-202.
- Barrande, M, Bouchet, R, Denoyel, R, *Tortuosity of Porous Particles*, Analytical Chemistry 79 (2007) 9115-9121.
- Bastiaens, W, Demarche, M, *The extension of the URF HADES: realization and observation*. Proceedings of the WN'03 Conference, Tuscon, USA (2003).
- Bastiaens, W, Bernier, F, Li, X, (2006) *An overview of long-terms HM measurements around HADES URF*. Proceedings of International Symposium on mutliphysics coupling and long-term behaviour in rock mechanics, Lieege (2006).
- Bastiaens, W, Bernier, F, and Li, X, (2007) *SELFRAC: experiments and conclusions on fracturing, self-healing and self-sealing processes in clays*, Physics and Chemistry of the Earth, Parts A/B/C 32 (2007) 600-615.
- Bear, J, *Dynamics of fluids in porous media*, Elsevier New York (1972) 764p.

- Been, K, Sills, G C, *Self-weight consolidation of soft soils: an experimental and theoretical study*, Geotechnique 31 (1981) 519-535.
- Beerten, K, Leterme, B, *Physical geography of north-eastern Belgium - the Boom Clay outcrop and sub-crop zone SCK-CEN report ER-2012/Kbe/P-2* 60p.
- Beerten, K, De Craen, M, wouters, L, *Patterns and estimates of post Rupelian burial and erosion in the Campine area, north-eastern Belgium*. Physics and Chemistry of the Earth, 64 (2013)12-20.
- Belanteur, N, Tacherifet, S, Pakzad, M, *Study of mechanical, thermos-mechanical and hydro-mechanical behaviour of swelling and unswelling highly compacted clay*, Geotechnique 78 (1997) 31-50.
- Benazzouz, BK, Zaoui, A, *Thermal behaviour and superheating temperature of Kaolinite from molecular dynamics*, Applied Clay Science 58(0) (2012) 44-51.
- Bernier, F, Neerdel, B, *Overview of in-situ thermomechanical experiments in clay: Concepts, results and interpretation*, Engineering Geology 41 (1996) 51-64.
- Bernier, F, Li, XL, Bastiaens, W, *Twenty-five years' geotechnical observation and testing in the Tertiary Boom Clay formation*, Géotechnique 57(2) (2007) 229-237.
- Bertrand, B, Laloui, L, Laurent, C, *Thermo-hydro-mechanical simulation of ATLAS in situ large scale test in Boom Clay*, Computers and Geotechnics 36 (2009) 626-640.
- Besuelle, P, Viggiani, G, Desrues, J, Coll, C, Charrier, P, *A Laboratory Experimental Study of the Hydromechanical Behaviour of Boom Clay*, Rock Mechanics and Rock Engineering 47 (2013)143-155.
- Biot, M, *General theory of three-dimensional consolidation*, Journal of Applied Physics 2 (1941) 155-164.
- Bishop, A, Webb, D, Skinner, A, *Triaxial tests on soil at elevated cell pressures*, Proceedings of the 6th International Conference on Soil Mechanics and Foundation Engineering (1965).
- Bjerrum, L, *Progressive failure in slopes of overconsolidated plastic clay and clay shales*, Journal of Soil Mechanics and Foundation Divisions 93 (1967).
- Blanchart, P, Faure, P, De Craen, M, Bruggeman, C, Michels, R, *Experimental investigation on the role of kerogen and clay minerals in the formation of bitumen during the oxidation of Boom Clay*, Fuel 97 (2012) 344-351.
- Blümling, P, Bernier, F, *The excavation damaged zone in clay formations time-dependent behaviour and influence on performance assessment*, Physics and Chemistry of the Earth, Parts A/B/C (2007) 1-31.
- Bock, H, Dehandschutter, B, Derek Martin, C, Mazurek, M, de Haller, A, Skoczylas, F, Davy, C, *Self-sealing of Fractures in Argillaceous Formations in the Context of Geological Disposal of Radioactive Waste*, Review and Synthesis, NEA report 8184, (2010).
- Boivin-Jahns, V, Ruimy, R, *Bacterial diversity in a deep-subsurface clay environment*, Appl. Environ. Microbiol. 62 (1996) 3405-3412.

- Bouazza, A, Impe, W, Haegeman, W, *Some mechanical properties of reconstituted Boom clay*, Geotechnical and Geological Engineering 14 (1996) 341-352.
- Britto, AM, Savvidou, C, Maddocks, DV, Gunn, MJ, Booker, JR, *Numerical and centrifuge modelling of coupled heat flow and consolidation around hot cylinders buried in clay*, Géotechnique (1989) 13-25.
- Brown, ET, Bray, JW, Ladanyi, B, Hoek, E, *Ground response curves for rock tunnels*, Journal of Geotechnical Engineering 109 (1983) 15-39.
- Brunauer, S, Emmett, PH, Teller, E, *Adsorption of gases in multimolecular layers*, Journal of the American chemical society 60 (1938) 309-319.
- Burland, JB, *On the compressibility and shear strength of natural clays*, Geotechnique 40 (1990) 329-378.
- Byerlee, JD, *The fracture strength and frictional strength of Weber sandstone*, In International Journal of Rock Mechanics and Mining Sciences and Geomechanics Abstracts 12 (1975) 1-4.
- Casagrande, A, *The determination of the pre-consolidation load and its practical significance*, Proceedings of the international conference on soil mechanics and foundation engineering 33 (1936) 60-64.
- Castellanos, E, Villar, MV, Romero, E, Lloret, A, Gens, A, *Chemical impact on the hydro-mechanical behaviour of high-density FEBEX bentonite*, Physics and Chemistry of the Earth, Parts A/B/C 33 (2008) S516-S526.
- Chan, HR Kenney, TC, *Laboratory investigation of permeability ratio of New Liskeard varved soil*, Canadian Geotechnical Journal 10 (1973) 453-472.
- Chen, GJ, Sillen, X, Verstricht, J, Li, XL, *ATLAS III in situ heating test in boom clay: Field data, observation and interpretation*, Computers and Geotechnics, 38(5) (2011) 683-696.
- Chen, L, Liu, YM, Wang, J, Cao, S F, Xie, J L, Ma, L K Liu, J, *Investigation of the thermal-hydro-mechanical (THM) behaviour of GMZ bentonite in the China-Mock-up test*, Engineering Geology 172 (2014) 57-68.
- Clarke, BG, Smith, A, *Self-boring pressuremeter tests in weak rocks*, Construction and Building Materials 6 (1992) 91-96.
- Clayton, C, Hay, S, *Gas migration mechanisms from accumulation to surface*, Bulletin of the Geological Society of Denmark, 41(1) (1994) 12-23.
- Coll, C, *Endommagement des Roches Argileuses et Perméabilité Induite au Voisinage d'Ouvrages Souterrains*, PhD Thesis, Université Joseph Fourier, Grenoble (2005).
- Cui, Y, Tang, AM, *On the chemo-thermo-hydro-mechanical behaviour of geological and engineered barriers*, Journal of Rock Mechanics and Geotechnical Engineering 5(3) (2013) 169-178.
- Cui, YJ, Delage, P, *Yielding and plastic behaviour of an unsaturated compacted silt*, Geotechnique 46 (1996) 291-311.

Cui, YJ, Delage, P, Le, TT, Li, XL, Tang, AM, *Investigating the time-dependent behaviour of Boom clay under thermomechanical loading*, *Géotechnique*, 59(4) (2009) 319-329.

Cui, YJ, Tang, AM, *On the chemo-thermo-hydro-mechanical behaviour of geological and engineered barriers*, *Journal of Rock Mechanics and Geotechnical Engineering* 5(3) (2013) 169-178.

Cuss, R, *An experimental investigation of the mechanical behaviour of sandstones with reference to borehole stability*, Ph.D. Thesis, The University of Manchester (1999).

Cuss, R, Horseman, S, *The use of Critical State Mechanics to predict the Deformation within the Reservoir Setting*, *Faults and Top Seals: What do we know and where do we go?* (2003).

Cuss R, Rutter, E, Holloway, R, *The application of critical state soil mechanics to the mechanical behaviour of porous sandstones*. *International Journal of Rock Mechanics and Mining Sciences* 40(6) (2003) 847-862.

Cuss, R, Harrington, J, *Update on Dilatancy Associated with Onset of Gas Flow in Callovo-Oxfordian Claystone*, Progress report on test SPP_COx-2. British Geological Survey Commissioned Report CR/11/110 (2011).

Cuss, R, Harrington, J, Noy, D, *Large-scale gas injection test (Lasgit) performed at the Äspö Hard Rock Laboratory*, Summary report 2008, Swedish Nuclear Fuel and Waste Management Co., Stockholm (Sweden) (2010).

Cuss, R, Harrington, J, Noy, D, Wikman, A, Sellin, P, *Large-scale gas injection test (Lasgit): Results from two gas injection tests*, *Physics and Chemistry of the Earth, Parts A/B/C*, 36(17-18) (2011) 1729-1742.

Cuss, R, Harrington, J, Giot, R, Auvray, C, *Experimental observations of mechanical dilation at the onset of gas flow in Callovo-Oxfordian claystone*, *Geological Society of London Special Publications* 400 (2014).

Davies, P, *Evaluation of the role of threshold pressure in controlling flow of waste-generated gas into bedded salt at the Waste Isolation Pilot Plant*, Sandia National Laboratory Report (1991).

De Beer, E, *Shear strength characteristics of the Boom clay*, Proceedings of the Geotechnical Conference, Oslo, (1967).

De Beer, E, *Some considerations concerning the geological, physical and mechanical properties of Boom clay*, Technical Report (1977).

De Bruyn, D, Thimus, JF, *The influence of temperature on mechanical characteristics of Boom Clay: The results of an initial laboratory programme*, *Engineering Geology*, 41 (1996) 117-126.

De Bruyn, D, Labat, S, *The second phase of ATLAS: the continuation of a running THM test in the HADES underground research facility at Mol*, *Engineering Geology* 64 (2002) 309-316.

- De Craen, M, Beerten, K, Honty, M, Gedeon, M, *Geo-scientific evidence to support the 12 isolation function (geology and long-term evolution) as part of the Safety and Feasibility Case 1 (SFC1) SCK-CEN report ER-184 12/MDC/P-11 March 2012 (2012).*
- De Craen, M, Swennen, R, Keppens, EM, Macaulay, CI, Kiriakoulakis, K, *Bacterially mediated formation of carbonate concretions in the Oligocene Boom Clay of northern Belgium*, Journal of Sedimentary Research 69 (1999) 1098-1106.
- De Craen, M, Wang, L, Van Geet, M, Moors, H, *Geochemistry of Boom Clay pore water at the Mol site*, SCK-CEN scientific report BLG-990. Waste and Disposal Department SCK-CEN (Mol, Belgium) (2004).
- De Craen, M, Wang, L, Van Geet, M, Moors, H, *Geochemistry of Boom Clay pore water at the Mol site*, SCK-CEN-BL-990 04/MDC/P-48, SCK-CEN (2004b).
- De Craen, M, Van Geet, M, Honty, M, Weetjens, E, Sillen, X, *Extent of oxidation in Boom Clay as a result of excavation and ventilation of the HADES URF: Experimental and modelling assessments*, Physics and Chemistry of the Earth, Parts A/B/C 33 (2008) 350-362.
- De Marsily, G, *Quantitative Hydrogeology*, Groundwater Hydrology for Engineers. Academic Press, New York, (1986).
- Decler, J, Viaene, W, Vandenberghe, N, *Relationship between chemical, physical and mineralogical characteristics of the rupelian Boom clay*, Clay minerals 26 (1983) 389-401.
- Dehandschutter, B, Vandycke, S, Sintubin, M, Vandenberghe, N, Gaviglio, P, Sizun, JP, Wouters, L, *Microfabric of fractured Boom Clay at depth: a case study of brittle-ductile transitional clay behaviour*, Applied Clay Science, 26(1-4) (2004) 389-401.
- Dehandschutter, B, Vandycke, S, Sintubin, M, Vandenberghe, N, Wouters, L, *Brittle fractures and ductile shear bands in argillaceous sediments: inferences from Oligocene Boom Clay (Belgium)*, Journal of Structural Geology 27(6) (2005a) 1095-1112.
- Dehandschutter, B, Gaviglio, P, Sizun, JP, Sintubin, M, Vandycke, S, Vandenberghe, N, Wouters, L, *Volumetric matrix strain related to intraformational faulting in argillaceous sediments*, Journal of the Geological Society 162 (2005b) 801-913.
- Delage, P, Cui, YJ, *Comportement élasto-plastique d'un limon compacté, érie II*, Mécanique physique, chimie, astronomie 320 (1995) 317-324.
- Delage, P, Sultan, N, Cui, YJ, *On the thermal consolidation of Boom clay*, Canadian Geotechnical Journal 37 (2000) 343-354.
- Delage, P, Cui, YJ, Sultan, N, *On the thermal behaviour of Boom clay*. EUROSAFE Forum, Berlin (2004).
- Delage, P., Le, T. T., Cui, Y.-J., Li, X. L., and Tang, A. M., 2009. Investigating the time-dependent behaviour of Boom clay under thermomechanical loading. Géotechnique, 59(4), 319-329.
- Deng, YF, Cui, YJ, Tang, AM, Nguyen, XP, Li, XL, Van Geet, M, *Investigating the pore water chemistry effects on the volume change behaviour of Boom clay*, Physics and Chemistry of the Earth, Parts A/B/C, 36(17-18) (2011) 1905-1912.

Deng, YF, Cui, YJ, Tang, AM, Li, XL, Sillen, X, *An experimental study on the secondary deformation of Boom clay*, Applied Clay Science 59-60 (2012) 19-25.

Deniau, I, Derenne, S, Beucaire, C, Pitsch, H, Largeau, C, *Morphological and chemical features of a kerogen from the underground Mol laboratory (Boom Clay Formation, Oligocene, Belgium): structure, source organisms and formation pathways*, Organic geochemistry 32 (2001) 1343-1356.

Derjaguin, BV, Churaev, NV, Muller, VM, *Wetting films. Surface Forces*, Springer U.S. (1987) 327-362.

Desbois, G, Urai, JL, De Craen, M, *In-situ and direct characterization of porosity in Boom Clay (Mol site, Belgium) by using novel combination of ion beam cross-sectioning, SEM and cryogenic methods*, SCK CEN External Report (2010).

Desbois, G, Urai, JL, Hermes, S, Brassinnes, S, De Craen, M, Sillen, X, *Nanometer-scale pore fluid distribution and drying damage in preserved clay cores from Belgian clay formations inferred by BIB-cryo-SEM*, Engineering Geology 179 (2014) 117-131.

Di Maio, C, Santoli, L, Schiavone, P, *Volume change behaviour of clays: the influence of mineral composition, pore fluid composition and stress state*, Mechanics of Materials 36(5-6) (2004) 435-451.

Dias Junior, MS, Pierce, JF, *A simple procedure for estimating preconsolidation pressure from soil compression curves*, Soil Technology 8 (1995) 139-151.

Donohew, AT, Horseman, S, Harrington, JF, *Chapter 18: Gas entry into unconfined clay pastes between the liquid and plastic limits*, Environmental Mineralogy, Mineralogical Society Series No. 9, London (2000) 369-394.

Drucker DC, Prager W, *Soil mechanics and plastic analysis or limit design*, Quarterly Applied Math, 10 (1952) 157-165.

Dullien, FAL, *Prediction of "tortuosity factors" from pore structure data*, AIChE Journal 21(4) (1975) 820-822.

Dzenvashir, RD, Buryakovskiy, LA, Chilingarian, GV, *Simple quantitative evaluation of porosity of argillaceous sediments at various depths of burial*, Sedimentary Geology 46 (1986)169-175.

Ehlers, J, *Reconstructing the dynamics of the north-west European Pleistocene ice sheets*, Quaternary Science Reviews 9 (1990) 71-83.

Elkhoury, JE, Niemeijer, A, Brodsky, EE, Marone, C, *Laboratory observations of permeability enhancement by fluid pressure oscillation of in situ fractured rock*, Journal of Geophysical Research: Solid Earth 116(B2) (2011) B02311.

Ewy, RT, *Wellbore-stability predictions by use of a modified Lade criterion*, SPE Drill and Completion, 14 (1999) 85-91.

Fallico, C, De Bartolo, S, Troisi, S, Veltri, M, *Scaling analysis of hydraulic conductivity and porosity on a sandy medium of an unconfined aquifer reproduced in the laboratory*, Geoderma, 160(1) (2010) 3-12.

- Flynn, TM, Sanford, RA, Bethke, CM, *Attached and suspended microbial communities in a pristine confined aquifer*, Water Resources Research 44 (2008).
- François, B, Laloui, L, Laurent, C, *Thermo-hydro-mechanical simulation of ATLAS in situ large-scale test in Boom Clay*, Computers and Geotechnics 36(4) (2009) 626-640.
- Fritz, JJ, *Ideality of clay membranes in osmotic processes: A review*, Clays and Clay Minerals 34 (1986) 214-223.
- Fritz, SJ, Marine, IW, *Experimental support for predictive osmotic model of clay membranes*, Geochemica et Cosmochimica Acta 47 (1983) 1515-1522.
- Fukunaga, S, Jintoku, T, Iwata, Y, Nakayama, M, Tsuji, T, Sakaya, N, Mogi, KL, Ito, M, *Investigation of microorganisms in bentonite deposits*, Geomicrobiology Journal 22 (2005) 361-370.
- Garavito, AM, De Cannière, P, Kooi, H, *In situ chemical osmosis experiment in the Boom Clay at the Mol underground research laboratory*, Physics and Chemistry of the Earth, Parts A/B/C 32(1-7) (2007) 421-433.
- Gedeon, M, Wemaere, I, Labat, S, *Characterization of groundwater flow in the environment of the Boom Clay formation*, Physics and Chemistry of the Earth, Parts A/B/C 36(17-18) (2012) 1486-1495.
- Gens, A, Alonso, E, *A framework for the behaviour of unsaturated expansive clays*, Canadian Geotechnical Journal. Retrieved from <http://www.nrcresearchpress.com/doi/abs/10.1139/t92-120> (1992)
- Gerard, P, Harrington, J, Charlier, R, Collin, F, *Modelling of localised gas preferential pathways in claystone*, International Journal of Rock Mechanics and Mining Sciences 67 (2014) 104-114.
- Gerogiannopoulos, GN, Brown, ET, *The Critical State Concept Applied to Rock*, International Journal of Rock Mechanics and Mining Science and Geomechanics 15 (1978) 1-10.
- Gibson, RE, *The progress of consolidation in a clay layer increasing in thickness with time*, Geotechnique 8 (1958) 171-182.
- Gibson, RE, Henkel, D, *Influence of duration of tests at constant rate of strain on measured 'drained' strength*, Geotechnique 4 (1954) 6-15.
- Gonçalvès, J, Trémosa, J, *Estimating thermo-osmotic coefficients in clay-rocks: I. Theoretical insights*, Journal of colloid and interface science 342(1) (2010) 166-174.
- Gonçalvès, J, de Marsily, G, Tremosa, J, *Importance of thermo-osmosis for fluid flow and transport in clay formations hosting a nuclear waste repository*, Earth and Planetary Science Letters 339 (2012) 1-10.
- Graham, CC, Harrington, JF, Cuss, RJ, Sellin, P, *Gas migration experiments in bentonite: Implications for numerical modelling*, Mineralogical Magazine 76(8) (2012) 3279-3292.
- Graham, CC, Harrington, JF, *Final Report of FORGE 3.2.1: Key gas migration process in Compact Bentonite*, BGS Commissioned Report FORGE FP7 D3.33, CR/14/064 (2014) 60pp.

Graham, CC, Harrington, JF, Cuss RJ, Sellin, P, *Pore-pressure cycling experiments on Mx80 bentonite*, In: *Clays in Natural and Engineered Barriers for Radioactive Waste Confinement*, Geological Society, London, Special Publications, 400 (2015).

Gray, DH, Mitchell, JK, *Fundamental aspects of electro-osmosis in soils*, *Journal of Soil Mechanics and Foundations Div* 93(SM6) (1967) 209-236.

Haberfield, C, *Towards a universal approach to soil and rock engineering: Fact or fallacy*, *The Geotechnics of Hard Soils-Soft Rocks*. Proceedings of the 2nd International Symposium of Hard Soils-Soft Rocks (1998).

Haijntink, B, Rodwell, W, *Project on the effects of gas in underground storage facilities for radioactive waste (Pegasus project)*, Proceedings of a progress meeting held in Mol, Belgium, 28th and 29th May 1997 (1998).

Hanor, JS, *On the non-importance of membrane filtration as a mechanism for producing subsurface brines in the Louisiana Gulf Coast*, In: Proceedings 21st Clay Min. Soc. Annual Meeting, Baton Rouge, USA (1984).

Hansbo, S, *Consolidation of clay, with special reference to influence of vertical sand drains*, Proceedings of Swedish Geotechnical Institute, 18 (1960).

Hansbo, S, *Influence of mobile particles in soft clay on permeability*, Proceedings International Symposium on Soil structure (1973).

Hanshaw, BB, *Membrane properties of compacted clays*, Ph. D Thesis, Harvard University (1962).

Hantush, MS, *Modification of the theory of leaky aquifers*, *Journal of Geophysical Research*, 65(11) (1960) 3713-3725.

Harrington, JF, Horseman, ST, *Gas migration in clay. 153-173 in: Projects on the effects of gas in underground storage facilities for radioactive waste (Pegasus project)*, Proceedings of a progress meeting held in Mol, Belgium, 28 and 29 May 1997 (B. Haijntink and W. Rodwell, editors). European Science and Technology Series (1998) EUR 18167 EN (1997).

Harrington, J, Horseman, S, Noy, D, *Measurements of water and gas flow in Opalinus Clay using a novel guard-ring methodology*, British Geological Survey Technical Report CR/03/32 (2003).

Harrington, JF, Birchall, DJ, Noy, DJ, Cuss, RJ, *Large scale gas injection test (Lasgit) performed at the Aspo Hard Rock Laboratory*, Summary report (2007).

Harrington, JF, de la Vaissière, R, Noy, DJ, Cuss, RJ, Talandier, J, *Gas flow in Callovo-Oxfordian claystone (COx): results from laboratory and field-scale measurements*, *Mineralogical Magazine*, 76(8) (2012) 3303-3318.

Harrington, JF, Horseman, ST, *Gas migration in clay* Pp. 153-173 in: *Projects on the effects of gas in underground storage facilities for radioactive waste (Pegasus project)*. Proceedings of a progress meeting held in Mol, Belgium, 28 and 29 May 1997 (B. Haijntink and W. Rodwell, editors). European Science and Technology Series (1998).

Harrington, JF, Horseman, ST, *Gas transport properties of clays and mudrocks*. In: Aplin, A.C., Fleet, A.J., Macquaker, J.H.S. (Eds.), *Muds and Mudstones: Physical and Fluid Flow Properties*. Geological Society, London, (1999) pp. 107-124.

Harrington, JF, Horseman, ST, *Gas migration in KBS-3 buffer bentonite Sensitivity of test parameters to experimental boundary conditions*, Projects on the effects of gas in underground storage facilities for radioactive waste (Pegasus project): Proceedings of a progress meeting held in Mol, Belgium, 28 and 29 May 1997. European Commission, Brussels, (2003) pp. 153-172.

Harrington, JF, Noy, DJ, Horseman, ST, Birchall, JD Chadwick, RA, *Laboratory study of gas and water flow in the Nordland Shale, Sleipner, North Sea*, In *Carbon Dioxide Sequestration in Geological Media - State of the Science*. (editors M. Grobe, J.C., Pashin and R.L. Dodge). AAPG studies in Geology 59 (2009) 521-543.

Harrington, JF, Milodowski, AE, Graham, CC, Rushton, JC, Cuss, RJ, *Evidence for gas-induced pathways in clay using a nanoparticle injection technique*, *Mineralogical Magazine*, 76(8) (2012b) 3327-3336.

Harrington, JF, Volckaert, G, Noy, DJ, *Long-term impact of temperature on the hydraulic permeability of bentonite*, Geological Society, London, Special Publications (2014).

Hedberg, HD, *Relation of methane generation to undercompacted shales, shale diapirs and mud volcanoes*. AAPG Bulletin (1974).

Heister, K, Kleingeld, PJ, Gustav Loch, JP, *Induced membrane potentials in chemical osmosis across clay membranes*, *Geoderma* 136(1-2) (2006) 1-10.

Hemes, S, Desbois, G, Urai, JL, De Craen, M, Honty, M, *Comparative study on porosity in fine and coarse-grained Boom Clay Samples (Mol-Dessel reference site, Belgium)*, SCK CEN External Report (2011).

Hemes, S, Desbois, G, Urai, JL, De Craen, M, Honty, M, *Variations in the morphology of porosity in the Boom Clay Formation: insights from 2D high resolution BIB-SEM imaging Mercury Injection Porosimetry*, *Netherlands Journal of Geosciences* 92 (2013) 275-300.

Hemes, S, Desbois, G, Urai, JL, Schroppel, B, Schwarz, JO, *Multi-scale characterization of porosity in Boom Clay (HADES-level, Mol, Belgium) using a combination of X-ray μ -CT, 2D BIB-SEM and FIB-SEM tomography*, *Microporous and Mesoporous Materials* 208 (2015) 1-20.

Herbert, HJ, Kasbohm, J, Sprenger, H, Fernández, AM, Reichelt, C, *Swelling pressures of MX-80 bentonite in solutions of different ionic strength*, *Physics and Chemistry of the Earth, Parts A/B/C*, 33, Supplement 1 (2008) 327-342.

Hildenbrand, A, Schlomer, S, Krooss, BM, *Gas breakthrough experiments on fine-grained sedimentary rocks*, *Geofluids* 2 (2002) 3-23.

Hildenbrand, A, Schlomer, S, Krooss, BM, Littke, R, *Gas breakthrough experiments on polycrystalline rocks: comparative study with N_2 , CO_2 and CH_4* , *Geofluids* 4 (2004) 61-80.

Hobbs, PR, Jones, LD, *The shrinkage and swelling behaviour of UK Soils: methods of testing for swelling and shrinkage of soils*. British Geological Survey Technical Report, WN/95/15 (1995).

Hoek, E, Brown, E, *Empirical strength criterion for rock masses*, Journal of Geoenvironmental Engineering 106 (1980) ASCE 15715.

Hoek, E, Wood, D, Shah, S, *A modified Hoek-Brown criterion for jointed rock masses*, Proceedings of Rock Characterisation Symposium of the International Society for Rock Mech: Eurock (1992).

Holland, M, Schultheiss, P, Roberts, J, Druce, M, *Observed gas hydrate morphologies in marine sediments*, 6th International Conference on Gas Hydrates (ICGH 208), Vancouver, Canada (2008).

Holm, PE, Nielsen, PH, Albrechsten, HJ, Christensen, TH, *Importance of unattached bacteria and bacteria attached to sediment in determining potentials for degradation of xenobiotic organic contaminants in an aerobic aquifer*, Applied and Environmental Microbiology 58 (1992) 3020-3026.

Honty, M, De Craen, M, *Boom Clay mineralogy - qualitative and quantitative aspects*, SCK CEN contract: CO-90-08-2214-00 NIRAS/ONDRAF contract: CCHO 2009-0940000, Research Plan Geosynthesis (2011).

Horseman, S, Harrington, J, *Migration of repository gases in an overconsolidated clay*, British Geological Survey, Keyworth (United Kingdom), Fluid Processes Research Group (1994).

Horseman, ST, McEwen, TJ, *Thermal constraints on disposal of heat-emitting waste in argillaceous rocks*, Engineering Geology 41(1-4) (1996) 5-16.

Horseman, S, Harrington, J, *Study of gas migration in Mx80 buffer bentonite*, British Geological Survey, Technical Report WE/97/7 (1997).

Horseman, S, Harrington, J, *Evidence for thresholds, pathways and intermittent flow in argillaceous rocks*, Proceedings of a joint NEA/EC workshop on fluid flow through Faults and Fractures in Argillaceous Formations, Berne, Switzerland. NEA/OECD, Paris, (1998) 85-103.

Horseman, ST, Harrington, JF, *Gas migration under isotropic and K0 stress conditions*, In: Research into Gas Generation and Migration in Radioactive Waste Repository Systems (PROGRESS Project), Editor Rodwell, W.R., European Commission (2000).

Horseman, S, Winter, M, Entwistle, D, *Geotechnical characterisation of Boom Clay in relation to disposal of radioactive waste*, Report EUR 10987, Luxembourg: Commission of the European Communities (1987).

Horseman, ST, Winter, MG, Entwistle, DC, *Triaxial experiments on Boom Clay*. In: Cripps, J.C., Coulthard, J.M., Culshaw, M.G., Forster, A., Hencher, S.R., Moon, C.F. (Eds.), The Engineering Geology of Weak Rock. Balkema, Rotterdam, (1993) 36-43.

Horseman, S, Higgo, JJW, Alexander, J, Harrington, JF, *Water, Gas and Solute Movement through Argillaceous Media*, Nuclear Energy Agency, OECD, Paris (1996).

Horseman, ST, Harrington, JF, Sellin, P, *Gas migration in Mx80 buffer bentonite*. MRS Symposia Proceedings, 465 (1997) 1003-1010.

Horseman, ST, Harrington, JF, Sellin, P, *Gas migration in clay barriers*, Engineering Geology 54 (1999) 139-149.

Horseman, S.T, Cuss, RJ, Reeves, HJ, *Clay Club initiative: Self-healing of fractures in clay-rich host rocks*, Stability and Buffering Capacity of the Geosphere for Long-term Isolation of Radioactive Waste, (2004) 117.

Horseman, ST, Harrington, JF, Noy, DJ, *Swelling and osmotic flow in a potential host rock*, Physics and Chemistry of the Earth, Parts A/B/C 32 (2007) 408-420.

Hovland, M, Svensen, H, Forsberg, CF, Johansen, H, Fichler, C, Fossa, J, Rueslatten, H, *Complex pockmarks with carbonate-ridges off mid-Norway: products of sediment degassing*, Marine Geology 218(1) (2005) 191-206.

Hubbert, MK, Rubey, WW, *Role of fluid pressure in mechanics of overthrust faulting, I. Mechanics of fluid-filled porous solids and its application to overthrust faulting: reply to discussion by Francis Birch*, Geological Society of America Bulletin 72 (1961) 1445-1451.

Hueckel, T, Pellegrini, R, *Modeling of thermal failure of saturated clays*, Proc. 3rd Int. Symp. On Numerical Models in Geomechanics, Niagara falls (1989) 81-90.

Hueckel, T, Pellegrini, R, *Effective stress and water pressure in saturated clays during heating-cooling cycles*, Canadian Geotechnical Journal 29 (1989) 1095-1102.

Hueckel, T, François, B, Laloui, L, *Explaining thermal failure in saturated clays*, Géotechnique 59 (2009) 197-212.

Incropera, FP, Dewitt, DP, Bergman, TL, Lavine, AS, (2007) *Fundamentals of Heat and Mass Transfer*, John Wiley and Sons, Inc, 997 pp. J.H.S. Macquaker, editors). Geological Society of London, Special Publication (2009) 158

Jacops, E, Volckaert G, Maes N, Weetjens E, Govaerts J, *Determination of gas diffusion coefficients in saturated porous media: He and CH₄ diffusion in Boom Clay*, Applied Clay Science 83-84 (2013a) 271-223.

Jacops, E, Maes, N, Maes, T, Volckaert, G, Weetjens, E, *Results and interpretation of gas-driven radionuclide transport in undisturbed and disturbed Boom Clay*, FORGE Report D4.17, SCK•CEN-ER-222, 13/EJa/P-42 (2013b).

Jacops, E, Wouters, K, Volckaert, G, Moors, H, Maes, N, Gruggeman, C, Swennen, R, Littke, R, *Measuring the effective diffusion coefficient of dissolved hydrogen in saturated clay*, Applied Geochemistry 61 (2015) 175-184.

Jaeger, J, Cook, N, Zimmerman, R, *Fundamentals of rock mechanics*, John Wiley & Sons, (2009).

Judd, A, Sim, R, *Shallow gas migration mechanisms in deep water sediments*, Offshore Site Investigation and Foundation Behaviour, New Frontiers: Proceedings of an International Conference, Society of Underwater Technology (1998).

Katchalsky, A, Curran, PF, *Nonequilibrium Thermodynamics in Biophysics*, Harvard University Press, Cambridge, MA (1967).

Kemper, WD, Evans, NA, *Movement of water as effected by free energy and pressure gradients: III. Restriction of solutes by membranes*, Soil Science Society of America Proceedings 27 (1963) 485-490.

Kemper, WD, Rollins, JB, *Osmotic efficiency coefficients across compacted clays*, Soil Science Society of America 30 (1966) 529-534.

Koenen, M, Griffioen, J, *Mineralogical and geochemical characterization of the Boom Clay in the Netherlands*, OPERA-PU-TNO521-1, (2014) 77 p.

Kool, JB, Parker, JC, *Estimating soil hydraulic properties from transient flow experiments: SFIT user's guide*, Electric Power Research Institute, Palo Alto, California, (1987) 60.

Koponen, A, Kataja, M, Timonen, J, *Tortuous flow in porous media*. Physical Review E, 54(1) (1996) 406-410.

Kranz, RL, Saltzman, JS, Blacic, JD, *Hydraulic diffusivity measurements on laboratory rock samples using an oscillating pore pressure method*, International Journal of Rock Mechanics and Mining Sciences and Geomechanics Abstracts, 27(5) (1990) 345-352.

Kutelek, M, *Non-Darcian flow of water in soils (Laminar Region)*, 1st IAHR Symposium on Fundamentals of Transport Phenomena in Porous Media, Haifa, Israel (1969).

Kwon, O, Kronenberg, AK, Gangi, AF, Johnson, B, *Permeability of Wilcox shale and its effective pressure law*, Journal of Geophysical Research 106 (2001) 19339-19353.

Laban, C, Jaap, JM, van der M, *Pleistocene Glaciation in The Netherlands Developments in Quaternary Science*, 15 (2011) 247-260.

Lade, P, *Elasto-plastic stress-strain theory for cohesionless soil with curvey yield surfaces*, International Journal of Solids and Structures 13 (1977) 1019-1035.

Lambe, TW, *A mechanistic picture of shear strength in clay*, Research Conference on shear strength of cohesive soils, ASCE (1960) 555-580.

Lambeck, K, Purcell, A, Funder, S, Kjaer, K H, Larsen, E, Moller, P, *Constraints on the Late Saalian to early Middle Weichselian ice sheet of Eurasia from field data and rebound modelling*, Boreas International Journal of Quaternary Research, 35 (2006) 539-575.

Leddra, MJ, Petley, DN, Jones, ME, *Fabric changes induced in a cemented shale through consolidation and shear*, In The 33rd U.S. symposium on Rock Mechanics. American Rock Mechanics Association (1992).

Lehman, RM, *Understanding of aquifer microbiology is tightly linked to sampling approaches*, Geomicrobiology Journal 23 (2007) 331-341.

Li, X, TIMODAZ, *Thermal Impact on the Damaged Zone Around a Radioactive Waste Disposal in Clay Host Rocks, Final Report*. European Commission (2007).

Li, X, TIMODAZ: *A successful international cooperation project to investigate the thermal impact on the EDZ around a radioactive waste disposal in clay host rocks*, Journal of Rock Mechanics and Geotechnical Engineering, 5(3) (2013) 231-242.

- Li, X L, Bastiaens, W, Bernier, F, *Twenty-five years' geotechnical observation and testing in the Tertiary Boom Clay formation*, Géotechnique 57(2) (2007) 229-237.
- Li, XL, Bastiaens, W, Van Marcke, P, Verstricht, J, Chen, GJ, Weetjens, E, Sillen, X, *Design and development of large-scale in-situ PRACLAY heater test and horizontal high-level radioactive waste disposal gallery seal test in Belgian HADES*, Journal of Rock Mechanics and Geotechnical Engineering 2 (2010) 103-110.
- Lima, A, Morales, ER, Pineda, J, Solé, A,G, *Low-strain shear modulus dependence on water content of a natural stiff clay*. Retrieved from <http://upcommons.upc.edu/handle/2117/9917> (2012a).
- Lima, A, Morales, ER, Díaz, YP, *Water retention properties of two deep Tertiary clay formations within the context of radioactive waste disposal*, (2012b) 315-321.
- Linder, E, *Swelling rock: A review*, Proceedings of Rock Engineering for Foundations and Slopes. ASCE, (1976) 1.
- Low, PF, *Structural component of the swelling pressure of clays*, Langmuir 3 (1987) 18-25.
- Low, PF, *Interparticle forces in clay suspensions: flocculations, viscous flow and swelling*, In CMS Workshop Lectures 4 (1992) 158-190.
- Malusis, AM, Shackelford, CD, Maneval, JE, *Critical review of couples flux formulations for clay membranes based on nonequilibrium thermodynamics*, Journal of Contaminant Hydrology 138 (2012) 40-59.
- Malusis, MA, Shackelford, CD, *Coupling effects during steady-state solute diffusion through a semipermeable clay membrane*, Environmental Science and Technology 36 (2002) 1312-1319.
- Mandl G, Harkness, R, *Hydrocarbon migration by hydraulic fracturing*, Geological Society, London, Special Publications 29(1) (1987) 39-53.
- Marschall, P, Horseman, S, Gimmi, T, *Characterisation of Gas Transport Properties of the Opalinus Clay, a Potential Host Rock Formation for Radioactive Waste Disposal*, Oil and Gas Science and Technology - Rev. IFP, 60(1) (2005) 121-139.
- Mauclaire, L, McKenzie, JA, Schwyn, B, Bossart, P, *Detection and cultivation of indigeneous microorganisms in Mesozoic claystone core samples from the Opalinus Clay Formation (Mont Terri Rock Laboratory)*, Physics and Chemistry of the Earth, Parts A/B/C 32 (2007) 232-240.
- Mauret, E, Renaud, M, *Transport phenomena in multi-particle systems—I. Limits of applicability of capillary model in high voidage beds-application to fixed beds of fibers and fluidized beds of spheres*, Chemical Engineering Science 52(11) (1997) 1807-1817.
- McClintock, FA, Walsh, JB, *Friction on Griffith cracks in rocks under pressure*, Proceedings of 4th U.S. National Congress on Applied Rock Mechanics, 2 (1962).
- Mertens, J, Vandenberghe, N, Wouters, L, Sintubin, M, *The origin and development of joints in the Boom Clay Formation (Rupelian) in Belgium*, Geological Society of London Special Publications 216 (2003) 309-321.

- Mertens, J, Bastiaens, W, Dehandschutter, B, *Characterisation of induced discontinuities in the Boom Clay around the underground excavations (URF, Mol, Belgium)*, Applied Clay Science 26(1-4) (2004) 413-428.
- Middtømme, K, Roaldset, E, Aagaard, P, *Thermal conductivity of selected claystones and mudstones from England*, Clay Minerals 33(1) (1998) 131-145.
- Mitchell, JK, *Fundamentals of Soil Behaviour*, John Wiley and Sons, New York (1976).
- Monfared, M, Sulem, J, Delage, P, Mohajerani, M, *On the THM behaviour of a sheared Boom clay sample: Application to the behaviour and sealing properties of the EDZ*, Engineering Geology 124 (2012) 47-58.
- Muñoz, J, Alonso, EE, Lloret, A, *Thermo-hydraulic characterisation of soft rock by means of heating pulse tests*, Géotechnique (2009) 293-306.
- Nickel, E, *Oligozäne Bodendynamik und Sequenzstratigraphie am Südrand des Nordwesteuropäischen Tertiärbecken*, Mathematisch-Naturwissenschaftlichen Fakultät, Rheinischen Friedrich-Wilhelms-Universität Bonn (2003).
- Neuzil, C, *How permeable are clays and shales?* Water Resources Research 39 (2) (1994) 145-150.
- Neuzil, C, *Osmotic generation of 'anomalous' fluid pressures in geological environments*, Nature 403 (2000) 182-184.
- Nguyen, XP, Cui, YJ, Tang, AM, Deng, YF, Li, XL, Wouters, L, *Effects of pore water chemical composition on the hydro-mechanical behaviour of natural stiff clays*, Engineering Geology 166 (2013) 52-64.
- Novello, EA, *Geomechanics and the critical state*, PhD Monash University, (1988).
- Oakes, DT, *Solids concentration on effects in bentonite drilling fluids*, Clays and clay minerals 8 (1960) 252-273.
- Ohnaka, M, *The quantitative effect of hydrostatic confining pressure on the compressive strength of crystalline rocks*, Journal of Physical Earth 21 (1973) 125-140.
- Olgaard, D, Nuesch, R, Ural, J, *Consolidation of water saturated shales at great depth under drained conditions*, 8th International Symposium on Rock Mechanics. International Society for Rock Mechanics (1995).
- Olsen, HW, *Deviations from Darcy's law in saturated clays*, Soil Science Society of America Journal 29 (2) (1965) 135-140.
- Olsen, HW, *Simultaneous Fluxes of Liquid and Charge in Saturated Kaolinite*, Soil Sci. Soc. Am. J. 33(3) (1969) 338-344.
- Ortiz L, Volckaert G, De Cannière, P, Put, M, Horseman, ST, Harrington, JF, Impey, M, Einchcomb, S, *European project MEGAS: Modelling and experiments on gas migration in repository host rocks. (Phase 2)-Final report*, European Commission report, EUR 17453 (1997).

- Ortiz, L, Volckaert, G, De Canniere, P, Put, M, Horseman, ST, Harrington, JF, Impey, M and Einchomb, S, *MEGAS - Modelling and Experiments on Gas Migration in Repository Host-rocks*, EU PEGASUS Meeting Nuclear Science and Technology Series, Rapolina-Terme, Italy (1996).
- Parker, JC, *Multiphase flow and transport in porous media*, Reviews of Geophysics 27 (1989) 311-328.
- Patterson, MS, Wong, TF, *Experimental rock deformation- the brittle field*, Springer Science and Business Media (2005).
- Pedersen, K, *Microbial processes in radioactive waste*, SKB Technical Report TR-00-04 (2000).
- Pedersen, K, Motamedi, M, Karnland, O, Sandén, T, *Cultivability of microorganisms introduced into a compacted bentonite clay buffer under high-level radioactive waste repository conditions*, Engineering Geology 58(2) (2000) 149-161.
- Pelet, R, Tissot, B, *Nouvelles donnees sur les mecanismes de genese et de migration du petrole simulation mathematique et application a la prospection*, In 8th World Petroleum Congress, World Petroleum Congress (1971).
- Picard, J, Giraud, A, *Application of thermoporomechanics to problems of storage of radioactive waste*, Mechanics of Porous Media, Charlez. Balkema, Rotterdam (1995).
- Pierik, HJ, *An integrated approach to reconstruct the Saalian glaciations*, MSc thesis (Utrecht University / Province of Drenthe) (2010) 140p.
- Priest, S, *Discontinuity analysis for rock engineering*, Springer Science and Business Media (1993).
- Pusch, R, Forsberg, T, *Gas migration through bentonite clay*, Svensk Kaernbraenslefoersoerjning AB, Stockholm (1983).
- Pusch, R, Ranhagen, L, Nilsson, K, *Gas migration through Mx-80 bentonite*, Final report, Nagra Technical Report (1985) 85-36.
- Rieke, HH, Chilingarian, GV, *Compaction of argillaceous sediments*, Elsevier (1974).
- Rijkers, RHB, Huisman, DJ, De Lange, G, Weijers, JP, Witmans-Parker, N, *Inventarisatie geomechanische, geochemische en geohydrologische eigenschappen van Tertiaire kleipakketten - CAR Fase II*, TNO report NITG 98-90-B (1998) 167 p.
- Rodwell, WRE, *Research into Gas Generation and Migration in Radioactive Waste Repository Systems (PROGRESS Project)*, EUR 19133 EN, European Commission, Belgium (2000).
- Rodwell, WR, Harris, AW, Horseman, ST, Lalieux, P, Müller, W, Ortiz Amaya, L Pruess, K, *Gas Migration and Two-Phase Flow through Engineered and Geological Barriers for a Deep Repository for Radioactive Waste*, European Commission, Nuclear Energy Agency, Belgium (1999).

- Romero, E, Simms, P, *Microstructure Investigation in Unsaturated Soils: A Review with Special Attention to Contribution of Mercury Intrusion Porosimetry and Environmental Scanning Electron Microscopy*, Geotechnical and Geological Engineering 26 (2008) 705-727.
- Romero, E, Gens, A, Lloret, A, *Water permeability, water retention and microstructure of unsaturated compacted Boom clay*, Engineering Geology 54 (1999) 117-127.
- Romero, E, Senger, R, Marschall, P, *Air Injection Laboratory Experiments on Opalinus Clay, Experimental techniques, Results and Analyses*, 3rd EAGE Shale Workshop-Shale Physics and Shale Chemistry (2012).
- Romero, E, Lima, A, Gens, A, *Determination of the thermal parameters of a clay from heating cell tests*, Proceedings of the 18th International Conference on Soil Mechanics and Geotechnical Engineering, Paris (2013) 3403-3406.
- Rutter, EH, Brodie, KH, Evans, PJ, *Structural geometry, lower crustal magmatic underplating and lithospheric stretching in the Ivrea-Verbano zone, N. Italy*, Journal of Structural Geology 15 (1993) 647-662.
- Sato, R, Sasaki, T, Ando, K, Smith, PA, Schneider, JW, *Calculations of the Temperature Evolution of a Repository for Spent Fuel in Crystalline and Sedimentary Rocks, Switzerland*, NAGRA report, CH-5430 Wettingen (1998).
- Schlomer, S, Krooss, BM, *Experimental characterisation of the hydrocarbon sealing efficiency of cap rocks*, Marine and Petroleum Geology 14 (1997) 565-580.
- Schofield, AN, *The 'mohr-coulomb' error*, Cambridge University Press (1998).
- Schofield, AN, Wroth, CP, *Critical state soil mechanics*, McGraw-Hill (1968).
- SCK-CEN, HADES TOUR GUIDE (1997).
- Sen, MA, Horseman, ST, Harrington, JF, *Further studies on the movement of gas and water in an overconsolidated clay: Contribution to MEGAS Phase 2 Report (PEGASUS Project)*, Commission of European Communities (CEC), Brussels (1996).
- Senger, R, Romero, E, Ferrari, A, Marschall, P, *Characterization of gas flow through low-permeability claystone: laboratory experiments and two-phase flow analyses*, Geological Society, London, Special Publications, 400 (2014) 15.
- Senol, A, *Determination of Pre-consolidation Pressure*, Ph.D Thesis, Istanbul Technical University, The Institute of Science and Technology (1997).
- Şenol, A, Sağlamer, A, *Determination of Preconsolidation Pressure with New Method (Strain Energy-Log Stress)*, Electronic Journal of Geotechnical Engineering, 5 (2000).
- Shackelford, CD, Moore, SM, *Fickian diffusion of radionuclides for engineered containment barriers: Diffusion coefficients, porosities, and complicating issues*, Engineering Geology 152(1) (2013) 133-147.
- Shah, KR, *An elasto-plastic constitutive model for brittle-ductile transition in porous rocks*, International Journal of Rock Mechanics and Mining Sciences 34 (1997) 283.

Shen, L, Chen, Z, *Critical review of the impact of tortuosity on diffusion*, Chemical Engineering Science, 62(14) (2007) 3748-3755.

Sillen, X, Marivoet, J, *Thermal impact of a HLW repository in clay*, SCK-CEN (2007).

Sillen, X, Leupin, OX, *The use of clay as a n engineered barrier in radioactive-waste management - a review*, Clays and Clay Minerals 61 (2013) 477-498.

Skempton, AW, *First-time slides in over-consolidated clays*, Geotechnique 20 (1970) 320-324.

Skurtveit, E, Aker, E, Soldal, M, Angeli, M, Hallberg, E, (2010) *Influence of micro fractures and fluid pressure on sealing efficiency of caprock: a laboratory study on shale*, GHGT-10 (2010).

Skurtveit, E., Aker, E., Soldal, M., Angeli, M. and Wang, Z., 2012. Experimental investigation of CO₂ breakthrough and flow mechanisms in shale. Petroleum Geoscience, 18(1): 3-15.

Sposito, G., 1984. The surface chemistry of soils. New York: Oxford University Press.

Stroes-Gascoyne, S., Haveman, S. A., Hamon, C. J., Delaney, T.-L., Pedersen, K., Arlinger, J. and Daumas, S., 1997. Occurrence and identification of microorganisms in compacted clay-based buffer material designed for use in a nuclear fuel waste disposal vault. Canadian Journal of Microbiology, 43(12), 1133-1146.

Stroes-Gascoyne, S., Schippers, A., Schwyn, B., Poulain, S., Sergeant, C., Simonoff, M. and Matray, J. M., 2007. Microbial Community Analysis of Opalinus Clay Drill Core Samples from the Mont Terri Underground Research Laboratory, Switzerland. Geomicrobiology Journal, 24(1), 1-17.

Stroes-Gascoyne, S., Hamon, C. J., Maak, P. and Russell, S., 2010. The effects of the physical properties of highly compacted smectitic clay (bentonite) on the culturability of indigenous microorganisms. Applied Clay Science, 47(1-2), 155-162.

Sultan, N., Delage, P. and Cui, Y.J., 2002. Temperature effects on the volume change behaviour of Boom clay. Engineering Geology, 64: 135-145.

Sultan, N., Cui, Y.J. and Delage, P., 2010. Yielding and plastic behaviour of Boom clay. Geotechnique, 60 (9), 657-666.

Sun, Z., Tang, X. and Cheng, G., 2013. Numerical simulation for tortuosity of porous media. Microporous and Mesoporous Materials, 173(0): 37-42.

Tarandi, T., 1983. Calculated temperature field in and around a repository for spent nuclear fuel, SKB.

Tavenas, F., Des Rosiers, J.P., Leroueil, S., La Rochelle, P. and Roy, M., 1979. The use of strain energy as a yield and creep criterion for lightly overconsolidated clays. Geotechnique, 29, 285-303.

Terzaghi, K., 1943. Theoretical soil mechanics. Wiley.

Thunvik, R. and Braester, C., 1991. Heat propagation from a radioactive waste repository. SKB 91 reference canister, SKB.

Tsang, C. F., Barnichon, J. D., Birkholzer, J., Li, X. L., Liu, H. H. and Sillen, X., 2012. Coupled thermo-hydro-mechanical processes in the near field of a high-level radioactive waste repository in clay formations. *International Journal of Rock Mechanics and Mining Sciences*, 49: 31-44.

Urios, L., Marsal, F., Pellegrini, D. and Magot, M., 2012. Microbial diversity of the 180 million-years-old Toarcian argillite from Tournemire, France. *Applied Geochemistry*, 27, 1442-1450.

Van Genuchten, M.T., 1980. A closed-form equation for predicting the hydraulic conductivity of unsaturated soils. *Soil science society of America journal*, 44, 892-898.

Van Kote, F, Peres, J.M, Olivier, M, Lewi, J, Assouline, M, Mejon-Goula, MJ, *Performance assessment of geological isolation systems for radioactive waste Disposal in granite formations*, Commission of the European Communities (CEC) (1988).

Van Oort, E, *A novel technique for the investigation of drilling fluid induced borehole instability in shales*, Proceedings of Conference on Rock Mechanics in Petroleum Engineering, Delft, SPE (1994).

Vardoulakis, I, Sulem, J, *Bifurcation analysis in geomechanics*. Chapman and Hall (1995).

Verhoef, E, Neeft, E, Grupa, J, Poley, A, *Outline of a disposal concept in clay*, OPERA-PG-COV008, (2011); revised in 2014.

Vardon, PJ, Buragohain, P, Hicks, MA, Haart, J, Fokker, PA, Graham, CC, *Technical feasibility of a Dutch radioactive waste repository in Boom Clay: Thermo-hydro-mechanical behaviour*, OPERA-PU-TUD321c (2016).

Vis, GJ, Verweij, JM, *Geological and geohydrological characterization of the Boom Clay and its overburden*, OPERA-PU-TNO411 (2014).

Volckaert, G, Canniere, PD, Hooker, P, Fioravante, V, Grindrod, P, Impey, M, *MEGAS Modelling and experiments on gas migration in repository host rocks*, EUR 16235 EN, European Commission, Brussels, Belgium (1994).

Waltham, AC, *Foundations of Engineering Geology*, CRC Press (1994).

Wang, Y, *The effect of a non linear Mohr-Coulomb criterion on borehole stresses and damage-zone estimate*, *Canadian Geotechnical Journal* 31 (1994) 104-109.

Wang, Q, Cui, YJ, Tang, AM, Delage, P, Gatmiri, B, Ye, WM, *Long-term effect of water chemistry on the swelling pressure of a bentonite-based material*, *Applied Clay Science* 87 (2014) 157-162.

Weetjens, E, Sillen, X, *Gas generation and migration in the near field of a supercontainer-based disposal system for vitrified high-level radioactive waste*, Proceedings of the 11th International High-level Radioactive Waste management Conference (IHLRRWM), Las Vegas, United States, 30th April-4th May, American Nuclear Society (ANU) (2006) 667-684.

Wemaere, I, Marivoet, J, *Can we extrapolate hydraulic parameters of the Boom Clay from the local to regional scale*, Boom Clay Seminar (1997).

Wemaere, I, Marivoet, J, Labat, S, *Hydraulic conductivity variability of the Boom Clay in north-east Belgium based on four core drilled boreholes*, Physics and Chemistry of the Earth, Parts A/B/C 33 (2008) 24-36.

Wersin, P, Johnson, LH, McKinley, IG, *Performance of the bentonite barrier at temperatures beyond 100°C: A critical review*, Physics and Chemistry of the Earth, Parts A/B/C 32(8-14) (2007) 780-788.

Wersin, P, Stroes-Gascoyne, S, Pearson, FJ, Tournassat, C, Leupin, OX, Schwyn, B, *Biogeochemical processes in a clay formation in situ experiment: Part G - Key interpretations and conclusions, Implications for repository safety*, Applied Geochemistry 26(6) (2011) 1023-1034.

Wiebols, GA, Cook, NGW, *An energy criterion for the strength of rock in polyaxial compression*, International Journal of Rock Mechanics and Mineral Science, 5 (1968) 529-549.

Wiers, J, *A hydrogeological characterization and groundwater model of the Roer Valley Graben*, Msc Thesis, Centre of Hydrogeology Utrecht, Utrecht University and Netherlands Institute of Applied Geoscience TNO - National Geology Survey (2001).

Wildenborg, T, Bogdan, O, *Transport of radionuclides through a clay barrier*, TNO-NITG Information (2000) 8-12.

Wildenborg, AFB, Orlic, B, Thimus, JF, Lange, G, De Cock, S, De Leeuw, CS, De Veling, EJ, M, *Radionuclide transport in clay during climate change*, Netherlands Journal of Geosciences/Geologie En Mijnbouw 82(1) (2003) 19-30.

Wong, RC, *Swelling and softening behaviour of La Biche shale*, Canadian Geotechnical Journal 35 (1998) 206-221.

Wong, SW, Heidug, WK, *Borehole stability in shales: A constitutive model for the mechanical and chemical effects of drilling fluid invasion*, Rock Mechanics in Petroleum Engineering Society of Petroleum Engineers (1994).

Wong, RC, Wang, EZ, *Three-dimensional Anisotropic Swelling Model for Clay Shale - A fabric Approach*, International Journal of Rock Mechanics and Mining Sciences 34 (1997) 187-198.

Wong, T, Batjes, DAJ, de Jager, J, (Eds.) *Geology of the Netherlands*. Herent: Royal Netherlands Academy of Arts and Sciences (2007).

Wouters L, Herron, M, Abeels V, Hagood M, Strobet, J, *Innovative applications of dual range Fourier transform infrared spectroscopy to analysis of Boom Clay mineralogy*, Aardk. Mededel 9 (1999) 159-168.

Wouters, K, Moors, H, Boven, P, Leys, N, *Evidence and characteristics of a diverse and metabolically active microbial community in deep subsurface clay borehole water*, FEMS Microbiology and Ecology 86 (2013) 458-473.

Wroth, C, *Some aspects of the elastic behaviour of overconsolidated clay*, Proceedings of the Roscoe Memorial Symposium: Stress-Strain behaviour of Soils (1972).

Wroth, CP, Wood, DM, *The correlation of index properties with some basic engineering properties of soils*, Canadian Geotechnical Journal 15 (1978) 137-145.

Ye, WM, Zhang, YW, Chen, YG, Chen, B, Cui, YJ, *Experimental investigation on the thermal volumetric behaviour of highly compacted GMZ01 Bent*, Applied Clay Science 83-84 (2013) 210-216.

Yeung, AT, *Coupled flow equations for water, electricity and ionic contaminants through clayey soils under hydraulic, electrical and chemical gradients*, Journal of Non-Equilibrium Thermodynamics 15 (1990) 247-262.

Yeung, AT, Mitchell, JK, *Coupled fluid, electrical and chemical flows in soil*, Geotechnique 43 (1993) 121-134.

Young, A, Low, PF, *Osmosis in argillaceous rocks*, AAPG 47 (1965) 1004-1008.

Yu, HD, Chen, WZ, Jia, SP, Cao, JJ, Li, XL, *Experimental study on the hydro-mechanical behaviour of Boom clay*, International Journal of Rock Mechanics and Mining Sciences 53 (2012) 159-165.

Yu, L, Rogiers, B, Gedeon, M, Marivoet, J, De Craen, M, *Variability in the hydraulic conductivity of the Boom clay in the Campine Basin, NE-Belgium*, From Clays in natural and engineered barriers for radioactive waste confinement (2012).

Yu, L, Rogiers, B, Gedeon, M, Marivoet, M, De Craen, M, Mallants, D, *A critical review of laboratory and in-situ hydraulic conductivity measurements for the Boom Clay in Belgium*, Applied Clay Science 75-76 (2013) 1-12.

Yu, L, Weetjens, E, Sillen, X, Vietor, T, Li, X, Delage, P, Labiouse, V, Charlier, R, *Consequences of the thermal transient on the evolution of the damaged zone around a repository for heat-emitting high-level radioactive waste in a clay formation: a performance assessment perspective*, Rock mechanics and rock engineering 47 (2014) 3-19.

Zeelmaekers, E, *Computerized qualitative and quantitative clay mineralogy: Introduction and application to known geological cases*, Unpublished PhD thesis, Katholieke Universiteit (K.U.) Leuven, Groep Wetenschap en Technologie (Heverlee, Leuven) (2011).

Zhou, S, *A program to model the initial shape and extent of borehole breakout*, Computers and Geosciences 20 (1994) 1143-1160.

Zhang, G, Samper, J, Montenegro, L, *Coupled thermo-hydro-bio-geochemical reactive transport model of CERBERUS heating and radiation experiment in Boom clay*, Applied Geochemistry 23(4) (2008) 932-949.

Zihms, S, Harrington, JF, *Thermal cycling: impact on bentonite permeability*, IGDTF Geodisposal 2014, Mineralogical Magazine Special Issue (In Press).

Appendix A: Symbols and Abbreviations

	- Denotes parallel to bedding	p' or σ_{eff}	- Effective stress
\perp	- Denotes perpendicular to bedding	P_b	- Gas breakthrough pressure
A	- Cross sectional area	P_{gp}	- Peak gas pressure
C	- Gas pumping rate	P_{bdt}	- Brittle ductile transition pressure
C_c	- Compression index	P_c	- Capillary pressure
C_d	- Drained cohesion	P_{co}	- Apparent capillary pressure
C_s	- Swelling index	P'_c	- Pre-consolidation pressure
C_u	- Undrained cohesion	P_{co}	- Apparent capillary pressure
D	- Diffusion coefficient	P_{gi}	- Pressure of the gas at upstream end
D_e	- Effective diffusion coefficient	P_{go}	- Pressure of the gas at downstream end
dh	- Decline in hydraulic head	P_i	- Pressure in phase i
dp	- Decline in pressure	P_p	- Pore pressure
dV_w	- Volume of water released from storage	P_w	- Pore water pressure
e	- Void ratio	P_{wo}	- Back pressure
E	- Young's Modulus	q	- Darcy velocity or specific discharge
e_a	- Intercept of the Critical State Line	Q	- Volumetric flow
e_c	- Critical specific void ratio	q'	- Differential stress
E_d	- Drained Young's Modulus	q_i	- Darcy velocity vector for phase i
E_{oed}	- Oedometer Modulus	Q_{st}	- Volumetric flow rate under STP
E_u	- Undrained Young's Modulus	q_u	- Uniaxial Compressive Strength
F	- Force	R	- Gas constant
G	- Acceleration due to gravity	S^*	- Effective wetting phase saturation
G	- Shear Modulus	S_c	- Shear strength
G_s	- Specific gravity	S_i	- Saturation of phase i
H	- Porewater specific enthalpy	S_{rg}	- Residual non-wetting phase saturation
H_c	- Soil constant	S_{rw}	- Residual wetting phase saturation
h	- Soil constant	S_w	- Wetting phase saturation
J	- Flux of solutes	S_s	- Specific storage
J_H	- Heat flux	S_u	- Undrained shear strength
J_s^d	- Solute mass flux	T	- Temperature
k	- Permeability	T_0	- Tensile strength
k_w	- Permeability of wetting phase	λ	- Slope of the Normal Consolidation Line
k_{rw}	- Permeability of residual wetting phase	μ	- Fluid viscosity
k_g	- Gas permeability	v	- Specific volume
k_i	- Intrinsic permeability	V_0	- Initial volume of rock
k_{ri}	- Relative permeability of phase i	V_a	- Bulk volume of rock from which water is released
K_{Sw}	- Thermal conductivity of sample matrix	V_a	- Volume of accessible porosity
K_{Tw}	- Thermal conductivity of water	V_b	- Bulk volume of rock
K_T	- Thermal conductivity	V_c	- Critical specific volume
l_0	- Initial length	V_p	- Total volume of voids
L_p	- Plasticity index	V_{st}	- Molar volume of gas at STP
M	- Slope of the Critical State Line	w	- Water content
M_s	- Mass of solid volume	W_c	- Width of gas filled fracture
M_s	- Molar mass of the solute	W_l	- Liquid limit
		x	- Flow direction

z - Depth below surface
 α - Linear expansion coefficient
 β - Volumetric expansion coefficient
 γ_w - Specific weight of water
 δ - Aperture of the gas filled fracture
 ΔH - Macroscopic volume-averaged excess specific enthalpy
 Δl - Change in length
 ΔV - Change in volume
 ε - Strain
 $\varepsilon_1, \varepsilon_3$ - Maximum and minimum principal strain components
 ε_v - Volumetric strain
 η - Empirical constant
 η_g - Viscosity of gas
 η_i - Viscosity of phase i
 η_w - Absolute viscosity of water
 κ - Hydraulic Conductivity
 κ_H - Horizontal hydraulic conductivity
 κ_v - Vertical Hydraulic Conductivity
 η_i - Viscosity of phase i
 ν - Poisson's Ratio
 ν_d - Drained Poisson's Ratio
 ν_u - Undrained Poisson's Ratio
 ρ_b - Bulk Density
 ρ_d - Dry density
 ρ_f - fluid density
 ρ_i - phase density for phase i
 ρ_s - Particle density
 ρ_w - Density of water
 σ - Stress
 $\sigma_1, \sigma_2, \sigma_3$ - Maximum, Intermediate and Minimum principal stress components
 σ_d - Differential stress
 σ_H and σ_h - Horizontal stress components
 σ_{max} - Maximum stress
 σ_N - Normal stress
 σ_{total} - Applied total stress
 σ'_v - Effective vertical stress
 σ_v - Total vertical stress
 σ_τ - Shear stress
 τ_0' - Cohesion intercept
 τ_c - Shear stress at failure
 τ_o - Cohesion
 ϕ - Internal angle of friction
 φ - Porosity
 ϕ_d - Drained internal angle of friction
 φ_e - Effective porosity
 φ_t - Total porosity
 ϕ_u - Undrained internal angle of friction

ω - Solute mass fraction
 γ - Shear strain
 Z - Osmotic reflection coefficient

Abbreviations

BIB - Broad Ion Beam
 CSL - Critical State Line
 EDZ - Excavation Damage Zone
 FIB - Focused Ion Beam
 GDF - Geological Disposal Facility
 MIP - Mercury Injection Porosimetry
 NCL - Normal Consolidation Line
 OCR - Over Consolidation Ratio
 RRL - Recompression/Rebound Line
 SEM - Secondary Electron Microscope
 TL - Tension Line
 UCS - Uniaxial Compressive Strength
 URL - Underground Research Facility
 VCL - Virgin Compression Line
 XRD - X-Ray Diffraction

Appendix B: Data and properties

	Decler <i>et al.</i> (1983)	Al-Mukhtar <i>et al.</i> (1996)	Nguyen <i>et al.</i> (2013)	Coll (2005)	TIMODAZ (2007)
Clay minerals	50	62	40	55	23-59
Illite	12	16	10	20-30	
Kaolinite	5	13	30	20-30	5-15
Smectite	33	33		10	
2:1 clays and micas					35-50
Vermiculite/chlorite					1-4
Quartz	35		60	25	23-57
Calcite	1				1-5
Pyrite	1				1-5
Feldspar				20	
Microcline	9	4-5			6-11
Plagioclase	4	4-5			0-3

Table B-1. Reported mineral composition of the Boom Clay in Belgium

Reference composition	Qtz	Albite	K-felds	Siderite	Calcite	Apatite	Pyrite	Illite/ Muscovite	Smectite + illite/smectite	Kaolinite	Chlorite
Wt%	22-72	0-6.3	0.4-17.3	0-1.5	0-4.6	0-2	0.3-5	5-37	6.8-35	2-16	1-4

Table B-2. Reference mineral composition of the Boom Clay in Belgium, as reported by SCK-CEN (The Belgian Nuclear Research Centre) (Honty and De Craen, 2011).

Ion	mg/l	mmol/l	Ion	mg/l	mmol/l	Property	Unit	Value
Ca	2.0	0.05	Total S	0.77	0.02	pH		8.5
Fe	0.2	0.003	Cl -	26	0.7	pCO ₂	Atm	10 ^{-2.62}
Mg	1.6	0.06	SO ₄ ²⁻	2.2	0.02	Eh	mV	-274
K	7.2	0.2	HCO ₃ ⁻	878.9	14.4	Ionic strength		0.016
Si	3.4	0.1						
Na	359	15.6						
Al	0.6 × 10 ⁻³	2.4 × 10 ⁻⁵						

Table B-3. Reference Boom Clay pore water after De Craen et al. (2004b).

Boom Clay Geotechnical Parameters								
Parameter	Bulk density	Dry density	Water content	Void ratio	Porosity	Specific gravity	Liquid limit	Plasticity index
Symbol (Units)	ρ_b g/cm ³	ρ_d g/cm ³	w %	e	ϕ %	G_s g/cm ³	W_l %	L_p %
De Beer <i>et al.</i> (1977)	1.93	1.53	26	0.529-0.786	34.6-44.4		82	49
Horseman <i>et al.</i> (1987) ^a	2.05	1.66	24	0.646	39.2	2.70	66	47
Anon. (1979) ^b	1.914-2.105	1.484-1.726	18-29	0.529-0.80	34.6-44.4		64	40
Al-Mukhtar (1996)						2.67	70	45
Belanteur <i>et al.</i> (1997)						2.67		
Wildenborg <i>et al.</i> (2000)				0.37-0.47	27 ^c , 32 ^d			
Bernier <i>et al.</i> (2007)					39			
TIMODAZ (2007)	2.026		22-27	0.64	39		55-80	32-51
Deng <i>et al.</i> (2012)				0.49-0.67	32.9-40.1	2.67	59-83	
Deng <i>et al.</i> (2012) ^e				0.785	44.0	2.65	78	45
Lima <i>et al.</i> (2012a)	1.9-2.05	1.65-1.71	21-25	0.560-0.618	35.8-38.2		55.7	27 ^f
Lima <i>et al.</i> (2012b)	2.05	1.65	~25	0.60-0.62	37.5-38.3		56	27 ^f
Yu <i>et al.</i> (2012)	2.04 ^g	1.64	23.9 ^g	0.685 ^g	40.6 ^g			
Bésuelle <i>et al.</i> (2013)					36.5			

Table B0-4. Summary of geotechnical properties for the Boom Clay. All samples were derived from Mol, Belgium, at an approximate repository depth of 223m, unless otherwise denoted. Elastic parameters can be found in Chapter 3 (Table 3.1)

^a Values quoted relate to a depth of 247 m.

^b Quoted by Horseman *et al.* (1993). Relates to a depth range between 168 m and 266 m.

^c Value quoted relates to a depth interval of 738-888 m.

^d Value quoted relates to a depth interval of 1415-1495 m.

^e These values relate to core material derived from Essen at a depth interval (218.9-219.91 m) reasonably comparable to that of Mol stratigraphically.

^f Low value suggests this is a misquote and is, instead, the measured plasticity limit.

^g Average taken from a wider dataset.

Boom Clay Mechanical Parameters

Parameter State Symbol (Units)	Young's modulus		Poisson's ratio		Internal friction angle		Cohesion		UCS q_u MPa	Preconsolidation pressure P_c' MPa
	Drained E_d MPa	Undrained E_u MPa	Drained ν_d	Undrained ν_u	Drained ϕ_d	Undrained ϕ_u	Drained c_d MPa	Undrained c_u MPa		
Horseman <i>et al.</i> (1993)		152 ^h , 197 ⁱ								5 ^j , 6 ^k
Bouazza <i>et al.</i> (1996)					18.5		0.01			
Barnichon and Volckaert (2003)	300		0.125		18		0.3			
Wildenborg <i>et al.</i> (2003)										6.8 ^l , 7.4 ^m , 7.5 ^m
Bernier <i>et al.</i> (2007)	300				18		0.3			2
TIMODAZ (2007)	300				18-25	2.0-4.0	-0.3	0.5-1.3		-5-6
Deng <i>et al.</i> (2012) ⁿ					13.0 ^o					1.74
Lima <i>et al.</i> (2012b)					20 ^p					5.2
Tsang <i>et al.</i> (2012)									2 ^k	
Yu <i>et al.</i> (2012)										5
Bésuelle <i>et al.</i> (2013)	150 ^q 500 ^{q,r}		0.125		18-24		0.08		2.5	-5

Table B0-5. Summary of the mechanical properties of the Boom Clay, as reported in the literature. All samples were derived from Mol, Belgium, at an approximate depth of 223m, unless otherwise denoted.

^h Secant modulus.

ⁱ Tangent modulus.

^j Parallel to bedding.

^k Perpendicular to bedding.

^l Average value for samples taken from Weelde (Belgium) core at a depth of 313m.

^m Samples taken from Blija borehole at depths of 453m and 561m, respectively.

ⁿ Samples taken from Essen borehole.

^o Drainage state assumed, based on chosen strain rate.

^p Methodology appears unpublished.

^q Not immediately apparent at which stress conditions (during loading) these values are derived from.

^r On reloading.

Boom Clay Hydraulic Parameters

Parameter	Methodology	Location/Depth	Void ratio	Effective stress	Hydraulic conductivity (⊥)	Hydraulic conductivity ()	Anisotropy ratio	Specific storage
Symbol (Units)		x, z m	e	σ_{eff} MPa	K_{\perp} m/s	$K_{ }$ m/s	/⊥	S_s m ⁻¹
Horseman et al. (1993; 1987)	Triaxial cell	Mol, 247	0.646	2.5	$2.83 \times 10^{-12} \text{ }^s$	5.5×10^{-12}	1.94	1.7×10^{-6}
Horseman and Harrington (1994)	Isotropic, constant flow rate	Mol			$1 \times 10^{-12} \text{ }^s$	3×10^{-12}	-3	$\pm 8.57 \times 10^{-5} \text{ }^s \text{ }^t$
Volckaert et al. (1995), SCK.CEN	Constant head	Mol	$\perp 0.673^s$ $ 0.634^s$		$1.3 - 3.4 \times 10^{-12} \text{ }^s$	$3.6 \times 10^{-12} \text{ }^s$	1.1-2.8	
Volckaert et al. (1995), SCK.CEN	<i>In situ</i> testing	Mol			$2.3 \times 10^{-12} \text{ }^t$	5.3×10^{-12}	2.3	$\pm 8.1 \times 10^{-6} \text{ }^t$
Haijtkink and Roswell (1998), BGS	Isotropic, constant flow rate	Mol		1.7 - 2.15	$1.39 \times 10^{-12} \text{ }^s$	$4.27 \times 10^{-12} \text{ }^s$	3.1	$ 9.3 \times 10^{-5} \text{ }^s \text{ }^t$
Harrington and Horseman (1999)	Isotropic, constant flow rate	Mol, 224	$\perp 0.638^s$ $ 0.616^s$	$\perp 2.22,$ $ 2.19$	7.7×10^{-13}	2.7×10^{-12}	3.51	
Wildenborg et al. (2003)	Not given, oedometer arrangement	313 - 561			$7.6 \times 10^{-14} -$ 1.1×10^{-13}			
Aertsens et al. (2004)	Low pressure constant head	190 - 290		Not at <i>in situ</i> conditions	$2.3 \times 10^{-12} \text{ }^s$		-2	
Bernier et al. (2007)	<i>In situ</i> testing	Mol, ~220		2.3 ^t	$2 - 4 \times 10^{-12}$			
Lima et al. (2012a)	Not given	Not given	0.56-0.618	Not given	3.0×10^{-12}			
Lima et al. (2012b)	Not given	Mol, 223	0.60-0.62	2.25 ^t	2.4×10^{-12}			
Bésuelle et al. (2013)	Constant head, repeated	Mol, 223	0.574	2.3 ^t	1.92×10^{-12}			

^s Averaged value calculated from larger dataset.

^t Vertical effective stress.

Boom Clay Hydraulic Parameters (continued)								
Parameter	Methodology	Location/Depth	Void ratio	Effective stress	Hydraulic conductivity (⊥)	Hydraulic conductivity ()	Anisotropy ratio	Specific storage
Hildenbrand et al. (2002)	Constant head	Mol, 220	0.558 ^u	Not at <i>in situ</i> conditions	1.25 x 10 ⁻¹³ ^u	3.55 x 10 ⁻¹³ ^w	2.84	
Hildenbrand et al. (2002)	Constant head	Molenbeersel, 1056	0.304 ^{s, v}	Not at <i>in situ</i> conditions	1.5 x 10 ⁻¹³ ^v	2.99 x 10 ⁻¹³ ^w	1.99	
Average for all Mol data ^w		Mol ~220	±0.619		1.6 x 10 ⁻¹²	4.1 x 10 ⁻¹²	2.5	

Table B-06. Summary of hydraulic properties for the Boom Clay. All samples were derived from Mol, Belgium, at an approximate repository depth of 223 m, unless otherwise denoted.

^u Estimated based on water content. MIP analysis estimates a porosity of 0.316.

^v Estimate based on MIP analysis. Water content data is not given.

^w Average figures exclude data relating to samples taken from other depth intervals/locations or known to not be tested with Mol pore fluid chemistry.

Test	Gas pumping rate [C] $\mu\text{l hr}^{-1}$	Excess gas pressure [P _{gi} -P _{wo}]			Apparent capillary pressure [P _{co}] MPa	Gas permeability [k _g] m ² x10 ²⁰		Conf. stress [σ _c] MPa	Back-pressure [P _{wo}] MPa
		Break-through MPa	Peak MPa	Steady state MPa		Flow in	Flow out		
T1S1	375	1.21	1.27	1.21	-1.00	-25.8	-34.2	4.40	2.18 [¶]
T2S1	375	1.88	1.89	1.73	-1.00	79	6.5	4.40	2.18 [¶]
T2S2	375	1.93	1.93	1.46	-1.00	12.2	12.0	4.40	2.18 [¶]
	180			1.38	-1.00	7.0	8.3	4.40	2.18 [¶]
	90			1.27	-1.00	4.9	5.3	4.40	2.18 [¶]
	45			1.25	-1.00	2.6	4.7	4.40	2.18 [¶]
	375	1.60	1.75	1.64	-1.00	9.0	8.8	4.40	2.18 [¶]
	180			1.42	-1.00	6.4	5.1	4.40	2.18 [¶]
	90			1.26	-1.00	5.0	4.6	4.40	2.18 [¶]
T3S3	375	3.57	3.59	3.15	2.1	5.4	5.1	7.40	2.21 [¶]
	375	2.91		3.28	2.1	4.9	5.4	7.40	2.21 [¶]
	375	3.04	3.37	3.28	2.1	4.9	4.6	7.40	2.21 [¶]
	37500	3.92	4.75	4.57	2.5	28.5	300	7.40	2.21 [¶]
	3750000	4.78	5.13	-4.26	1.5	-28000	-2400	7.40	2.21 [¶]
T2S3	375	0.48	0.48	0.38	-0.3	66.2	63.7	4.40	2.21
T3S1	375	1.01	1.02	0.8	0.5	9.7	9.4	4.40	2.21
	375	0.83	0.95	0.90	0.5	7.7	8.0	4.40	2.21
T3S2	375	0.38	1.08	1.06	-0.2	3.6	3.7	4.40	2.21
	375			1.09	-0.2	3.4	3.2	4.40	2.21
T4S1	375	1.97	2.00	1.92	-1.00	6.4	5.6	4.40	2.23
	180			1.85	-1.00	3.3	2.4	4.40	2.23
	90			1.77	-1.00	1.8	1.3	4.40	2.23
	45			1.71	-1.00	1.0	0.4	4.40	2.23
	375	2.03	2.07	2.00	-1.00	5.9	5.3	4.40	2.23
	180			1.90	-1.00	3.1	2.6	4.40	2.23
	90			1.84	-1.00	1.7	1.3	4.40	2.23
	45			1.77	-1.00	0.9	0.5	4.40	2.23
T4S2	375	3.39	3.82	3.12	-1.00	3.0	2.8	8.70 [#]	2.22
	180			2.54	-1.00	1.9	1.8	8.70 [#]	2.22
	90			2.03	-1.00	1.3	1.3	8.70 [#]	2.22
	45			1.74	-1.00	0.9	0.8	8.70 [#]	2.22
	375	2.97	3.74	3.55	-1.00	2.2	2.0	8.70 [#]	2.22
	180			3.18	-1.00	1.2	1.1	8.70 [#]	2.22
	90			2.33	-1.00	0.8	0.4	8.70 [#]	2.22

Table B-7. Summarised gas transport properties of the Boom Clay taken from Horseman and Harrington (2000). Apparent capillary pressure is the extrapolated asymptote of the shut-in transient. This extrapolation is rather uncertain in some experiments. The symbol # signifies that the quoted value is the axial stress in a test performed under K₀ conditions. Tests marked ¶ denote samples orientated normal to bedding.

Prior to gas injection			
Test stage and flow rate $\mu\text{l}\cdot\text{hr}^{-1}$	Hydraulic conductivity $K \times 10^{-12} \text{ (m}\cdot\text{s}^{-1}\text{)}$	Specific storage $S_s \times 10^{-5} \text{ (m}^{-1}\text{)}$	Average effective stress σ_{eff}
T4S1-H1-5	4.4	9.3	2.13
T4S1-H1-10	4.7	9.5	2.10
T4S1-H1-20	4.8	9.3	2.03
T4S1-H1-10D	5.1	9.0	2.10
T4S1-H1-5D	5.1	-	2.14
After gas injection			
T4S1-H2-10	4.2	#	2.09
T4S1-H2-20	4.5	18.0	2.01
T4S1-H2-30	4.4	21.0	1.93
T4S1-H2-20D	4.3	12.0	2.01
T4S1-H2-10D	3.9	13.0	2.08

Table B-8. Hydraulic conductivity data from Harrington and Horseman (1997) for flow before and after gas injection. Test marked # was unreported since only a poor numerical fit to the data was achieved.

Clay	Thermal conductivity $\text{W}/\text{m}^{\circ}\text{C}$	Reference
Bentonite	0.75 (dry conditions)	Tarandi (1983)
	1.5 (saturated conditions)	
	0.75 (dry conditions)	Thunvik and Braester (1991)
	0.7 (dry conditions)	
	1.7 (saturated conditions)	Sato <i>et al.</i> (1998)
Claystone and siltstone	0.8-1.1 (dry conditions)	Van Kote <i>et al.</i> (1988)
	1.35-1.45 (saturated conditions)	
	0.8 - 1.25	
Shale	1.05 - 1.45	Midttømme <i>et al.</i> (1998)
Oxford Clay	1.57	
Kimmeridge Clay	1.51	Bernier <i>et al.</i> (1996) CERBERUS
Boom Clay	1.6	
	1.7	
Opalinus Clay	1.69	Bernier <i>et al.</i> (1996) CACTUS
	1.6	SCK-CEN (1997)
	1.6	Romero <i>et al.</i> (2013)
	1.7	Bock <i>et al.</i> (2010)

Table B-9. Thermal conductivities for clays and clay minerals.

Clay	Linear thermal expansion coefficient $\alpha \text{ (}^{\circ}\text{C}^{-1}\text{)}$	Reference
Boom Clay (drained)	4.2×10^{-5} **	Monfared <i>et al.</i> (2012)
Boom Clay (undrained)	1.16×10^{-4} **	
Opalinus Clay (parallel to bedding)*	1.5×10^{-5}	Bock <i>et al.</i> (2010)
Opalinus Clay (perpendicular to bedding)*	2×10^{-5}	
MX 80 Bentonite*	2×10^{-4}	Cui and Tang (2013)
GMZ01 Bentonite*	1×10^{-4}	Ye <i>et al.</i> (2013)

Table B-10. Linear thermal expansion coefficients (α). *no drainage conditions provided. ** Quoted as volumetric in original literature.

Clay	Volumetric thermal expansion coefficient β ($\text{m}^3/\text{m}^3 \times ^\circ\text{C}$)	Reference
Boom Clay (drained)	3×10^{-5}	Picard and Giraud (1995)
	1.26×10^{-4}	Monfared <i>et al.</i> (2012)
Boom Clay (undrained)	13×10^{-5}	Picard and Giraud (1995)
	3.47×10^{-4}	Monfared <i>et al.</i> (2012)
Opalinus Clay*	1.2×10^{-5}	Muñoz <i>et al.</i> (2009)
Water	2×10^{-4}	Britto <i>et al.</i> (1989)

Table B-11. Volumetric thermal expansion coefficients (β). * no saturation conditions provided

Reference	Sample type	Sample properties	Key parameters/properties measured	Test set-up	Test procedure	Temperature range
Baldi <i>et al.</i> (1988)	Boom Clay (HADES) Pontida Silty Clay Kaolin	L_p : 25.0% W_l : 66.6% w (initial): 12%	Pore pressure Hydraulic outflow Volumetric strain	Triaxial cell, one radial and two axial heaters	Isothermal, isotropic consolidation testing Isobaric thermal loading/unloading Drained conditions	Room temperature - 90 °C
Hueckel and Pelligrini (1992)	Boom Clay (HADES) Pasquasia Clay	Not given	Pore pressure Hydraulic outflow Volumetric strain	Triaxial cell, one radial and two axial heaters	Isobaric thermal loading/unloading Undrained conditions	Room temperature - 100 °C
Horseman <i>et al.</i> (1987; 1993)	Boom Clay (HADES)	ρ_b : 2.05g/cm ³ ρ_d : 1.66g/cm ³ w (initial): 24% e : 0.646 L_p : 47% OCR: -2.4	Differential stress Pore pressure Volumetric strain Friction angle, cohesion Critical state coefficient, M	Triaxial cell, electrical heating jacket	Shear testing Undrained conditions	Room temperature and 80 °C
De Bruyn and Thimus (1996)	Boom Clay (HADES)	w : 23.0 - 26.0 % ϕ : 39.4-40.5 %	Pore pressure Axial strain Friction angle, cohesion	Triaxial cell	Isotropic consolidation, isothermic shear testing	20°, 50°, 75° and 80 °C
Delage <i>et al.</i> (2000)	Boom Clay	L_p : 50% ϕ : 40% W_c : 24-30%	Net hydraulic flow Permeability	Isotropic compression cell	Saturation under 1 MPa P_{wo} and σ_{eff} of 30k Pa After saturation: isotropic consolidation under all around pressure of 4 MPa followed by unloading to 2 MPa - OCR =2	20, 60, 70, 80 and 90°C
Cui <i>et al.</i> (2009)	Boom Clay (HADES)	L_p : 37 - 50% C_c : 50 - 62% w (samples in this study): 19.5 - 21.6% OCR: 2.4	Net hydraulic flow	Triaxial cell with heating coil	Isothermal, isotropic consolidation testing Isobaric thermal loading/unloading	25 -80°C
Monfared <i>et al.</i> (2012)	Boom Clay (HADES)	ϕ : 39% C_c : 55% w (initial): 21 and 21.6%	Volumetric strain Pore pressure Permeability Net hydraulic flow	Triaxial cell with heating belt	Shear testing Thermal loading of fractured samples	25 - 80 - 25°C

Table B-12. Summary of elevated temperature studies conducted in Boom Clay. L_p : plasticity index; W_l : liquid limit; e : void ratio; C_c : clay content; OCR: over-consolidation ratio; ϕ : porosity; w : water content; P_{wo} back pressure; σ_{eff} : isotropic effective stress; ρ_b : bulk density; ρ_d : dry density

OPERA

Meer informatie:

Postadres
Postbus 202
4380 AE Vlissingen

T 0113-616 666
F 0113-616 650
E info@covra.nl

www.covra.nl

